**Universidade de Aveiro**
**Ano 2019**

Departamento de Ciências Médicas

**ANDREIA SOFIA RODRIGUES GARCIA**

# Influência das toxinas urémicas na translocação microbiana através da barreira epitelial intestinal na doença renal crónica

# Influence of uremic toxins on microbial intestinal epithelial barrier translocation in chronic kidney disease

**Universidade de Aveiro**
**Ano 2019**

Departamento de Ciências Médicas

**ANDREIA SOFIA RODRIGUES GARCIA**

# Influência das toxinas urémicas na translocação microbiana através da barreira epitelial intestinal na doença renal crónica

# Influence of uremic toxins on microbial intestinal epithelial barrier translocation in chronic kidney disease

Dissertação apresentada à Universidade de Aveiro para cumprimento dos requisitos necessários à obtenção do grau de Mestre em Biomedicina Molecular, realizada sob a orientação científica da Doutora Ana Margarida Domingos Tavares de Sousa, Professora Auxiliar Convidada do Departamento de Ciências Médicas da Universidade de Aveiro, e coorientação científica da Doutora Maria Benedita Almeida Garrett de Sampaio Maia Marques, Professora Auxiliar da Faculdade de Medicina Dentária da Universidade do Porto.

Apoio financeiro do FEDER - Fundo Europeu de Desenvolvimento Regional, através dos programas COMPETE 2020, PORTUGAL 2020 e NORTE 2020, e da FCT - Fundação para a Ciência e a Tecnologia.

Dedico este trabalho aos meus pais pelo incansável apoio.

**o júri**

presidente

Doutor Bruno Miguel Alves Fernandes do Gago
Professor Auxiliar do Departamento de Ciências Médicas da Universidade de Aveiro

Doutora Freni Tavaria
Professora Auxiliar Convidada da Escola Superior de Biotecnologia da Universidade Católica Portuguesa - Porto

Doutora Maria Benedita Almeida Garrett de Sampaio Maia Marques
Professora Auxiliar da Faculdade de Medicina Dentária da Universidade do Porto

**agradecimentos**

Em primeiro lugar gostaria de agradecer ao Professor Doutor Manuel Pestana, que me aceitou em primeira instância e me proporcionou a oportunidade de realizar a dissertação de mestrado no “Nephrology & Infectious Diseases R&D Group” do Instituto de Investigação e Inovação em Saúde da Universidade do Porto.

À Professora Doutora Benedita Sampaio Maia um agradecimento especial, por me acolher, pela orientação e pelo apoio incansável, foi sem dúvida um grande pilar.

À Professora Doutora Ana Margarida Sousa agradeço o acompanhamento e orientação.

Ao Professor Doutor Bruno Sarmento e ao Doutor André Maia agradeço o acompanhamento e as ajudas fundamentais para a concretização deste trabalho.

A toda a equipa do “Nephrology & Infectious Diseases R&D Group” agradeço o companheirismo, em especial à Maria Azevedo, à Carolina Costa e à Susana Braga, agradeço a amizade, as ajudas no trabalho de laboratório e todos os momentos de conversa e descontração que me proporcionaram.

À Helena Macedo um agradecimento especial pelo apoio incansável, foi um grande pilar.

À Ana Baião agradeço o companheirismo, a amizade e todos os momentos de conversa e descontração que me proporcionou.

Ao Instituto de Investigação e Inovação em Saúde da Universidade do Porto, a todos os colegas de outros grupos e a todos os funcionários, um sentido agradecimento por proporcionarem um bom ambiente de trabalho.

A todos os doentes do Serviço de Nefrologia do Centro Hospitalar Universitário de São João, o maior agradecimento pela disponibilidade em participarem no estudo.

Um agradecimento muito especial aos meus amigos mais próximos que me acompanharam ao longo de toda esta etapa, em especial à Ana Correia, à Sónia Miranda, à Marta Silva e à Sílvia Martins. O vosso apoio foi fundamental. Obrigada pela amizade incondicional.

E por último, e sem dúvida mais importante, agradeço profundamente à minha família, em especial aos meus pais e ao meu irmão. Obrigada por acreditarem sempre em mim, por serem o meu suporte e por todo o apoio incondicional. É a vós que dedico todas as minhas conquistas académicas e pessoais.

**palavras-chave**

Barreira epitelial intestinal, disbiose intestinal, doença renal crónica, microbioma, translocação microbiana, toxinas urémicas

**resumo**

Doença renal crónica (DRC) é um termo geral para distúrbios que afetam a estrutura e a função do rim. A perda progressiva da função renal conduz à acumulação de toxinas, toxinas urémicas, normalmente excretadas pelos rins. É nessas circunstâncias que o "estado urémico" é estabelecido. Estudos recentes relacionam o plasma urémico ao dano da função da barreira intestinal e à depleção dos constituintes proteicos das junções de oclusão (JO). No lúmen intestinal, a ureia é hidrolisada pela urease microbiana, formando grandes quantidades de amónia, o principal mediador da disrupção da barreira intestinal em condições urémicas, causando uma depleção das proteínas das JO epiteliais intestinais na DRC. Quando o ecossistema microbiano é afetado, espécies microbianas prejudiciais podem crescer excessivamente, assim como os seus produtos do metabolismo, conduzindo a um desequilíbrio do microbioma intestinal. Estudos recentes sugerem que o microbioma intestinal exerce influência na produção de toxinas urémicas e na progressão da DRC. Na DRC, o dano da função da barreira intestinal pode permitir a translocação de microrganismos intestinais, endotoxinas, antigénios e outros produtos microbianos do lúmen intestinal para a circulação sistémica, contribuindo para a patogénese de inflamação sistémica, risco cardiovascular e progressão da DRC. O nosso principal objetivo foi avaliar a aplicação de dois modelos *in vitro* de barreira epitelial intestinal para o estudo da translocação microbiana e avaliar o impacto de diferentes condições urémicas presentes na DRC nessa translocação microbiana. Para isso, analisamos o efeito do plasma de doentes com DRC e da toxina urémica ureia na translocação intestinal microbiana, assim como na integridade, permeabilidade e localização e quantidade das proteínas das JO nos modelos intestinais *in vitro*, monocultura Caco-2 e modelo triplo Caco-2/HT29-MTX/Raji B. Os resultados mostraram que as condições urémicas experimentais simuladas neste estudo não potenciaram a translocação microbiana, embora tenham interferido em certa medida com a integridade e a permeabilidade dos modelos de barreira epitelial intestinal. A translocação microbiana foi maior na monocultura Caco-2 do que no modelo triplo, sugerindo que o modelo triplo cria uma barreira mais eficaz e, portanto, aparentemente representa um modelo intestinal mais robusto do intestino humano. Este estudo permitiu concluir que o estado urémico influencia a integridade da barreira intestinal, mas que essa influência pode não estar diretamente relacionada com um aumento da translocação microbiana através do epitélio intestinal nos modelos *in vitro* estudados.

**keywords**

Chronic kidney disease, intestinal dysbiosis, intestinal epithelial barrier microbial translocation, microbiome, uremic toxins

**abstract**

Chronic kidney disease (CKD) is a general term for disorders affecting kidney structure and function. The progressive loss of renal function leads to the accumulation of toxins, the uremic toxins, normally cleared by the kidneys. It is under these circumstances that the “uremic state” is established. Recent studies relate uremic plasma to impaired intestinal barrier function and to depletion of the tight junctions (TJs) protein constituents. Within the intestinal lumen urea is hydrolyzed by microbial urease forming large quantities of ammonia, the major mediator of intestinal barrier disruption in uremic conditions, causing a depletion of the intestinal epithelial TJs proteins in CKD. When the microbial ecosystem is affected, harmful microbial species may overgrowth, as well their metabolism product, leading to an imbalance of the intestinal microbiome. Recent studies suggest that intestinal microbiome exert an influence over both the production of uremic toxins and the progression of CKD. In CKD, the impairment of the intestinal barrier function may allow the translocation of intestinal microorganisms, endotoxins, antigens and other microbial products from intestinal lumen to systemic circulation, contributing to the pathogenesis of systemic inflammation, cardiovascular risk and progress of CKD. Our main goal was to evaluate the application of two *in vitro* models of intestinal epithelial barrier for the study of microbial translocation and to evaluate the impact of different uremic conditions present in CKD on this microbial translocation. For that, we analyzed the effect of plasma of CKD patients and the uremic toxin urea on microbial intestinal translocation, as well as on integrity, permeability and localization and quantity of TJs proteins in the *in vitro* intestinal models, Caco-2 monoculture and Caco-2/HT29-MTX/Raji B triple model. The results showed that the experimental uremic conditions simulated in this study did not potentiate the microbial translocation, although interfered at some extent with the integrity and the permeability of intestinal epithelial barrier models. Microbial translocation was higher in Caco-2 monoculture than in triple model, suggesting that the triple model creates a more effective barrier and, therefore, apparently represents a more robust intestinal model of the human intestine. This study allowed to conclude that the uremic state influences the integrity of intestinal barrier, but this influence could not be directly translated in an increase in the microbial translocation through the intestinal epithelium in the *in vitro* models studied.

# INDEX OF CONTENTS

**Index of figures** ..... **xix**

**Index of tables** ..... **xxiii**

**Abbreviations** ..... **xxv**

**1 Introduction** ..... **3**

1.1 Chronic kidney disease ..... 3

1.1.1 Uremic syndrome ..... 6

1.1.1.1 Uremic toxins ..... 7

1.1.1.1.1 Urea ..... 8

1.2 Intestinal epithelial barrier ..... 10

1.2.1 Microfold cells ..... 11

1.2.2 Tight junctions ..... 12

1.2.3 Intestinal barrier dysfunction in chronic kidney disease ..... 15

1.2.4 Intestinal dysbiosis in chronic kidney disease ..... 16

1.3 Therapeutic approaches in chronic kidney disease ..... 19

1.4 *In vitro* intestinal models ..... 19

1.4.1 Caco-2 monoculture model ..... 20

1.4.2 Caco-2/HT29-MTX/Raji B triple model ..... 22

1.4.3 Assessment of intestinal models integrity ..... 24

1.4.3.1 Transepithelial electrical resistance ..... 24

1.4.3.2 Permeability assays using FITC-dextran ..... 26

1.4.3.3 Immunocytochemistry of tight junctions ..... 27

1.4.4 Microbial translocation studies ..... 28

**2 Aims** ..... **31**

**3 Materials and Methods** ..... **35**

3.1 *In vitro* intestinal models ..... 35

3.1.1 Cell culture ..... 35

3.1.2 Optic microscopy ..... 35

3.1.3 Cell viability ..... 35

3.1.4 *In vitro* intestinal models ..... 36

3.1.4.1 Caco-2 monoculture model ..... 36
3.1.4.2 Caco-2/HT29-MTX/Raji B triple model ..... 36
3.1.5 Measurement of transepithelial electrical resistance ..... 37
3.1.6 Cell count of mature intestinal models ..... 37
3.2 Exposure to uremic conditions ..... 38
3.2.1 Plasma of chronic kidney disease patients ..... 38
3.2.2 Urea ..... 38
3.2.3 Dextran sodium sulfate ..... 39
3.3 Assessment of the effect of uremic conditions on transepithelial electrical resistance ..... 39
3.4 Assessment of the effect of uremic conditions on permeability ..... 39
3.5 Assessment of the effect of uremic conditions on tight junctions ..... 40
3.5.1 Immunocytochemistry ..... 40
3.5.2 High-throughput widefield fluorescence microscopy image acquisition and analysis ..... 41
3.5.3 Quantification of tight junctions ..... 42
3.6 Assessment of the effect of uremic conditions on microbial translocation ..... 42
3.6.1 Identification of bacteria ..... 42
3.6.2 Bacterial translocation assay ..... 43
3.7 Statistical analysis ..... 45
3.8 Scheme of methodology ..... 45
**4 Results ..... 49**
4.1 Morphology of cell lines of intestinal models ..... 49
4.2 Integrity of intestinal epithelial barrier ..... 50
4.2.1 Transepithelial electrical resistance ..... 50
4.2.2 Paracellular permeability of intestinal epithelial barrier ..... 51
4.3 Microbial translocation in intestinal epithelial barrier ..... 52
4.4 Effect of uremic conditions on transepithelial electrical resistance ..... 52
4.4.1 Effect of plasma of chronic kidney disease patients ..... 53
4.4.2 Effect of urea ..... 54

4.4.3 Effect of dextran sodium sulfate ..... 55
4.5 Effect of uremic conditions on permeability ..... 56
4.5.1 Effect of plasma of chronic kidney disease patients ..... 57
4.5.2 Effect of urea ..... 58
4.6 Effect of uremic conditions on quantity of tight junctions ..... 60
4.6.1 Effect of plasma of chronic kidney disease patients and dextran sodium sulfate ..... 60
4.7 Effect of uremic conditions on microbial translocation ..... 64
4.7.1 Effect of plasma of chronic kidney disease patients and dextran sodium sulfate ..... 64
4.7.2 Effect of urea ..... 66
**5 Discussion** ..... **69**
**6 Final remarks** ..... **77**
**7 References** ..... **81**
**8 Supplementary figures** ..... **95**
**9 Acknowledgments** ..... **99**

# INDEX OF FIGURES

**Figure 1 -** Structure of the kidney ..... **3**

**Figure 2 -** Stages of CKD ..... **4**

**Figure 3 -** Summary of the pathophysiologic consequences in CKD patients. (A) In healthy conditions the intestinal barrier function is intact; (B) In CKD different alterations occurred: (1) altered microbiome composition (dysbiosis); (2) impaired barrier function; (3) intestinal immune activation; (4) bacterial translocation; (5) systemic inflammation and presence of bacterial products; (6) altered drug transporters..... **6**

**Figure 4 -** Urea molecule structural chemical formula ..... **9**

**Figure 5 -** Routes and mechanisms of transport of molecules across the intestinal epithelium: 1) paracellular; 2) transcellular passive diffusion; 3) transcytosis; 4) carrier-mediated uptake at the apical domain followed by passive diffusion across the basolateral membrane ..... **11**

**Figure 6 –** M cells structure and function ..... **12**

**Figure 7 -** TJs proteins: CLDN, OCLN and ZO. (A) Model of TJs structure with CLDN linking two cell membranes and protein ZO1 linking the cytoplasmic tail of CLDN to actin filaments. (B and C) Structure of CLDN and OCLN..... **14**

**Figure 8 -** Bacterial family or genera associated to CKD. CKD is associated with higher levels of families described in the upward green arrow and with lower levels of the families described in the downward red arrow ..... **17**

**Figure 9 -** Summary of the mechanisms underlying to CKD ..... **18**

**Figure 10 -** Schematic representation of Caco-2 monoculture on a microporous membrane.. **21, 36**

**Figure 11 -** Schematic representation of Caco-2/HT29-MTX/Raji B triple model on a microporous membrane..... **22, 37**

**Figure 12 -** TEER measurement with a voltohmmeter..... **25**

**Figure 13 -** Permeability assay test principle. (A) FITC-dextran is added to the semi-permeable insert coated with a cell monolayer. (B) FITC-dextran permeates the cell monolayer into the plate well. The resulting fluorescence in the plate well is measured and used as an indicator of the extent of monolayer permeability..... **26**

**Figure 14 -** General protocol steps in an ICC assay ..... **27**

**Figure 15 -** *E. coli* isolated from feces of a CKD patient, cultured in MacConkey Agar (Sigma-Aldrich, USA)..... **43**

**Figure 16 -** Calibration curve of *E. coli* from CKD patient..... **43**

**Figure 17 -** Schematic representation of the methodology. In sum, the effect of uremic conditions was evaluated in the cellular barrier integrity, the permeability, the localization and quantity of TJs proteins and the microbial translocation in epithelial barrier of Caco-2 monoculture and triple model ..... **45**

**Figure 18 -** Morphology of cell lines used in intestinal models. Images were obtained by optic microscopy, at 400× magnification, and demonstrate epithelial cells growing in monolayer (Caco-2 and HT29-MTX) and lymphocytes B in suspension (Raji B)..... **49**

**Figure 19 -** TEER variation over 24 days on both Caco-2 monoculture and triple model. TEER values are expressed in ohm.cm$^2$ as mean ± SD of eight independent Caco-2 monoculture models and fourteen independent triple culture models. The larger arrow represents the day of maturation (21$^{st}$ day). The smaller arrow represents the addition of Raji B cells at 14$^{th}$ day of differentiation of the triple model..... **50**

**Figure 20 -** Paracellular permeability increased from 21$^{st}$ to 25$^{th}$ days in triple model. FITC-dextran permeability assay was performed at three different days after maturation (21$^{st}$, 23$^{rd}$ and 25$^{th}$ day) with a concentration of 1000 µg/mL of FITC-dextran used on apical compartment of triple model. The graph shows the percentage of FITC-dextran that passed to the basolateral compartment in the three different days in eight time points. The results are expressed as mean ± SD of four replicates at 21$^{st}$ day, three replicates at 23$^{rd}$ day and four replicates at 25$^{th}$ day. Statistically significant differences are signed as (*) $p < 0.05$ compared with 21$^{st}$ day ..... **51**

**Figure 21 -** *E. coli* translocation was higher in Caco-2 monoculture than in triple model. Bacterial translocation assay was performed for 180 min, using MOI=5. The results are represented as $\log_{10}$(CFU/well) vs time and are the mean ± SD of five independent experiments. Statistically significant differences are signed as (*) $p < 0.05$ compared with triple model..... **52**

**Figure 22 -** Effect of CKD plasma on TEER. (A) CKD plasma decreased the TEER in Caco-2 monoculture. The graph shows the TEER values 24h after exposure to healthy and CKD plasma in Caco-2 monoculture. Results are expressed as mean ± SD of three independent experiments. Statistically significant differences are signed as (*) $p < 0.05$ compared with 0 hours (before exposure). (B) CKD plasma did not induce significant alteration on TEER in triple model. The graph shows the TEER values 24h after exposure to healthy and CKD plasma in triple model. Results are expressed as mean ± SD of six independent experiments..... **53**

**Figure 23 -** Effect of urea on TEER. (A) Uremic concentration of urea in the presence of urease decreased the TEER in Caco-2 monoculture. The graph shows the TEER values 24h after exposure to urea 20 mg/dL plus urease, urea 150 mg/dL plus urease, urea 150 mg/dL without urease and urease in Caco-2 intestinal model. Results are expressed as mean ± SD of three independent

experiments. Statistically significant differences are signed as (*) $p < 0.05$ compared with 0 hours (before exposure). (B) Urea did not induce significant alteration on TEER in triple model. The graph shows the TEER values 24h after exposure to urea 20 mg/dL plus urease, urea 150 mg/dL plus urease, urea 150 mg/dL without urease and urease in triple intestinal model. Results are expressed as mean ± SD of three independent experiments ..... **55**

**Figure 24 -** Effect of DSS on TEER. (A) DSS decreased the TEER in Caco-2 monoculture. The graph shows the TEER values 3h after exposure to DSS in Caco-2 intestinal model. Results are expressed as mean ± SD of three replicates. Statistically significant differences are signed as (**) $p < 0.01$ compared with 0 hours (before exposure). (B) DSS did not induce significant alteration on TEER in triple model. The graph shows the TEER values 3h after exposure to DSS in triple intestinal model. Results are expressed as mean ± SD of three replicates..... **56**

**Figure 25 -** Effect of CKD plasma on permeability. CKD plasma did not induce significant alteration on permeability in (A) Caco-2 monoculture and (B) triple model. FITC-dextran permeability assay was performed 24h after incubation with healthy and CKD plasma, with a concentration of 200 µg/mL of FITC-dextran used on apical compartment of intestinal model. The graph shows the percentage of FITC-dextran that passed to the basolateral compartment in eight time points. The results are expressed as mean ± SD of three replicates ..... **58**

**Figure 26 –** Uremic concentration of urea in the presence of urease increased the permeability in triple model. FITC-dextran permeability assay was performed 24h after exposure to urea 20 mg/dL plus urease, urea 150 mg/dL plus urease, urea 150 mg/dL without urease and urease, with a concentration of 200 µg/mL of FITC-dextran used on apical compartment of intestinal model. (A) The graph shows the percentage of FITC-dextran that passed to the basolateral compartment in eight time points. (B) Percentage of FITC-dextran that passed to the basolateral compartment at the end of experiment (time 240 min). All results are expressed as mean ± SD of three replicates. Statistically significant differences are signed as (**) $p < 0.01$ compared with control..... **59**

**Figure 27 -** Localization of TJs ZO1, OCLN, CLDN1 and CLDN2 in different conditions in Caco-2 monoculture. Images representative of localization of TJs ZO1, OCLN, CLDN1 and CLDN2 24h after exposure to healthy plasma and CKD plasma, and 3h after exposure to DSS..... **61**

**Figure 28 -** CKD plasma and DSS did not induce significant alteration on quantity of TJs in Caco-2 monoculture. Quantification of TJs represented in figure 27. Mean fluorescence intensity of (A) ZO1 (Alexa Fluor 488), (B) OCLN (Alexa Fluor 488), (C) CLDN1 (Alexa Fluor 594) and (D) CLDN2 (Alexa Fluor 594) at plasma membrane. All results are expressed as mean fluorescence intensity ± SD, normalized to fluorescence measured at the membrane without antibodies, obtained in three independent experiments..... **62**

**Figure 29 -** Localization of TJs ZO1, OCLN, CLDN1 and CLDN2 in different conditions in triple model. Images representative of localization of TJs ZO1, OCLN, CLDN1 and CLDN2 24h after exposure to healthy plasma and CKD plasma, and 3h after exposure to DSS..... **63**

**Figure 30 -** CKD plasma and DSS did not induce significant alteration on quantity of TJs in triple model. Quantification of TJs represented in figure 29. Mean fluorescence intensity of (A) ZO1 (Alexa Fluor 488), (B) OCLN (Alexa Fluor 488), (C) CLDN1 (Alexa Fluor 594) and (D) CLDN2 (Alexa Fluor 594) at plasma membrane. All results are expressed as mean fluorescence intensity ± SD, normalized to fluorescence measured at the membrane without antibodies, obtained in three independent experiments ..... **64**

**Figure 31 -** Effect of CKD plasma and DSS on microbial translocation. CKD plasma and DSS did not induce significant alteration in *E. coli* translocation in (A) Caco-2 monoculture and (B) triple model. Bacterial translocation assay was performed 24h after exposure to healthy and CKD plasma and 3h after exposure to DSS, for 180 min with a MOI=5. The results were represented as $log_{10}$(CFU/well) vs time and are the mean ± SD of five independent experiments..... **65**

**Figure 32 -** Effect of urea on microbial translocation. Urea did not induce significant alteration in *E. coli* translocation in (A) Caco-2 monoculture and (B) triple model. Bacterial translocation assay was performed 24h after exposure to urea 20 mg/dL plus urease, urea 150 mg/dL plus urease, urea 150 mg/dL without urease and urease, for 180 min with a MOI=5. The results were represented as $log_{10}$(CFU/well) vs time and are the mean ± SD of one independent experiment with 3 replicates ..... **66**

**Supplementary figure 1 -** Steps followed until quantification of TJs ..... **95**

# INDEX OF TABLES

**Table 1 -** Main known uremic retention solutes ..... **8**

**Table 2 -** Characteristics of Caco-2 cells ..... **20**

**Table 3 -** Number of epithelial cells at 22$^{nd}$ day of maturation in both Caco-2 monoculture and triple model. Values are expressed in cells/cm$^2$ as mean ± SD of three replicates ..... **44**

# ABBREVIATIONS

**BHI** Brain heart infusion

**BSA** Bovine serum albumin

**cAMP** Cyclic adenosine monophosphate

**CFU** Colony forming units

**CKD** Chronic kidney disease

**CLDN** Claudin

**CVD** Cardiovascular disease

**Da** Dalton

**DAPI** 4',6-diamidino-2-phenylindole

**DMEM** Dulbecco's Modified Eagle Medium

**DSS** Dextran sodium sulfate

***E. coli*** *Escherichia coli*

**EDTA** Ethylenediaminetetraacetic acid

**ESKD** End-stage kidney disease

**EUTox** European Uremic Toxin

**FBS** Fetal bovine serum

**FITC-dextran** Fluorescein isothiocyanate-dextran

**GFR** Glomerular filtration rate

**GIT** Gastrointestinal tract

**HA** Hippuric acid

**HBSS** Hank's balanced salt solution

**HD** Hemodialysis

**HIV** Human immunodeficiency virus

**IAA** Indole-3-acetic acid

**ICC** Immunocytochemistry

**IECs** Intestinal epithelial cells

**IL-6** Interleukin 6

**IS** Indoxyl sulfate

**JAMs** Junctional adhesion molecules

**LPS** Lipopolysaccharides

**M cells** Microfold cells

**MCP-1** Monocyte chemoattractant protein 1

**MOI** Multiplicity of infection

**mRNA** Messenger ribonucleic acid

**MW** Molecular weight

**NEAA** Non-essential amino acids

**OCLN** Occludin

**$O.D_{600\ nm}$** Optical density at 600 nm

**PBS** Phosphate-buffered saline

**PBS-T** PBS-Tween

**PCS** p-cresol sulfate

**PD** Peritoneal dialysis

**PET** Polyethylene terephthalate

**PFA** Paraformaldehyde

**P/S** Penicillin/streptomycin

**RT** Room temperature

**SD** Standard deviation

**TEER** Transepithelial/transendothelial electrical resistance

**TJs** Tight junctions

**TNF- α** Tumor necrosis factor-α

**ZO** Zonula occludens

# INTRODUCTION

# 1 INTRODUCTION

## 1.1 Chronic kidney disease

The kidneys are central to body homeostasis, by controlling excretion of excessive fluid, electrolytes and toxic waste products [1]. Blood, waste and water enter through the renal artery; filtered blood or water leave through the renal vein; excess water and toxic waste leave via the ureter, in form of urine (figure 1). The core function of the kidneys is, therefore, the excretion of the toxic products of metabolism in urine [2].

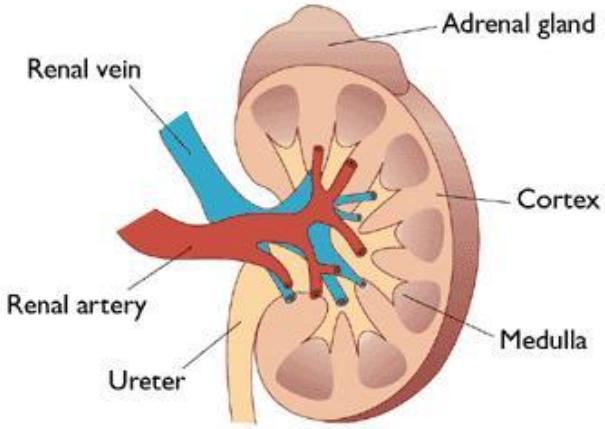


**Figure 1.** Structure of the kidney. Adapted from [3].

The dysfunction of the kidneys leads to disturbed renal metabolism and to impaired glomerular filtration [4].

Chronic kidney disease (CKD) is a general term for disorders affecting the structure and function of the kidney [5]. CKD is characterized by abnormalities of kidney structure or function for three or more months, irrespective of the cause. CKD may be detected by decreased glomerular filtration rate (GFR, <60 mL/min/1.73 $m^2$), by increased rates of urinary albumin excretion or by abnormal kidney structure detected by imaging. GFR refers to the flow rate of filtered blood through renal glomerulus [6].

According to the US National Kidney Foundation Clinical Practice Guidelines for Chronic Kidney Disease [7], CKD is classified into five stages on the basis of GFR, from normal kidney function (stage 1, >90 mL/min/1.73 $m^2$) to end-stage kidney disease (ESKD) (stage 5, <15 mL/min/1.73 $m^2$) (figure 2).


**Figure 2**. Stages of CKD. Adapted from [8].

ESKD require renal replacement therapy in the form of hemodialysis (HD), peritoneal dialysis (PD), or kidney transplant [7]. According to the National Institute of Diabetes and Digestive and Kidney Diseases [9], HD is defined as a treatment to filter waste and water from blood, as kidneys do when they are healthy, helping to control blood pressure and balance of minerals, such as potassium, sodium and calcium in blood. HD uses an artificial extra-body filtering membrane. According to the American Kidney Fund [10], PD is defined as treatment that uses the lining of the abdomen (belly area), called peritoneum, and a cleaning solution called dialysate to clean the blood. Dialysate absorbs waste and fluid from the blood, using the peritoneum as a filter, thus, implying an endogenous filtering membrane. According to The Official Foundation of the American Urological Association [11], kidney transplant is one of the most common organ transplant surgeries performed today and, in this surgery, kidney that is not working well is replaced by a healthy kidney from a donor.

Currently, CKD is an increasing public health issue, with high rates of morbidity and mortality. Its prevalence is estimated to be 8–16% worldwide [12]. In 2010, over 497 million adults in the world had CKD of which 236 million had moderate or severe decreases in kidney function presenting CKD stages 3-5 [13].

Diabetes and hypertension are the most common causes of CKD worldwide. Other causes can include glomerulonephritis, pyelonephritis and polycystic kidney disease [14].

On the other hand, cardiovascular disease (CVD) remains the major cause of morbidity and mortality in patients with CKD [15]. People with CKD have a 2- to 3-fold greater risk of cardiovascular mortality than people without CKD and are 20–30 times more likely to die from CVD than experience ESKD. CVD is frequently underdiagnosed and undertreated in patients with CKD [16]. CKD patients develop atheromatous vascular disease more frequently and earlier than the general population [17, 18]. Therefore, these patients should be acknowledged as having high cardiovascular risk that needs particular medical attention [16].

As CKD progresses, risk factors for CVD come into play. The altered quality of the blood in patients with CKD affects the peripheral vasculature, particularly the capillaries, in a way that requires increased force to propel the blood around the body [19], relating to cardiovascular damage. Studies have suggested that uremic toxins present in the blood of CKD patients are associated with vascular damage by inducing vasoactive substances related to atherogenesis such as chemokines, cytokines, or cell adhesion molecules [20-23]. Also, uremic toxins may contribute to inflammation and consequently CVD, in CKD patients [24].

CKD–related systemic inflammation is also a consequence of the alteration of microbiome composition, translocation of bacteria or their metabolism products across the intestinal barrier and increased serum levels of bacterial toxins. Therefore, uremia, established by the accumulation of uremic toxins in the blood [6], associates with alteration of intestinal microbiome, intestinal barrier dysfunction and bacterial translocation, leading to the state of persistent systemic inflammation in CKD [25] (figure 3). Plasma uremic toxins were associated with higher interleukin 6 (IL-6), monocyte chemoattractant protein 1 (MCP-1) and tumor necrosis factor-α (TNF-α) levels in CKD patients [24].

In sum, in CKD patients, the CVD is associated with reduced myocardial contractility, cardiac fibrosis and atherosclerosis, consequence of persistent systemic inflammation, endothelial dysfunction and oxidative stress, which in turn are consequence of uremia [15, 26].

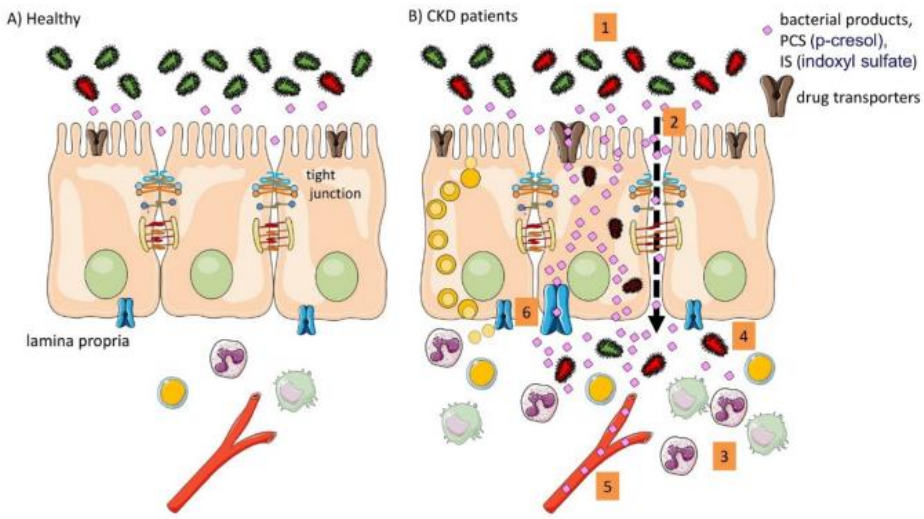


**Figure 3.** Summary of the pathophysiologic consequences in CKD patients. (**A**) In healthy conditions the intestinal barrier function is intact; (**B**) In CKD different alterations occurred: (1) altered microbiome composition (dysbiosis); (2) impaired barrier function; (3) intestinal immune activation; (4) bacterial translocation; (5) systemic inflammation and presence of bacterial products; (6) altered drug transporters. Adapted from [1].

### 1.1.1 Uremic syndrome

The progressive loss of renal function leads to the accumulation of organic waste products, normally cleared by the kidneys. It is under these circumstances that the "uremic state" is established [6]. Many of these products have been found to exert toxicity on virtually all systems of the human body, leading to the clinical syndrome of uremia [15].

The uremic syndrome can be defined as a deterioration of biochemical and physiological functions, in parallel with the progression of renal failure, resulting in complex and variable symptomatology [27-29]. The syndrome of uremia is related to irreversible loss of kidney function. Loss of kidney function results in structural and functional alterations of the intestinal barrier [1], that will be covered later.

#### 1.1.1.1 Uremic toxins

Organic waste products that accumulate in the uremic blood and tissues during the development of ESKD, due to a deficient renal clearance, are called uremic retention solutes or uremic toxins. These retention solutes may modify biochemical and physiological functions, contributing to the uremic syndrome [30]. In 2003, the European Uremic Toxin (EUTox) Work Group classified 90 retention solutes into three major categories based on the molecular weight (MW) and kinetic behavior of the uremic retention solutes during dialysis (table 1) [31]:

a) Small water-soluble molecules (MW ≤ 500 dalton [Da]), such as urea. Most toxins in this category are dialyzable with conventional HD. Some of them have been used in the evaluation of renal excretory function and monitoring removal efficiency of dialysis treatment, such as urea and creatinine.
b) Middle molecules (MW > 500 Da), whereas $\beta_2$-microglobulin is a prototype. Removal of middle molecules is more effective with PD than with conventional HD. This is probably because of the larger pore sizes and the longer dialysis duration of PD. HD techniques that increased the permeability of membranes (high-flux HD) or convection (hemofiltration/hemodiafiltration) provide superior clearance of these molecules.
c) Protein-bound compounds, for example, indoxyl sulfate (IS) and p-cresol sulfate (PCS). Twenty-five of the 90 listed toxins (27.8%) are protein-bound compounds, and twenty-three of them have an MW ≤ 500 Da. Among these uremic toxins, organic anions, such as IS, PCS, indole-3-acetic acid (IAA) and hippuric acid (HA), are low MW compounds. Nevertheless, they should be classified as high MW compounds in circulation because they are firmly bound to plasma proteins, primarily albumin (MW = 66 kDa). Therefore, this group of toxins is difficult to be dialyzed with conventional HD despite having molecular sizes small enough to pass through the dialysis membrane.

Alternatively, uremic toxins can be classified according to their origin: endogenous metabolism, microbial metabolism, or exogenous intake [32].

Most of the uremic toxins are secreted into the gut altering intestinal milieu, inducing changes in the structure, composition and function of the intestinal microbiome. Also, in the intestine of ESKD patients, secreted uremic toxins serve as alternative substrates for intestinal microbiome, which normally utilize indigestible complex carbohydrates [6].

**Table 1.** Main known uremic retention solutes. Adapted from [31].

| Small water soluble solutes | Protein-bound solutes | Middle molecules |
|---|---|---|
| Asymmetric dimethylarginine | 3-Deoxyglucosone | Adrenomedullin |
| Benzylalcohol | CMPF | Atrial natriuretic peptide |
| β-Guanidinopropionic acid | Fructoselysine | $\beta_2$-Microglobulin |
| β-Lipotropin | Glyoxal | β-Endorphin |
| Creatinine | Hippuric acid | Cholecystokinin |
| Cytidine | Homocysteine | Clara cell protein |
| Guanidine | Hydroquinone | Complement factor D |
| Guanidinoacetic acid | Indole-3-acetic acid | Cystatin C |
| Guanidinosuccinic acid | Indoxyl sulfate | Degranulation inhibiting protein I |
| Hypoxanthine | Kinurenine | Delta-sleep-inducing peptide |
| Malondialdehyde | Kynurenic acid | Endothelin |
| Methylguanidine | Methylglyoxal | Hyaluronic acid |
| Myoinositol | N-carboxymethyllysine | Interleukin 1β |
| Orotic acid | P-cresol | Interleukin 6 |
| Orotidine | Pentosidine | Kappa-Ig light chain |
| Oxalate | Phenol | Lambda-Ig light chain |
| Pseudouridine | P-OHhippuric acid | Leptin |
| Symmetric dimethylarginine | Quinolinic acid | Methionine-enkepahlin |
| Urea | Spermidine | Neuropeptide Y |
| Uric acid | Spermine | Parathyroid hormone |
| Xanthine | | Retinol binding protein |
| | | Tumor necrosis factor alpha |

CMPF is carboxy-methyl-propyl-furanpropionic acid.

#### 1.1.1.1.1 Urea

The reduction in urinary excretion of nitrogenous waste products in advanced CKD leads to their accumulation in the blood. The most abundant among these metabolites is urea [33].

Urea, with chemical formula $CO(NH_2)_2$ (figure 4), is a 60 Da small water-soluble compound, which has, among the presently known uremic retention solutes, the highest concentration in uremic serum [31]. It is a well-established surrogate marker of kidney function, uremic retention [34] and dialysis adequacy [35, 36], and its removal is directly related to patient survival [34].

Several studies point to an important pathophysiologic impact of urea:

- Urea inhibits $NaKCl_2$ cotransport in human erythrocytes [37], as well as several cell transport pathways. The $NaKCl_2$ cotransport is a ubiquitous process that serves numerous vital functions, among which cell volume and extrarenal potassium regulation are the most important [30].
- Urea also decreases cyclic adenosine monophosphate (cAMP) production [38], second messenger that plays fundamental roles in cellular responses to many hormones and neurotransmitters [39].
- Urea is a precursor of some of the guanidines, especially guanidinosuccinic acid, which by itself induces direct biochemical alterations [30].
- The presence of urea in the blood has been held responsible for a decreased affinity of oxygen for hemoglobin [40].
- Urea inhibits macrophage inducible nitric oxide synthesis at the posttranscriptional level [41].
- Urea induces apoptosis of vascular smooth muscle cells as well as endothelial dysfunction, thus directly promoting cardiovascular illness [42].
- Urea stimulates oxidative stress and dysfunction in adipocytes, leading to insulin resistance [42].

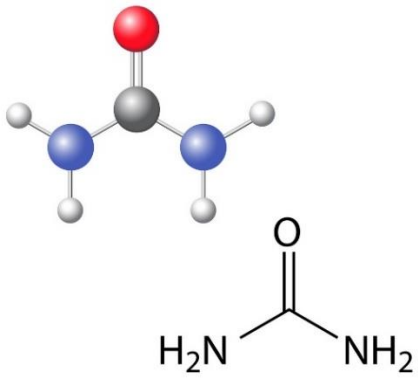


**Figure 4.** Urea molecule structural chemical formula. Available from [43].

## 1.2 Intestinal epithelial barrier

The gastrointestinal tract (GIT) plays an important role in the absorption and production of nutrients while protecting from invading pathogens and toxins [44]. The GIT functions as a barrier between the external environment and the internal milieu of the body. The epithelial layer of the GIT forms a selectively permeable barrier that permits the entry of nutrients, ions and water, and simultaneously restricts the entry of pathogens [45, 46] and other noxious compounds [47] into the underlying tissue compartments.

Intestine are divided into four layers: the mucosa (epithelium, lamina propria and muscularis mucosa), the submucosa, the muscularis propria (inner circular muscle layer, intermuscular space and outer longitudinal muscle layer) and the serosa [48]. An intact intestinal mucosa, with a normal intestinal permeability and barrier function, is essential for absorption, secretion and transport of compounds [49]. Some studies have shown that permeability of different molecules varies along the intestinal tract. In general, permeability decreases in the following order: jejunum > ileum > colon [50]. The intestinal mucosa is characterized by the presence of villi that constitute the anatomical and functional unit for absorption [51]. The presence of villi and microvilli provides a massive surface area for absorption (approximately 250 $m^2$ in a human). The mucosa consists of the epithelium, the lamina propria (fibroblasts, myofibroblasts, immune cells and collagen matrix containing blood and lymphatic vessels) and the muscularis mucosa. Therefore, any compound entering the bloodstream has to pass through the epithelial layer, part of the lamina propria and the wall of the respective vessel [52].

Intestinal epithelial cells (IECs) or enterocytes that line the intestinal mucosa can be regarded as the most outer defense barrier preventing microorganisms from reaching organs and tissues [53-56]. IECs play an important role in the interaction between luminal content and the immune system [54, 55, 57]. The intestinal barrier apparatus consists of the IECs and the apical junctional complex. The latter prevents paracellular passage of the luminal contents by sealing the gap between the adjacent epithelial cells [58] (figure 5).

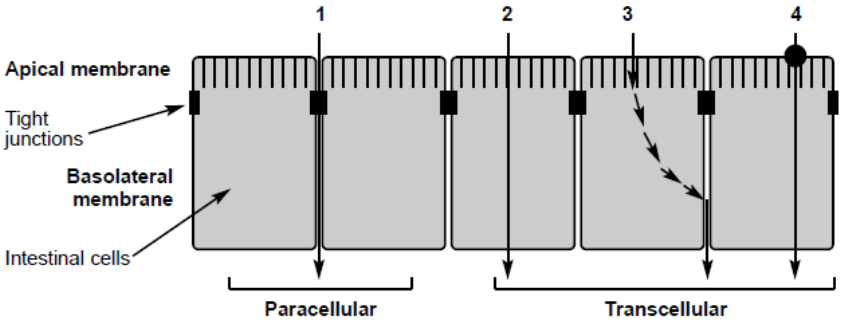


**Figure 5.** Routes and mechanisms of transport of molecules across the intestinal epithelium: 1) paracellular; 2) transcellular passive diffusion; 3) transcytosis; 4) carrier-mediated uptake at the apical domain followed by passive diffusion across the basolateral membrane. Adapted from [52].

### 1.2.1 Microfold cells

Microfold cells (M cells) are present in the intestinal epithelium and possess particular characteristics. Typical features of M cells include disorganization of apical microvilli, rearrangement of the cytoskeleton (expression of the actin associated to villin protein), decreased enzymatic activity (brush border hydrolase and sucrase isomaltase) and presence of a basolateral invagination which is associated to numerous B- and T-lymphocytes and dendritic cells [59-61] (figure 6). The specialized M cells serve as antigen-presenting cells of the intestinal innate immune system [62].

It is suggested that M cells result from the differentiation of enterocytes [63]. Moreover, as these changes only occur in a fraction of the cells, it is hypothesized that just a subpopulation of enterocytes is affected by the mediators released by lymphocytes [64], that allow the differentiation of enterocytes into M cells.

Unlike 'classical' enterocytes, M cells are able to translocate diverse particulates without digesting them. They act as pathways for microorganisms invasion and mediate the transcellular transport of intestinal microbiome and antigens [62] (figure 6). An ability to translocate the epithelial mucosa through M cells provides invasive pathogens with a rapid means of accessing the lymphoid tissues [65]. Several microorganisms have shown to be specifically transported by M cells, such as *Vibrio cholerae*, some strains of *Escherichia*

*coli* (*E. coli*), *Salmonella typhimurium*, *Yersinia enterocolitica*, *Shigella flexneri*, reovirus, poliovirus and human immunodeficiency virus (HIV) [66-73]. An ability to migrate through M cells has implications for the development of local immune responses and may act as a source of localized infection [65].

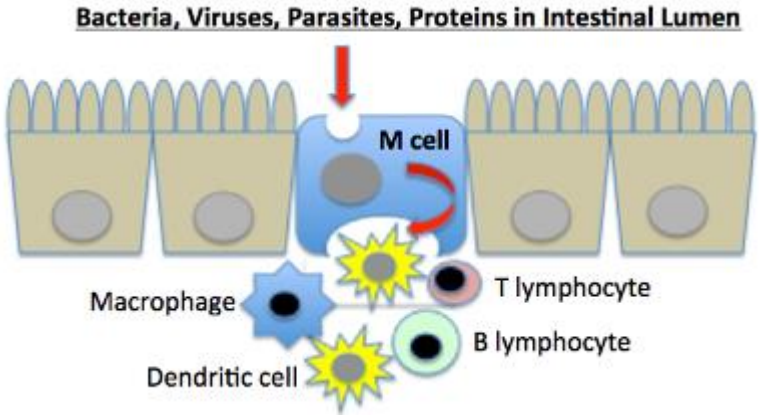


**Figure 6.** M cells structure and function. Adapted from [74].

### 1.2.2 Tight junctions

The permeability of the intestinal barrier is regulated by the integrity of cellular plasma membranes and tight junctions (TJs), as well as by epithelial cell processes mediating secretion and absorption [75].

TJs are multi-protein complexes consisting of transmembrane proteins, linked to the actin cytoskeleton via cytoplasmic proteins [76]. Approximately 50 TJs proteins have been identified. Transmembrane proteins, principally claudin (CLDN), occludin (OCLN) and junctional adhesion molecules (JAMs), contribute to the semi-permeable barrier, whereas cytosolic proteins link membrane components to the actin cytoskeleton and participate in signaling between TJs and the cell nucleus [77].

The intestinal epithelial TJs are the most apical intercellular junctions that connect individual cells in an epithelial layer, and form a seal that restricts paracellular passage [78]. The TJs forms an effective barrier against influx of microbes, microbial toxins, antigens, digestive enzymes, degraded food products and other noxious substances from the intestinal lumen to the internal milieu [47].

TJs are involved in the maintenance of epithelial cell polarity. Epithelial cells possess an apical cell surface, facing the organ lumen, and a basolateral domain that are biochemically and functionally distinct [78], that characterize the epithelial cell polarity.

The TJs apparatus consists of the three main components [45]:

1. Adhesive transmembrane proteins including OCLN and CLDN protein family, which link the plasma membranes of the adjacent cells to form a barrier to the diffusion of fluids and solutes.
2. The cytosolic proteins, including the zonula occludens (ZO) protein family, which serve as the anchor by, simultaneously, binding the intracellular domains of OCLN and CLDN and the perijunctional actin-myosin ring.
3. The perijunctional ring of actin and myosin, which modulate the structure and function of the TJs, regulating paracellular permeability.

**Occludin**

The amino acid sequence of OCLN codes for four transmembrane domains and two hydrophobic extracellular loops that are rich in tyrosine and glycine residues (figure 7). Movement of OCLN from the cell membrane into cytoplasmic vesicles occurs frequently during barrier function loss [79].

**Claudin**

CLDN has four transmembrane domains, but it is not related in sequence to OCLN. The extracellular domains of CLDN form pores along the TJs contacts. The cytoplasmic tails of CLDN interact with numerous proteins with roles as scaffolds and in actin binding, signaling and cell polarity (figure 7). Proteins of the CLDN family are the main component of TJs and form a seal that modulates paracellular transport in the intestinal epithelium [80]. It is known that CLDN-1, -3, -4, -5, -7 and -19 are pore-sealing CLDNs and, therefore, an increased expression of these proteins leads to a very tight epithelium and decreased permeability across the epithelial monolayer [81-83]. Conversely, CLDN2 and CLDN15 are considered as the pore-forming CLDNs, because of their ability to form paracellular anion/cation pores as well as water channels, leading to decrease epithelial tightness and

to increase solute permeability, allowing the passage of ions [84-86]. Together, CLDNs enable strict control over the paracellular flux of cations and anions [87].

**Zonula-occludens**

ZO are adapter proteins linking the transmembrane proteins to cytoplasmic proteins such as actin filaments [88, 89]. There are three ZO types: ZO1, ZO2 and ZO3. ZO1 plays a major role in the formation of TJs in epithelial cells compared with ZO2 and ZO3 [85]. Furthermore, ZO1 serves as an important linker between the TJs and the actin cytoskeleton and is thought to be a functionally critical TJs component (figure 7). It was also described that ZO1 is directly associated with OCLN [90].

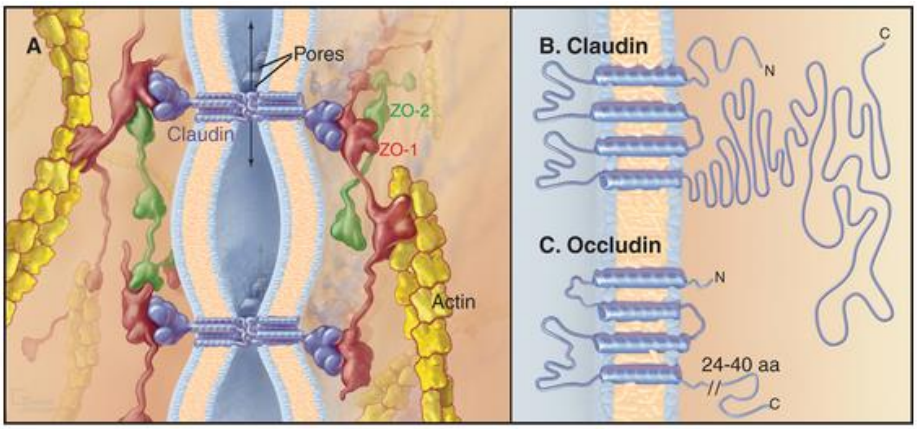


**Figure 7.** TJs proteins: CLDN, OCLN and ZO. **(A)** Model of TJs structure with CLDN linking two cell membranes and protein ZO1 linking the cytoplasmic tail of CLDN to actin filaments. **(B and C)** Structure of CLDN and OCLN. Adapted from [91].

The assessment of TJs integrity is complex, which is reflected by the finding that not only the quantity of messenger ribonucleic acid **(**mRNA) but also phosphorylation and folding together with localization of TJs proteins are of importance [92, 93].

In general, pathogens can disrupt the TJs by different mechanisms, including direct reorganization or degradation of specific TJs proteins, reorganization of the cell cytoskeleton and activation of host cell signaling events [94]. Additionally, it was reported

that some enteric pathogens appear to influence TJs functions by utilizing TJs proteins as receptors for internalization and breakdown of the epithelial barrier [95].

There are several molecules that can affect the intestinal epithelial barrier, such as dextran sodium sulfate (DSS). DSS is a compound that leads to disruption of TJs, adherens junctions and actin cytoskeleton leading to intestinal epithelium dysfunction [96]. Recent studies showed that DSS caused, *in vitro* and *in vivo,* intestinal barrier dysfunction and inflammatory response [97].

### 1.2.3 Intestinal barrier dysfunction in chronic kidney disease

Maintenance of the physical barrier in the intestine is dependent on the physical integrity of barrier components. Increased paracellular and transcellular permeability and epithelial cell damage will result in an increased intestinal barrier permeability [75].

Recent studies relate uremic plasma to impaired intestinal barrier function and to depleted the TJs protein constituents [47]. These findings point to the presence of as-yet unidentified products in the uremic plasma capable of depleting epithelial TJs and impairing barrier function.

The intestinal barrier dysfunction observed in CKD may allow the influx of endotoxins, that are bacterial toxins such as lipid component (lipid A) of the lipopolysaccharides (LPS) present in the outer wall of most Gram-negative bacteria that may be released in the blood when the bacterial cell wall is disrupted [6], and other noxious products contributing to the systemic inflammation and uremic toxicity [47]. There is mounting evidence pointing to the intestinal barrier dysfunction and its role in the pathogenesis of uremic toxicity and inflammation. These include presence of endotoxemia, that is, presence of endotoxins in the blood of uremic patients [6], increased intestinal permeability to large MW polyethylene glycols in the uremic patients and animals [98, 99], translocation of bacteria across the intestinal barrier and their detection in the mesenteric lymph nodes in uremic rats [100] and histological evidence of chronic inflammation throughout the GIT in patients in HD [101]. However, the mechanism by which uremic conditions result in degradation of the intestinal epithelial TJs proteins is unknown [47].

Disruption of TJs and barrier function induced by uremia is, in part, mediated by urea, which is generally considered to be a nontoxic retained metabolite [102]. Blood levels of urea rise with progressive decline in kidney function. Elevated urea at concentrations typically encountered in uremic patients induces disintegration of the intestinal epithelial barrier, leading to translocation of bacterial toxins into the bloodstream and systemic inflammation [42]. Intestinal barrier dysfunction in uremia may be due to diffusion of urea into the intestinal lumen and its conversion to ammonia by microbial urease [102]. Within the intestinal lumen urea is hydrolyzed by microbial urease forming large quantities of ammonia [$CO(NH_2)_2 + H_2O \rightarrow CO_2 + 2NH_3$] which is converted to ammonium hydroxide [$NH_3 + H_2O \rightarrow NH_4OH$] [103, 104]. Ammonium hydroxide, in turn, leads to a rise in the luminal fluid pH, causes mucosal irritation and promotes enterocolitis [101, 105]. Based on these observations, it was hypothesized that ammonium hydroxide may contribute to the epithelial barrier dysfunction and depletion of TJs protein constituents [102]. Ammonia, a product of urea metabolism by intestinal microbiome, was considered as a major mediator of intestinal barrier disruption in uremic conditions, causing a depletion of the intestinal epithelial TJs proteins in CKD [102, 106, 107].

### 1.2.4 Intestinal dysbiosis in chronic kidney disease

The human microbiome, defined by the NIH Human Microbiome Project as the collection of all genomes of microorganisms living in association with the human body, influences the well-being of the host by contributing to its nutrition, metabolism, physiology and immune function [108]. Also known as the “second human genome,” the intestinal microbiome plays important roles in both the maintenance of health and the pathogenesis of disease [109]. Microbiome metabolism is emerging as a modifiable non-traditional risk factor in nephrology [110].

Even amongst the beneficial bacteria of the microbiome, negative effects can arise. When the microbial ecosystem is affected, harmful microbial species may overgrowth as well their metabolism product [32, 111]. Intestinal dysbiosis can be defined as an imbalance of the intestinal microbiome that results in alterations of GIT activity producing deleterious

effects [6]. Dysbiosis have been shown to contribute to the pathogenesis of a range of diseases including obesity [112], liver disease [113], as well CKD [114].

Recent studies suggest that intestinal microbiome exert an influence over both the production of uremic toxins and the progression of CKD [44]. In addition to damaging the intestinal epithelial TJs and barrier function, uremia has been shown to result in profound alteration of the intestinal microbiome [114]. This ecosystem alteration is in part due to the bioavailability of uremic toxins that may promote the growth of microorganisms that are able to metabolize these uremic retention solutes. The microbial metabolization of the uremic retention solutes produces other uremic toxins, such as IS and PCS [6]. Dysbiosis is characterized by high levels of pathogenic bacteria that may lead to increase in uremic toxins and intestinal permeability. This allows the produced uremic toxins to cross the intestinal barrier into the bloodstream where the toxins can exacerbate declining kidney function and progression of CKD [44, 115].

CKD is associated with higher intestinal levels of Enterobacteriaceae, specially the genera *Escherichia*, *Enterobacter* and *Klebsiella* (figure 8) [6]. Enterobacteriaceae includes several species of bacteria, such as *E. coli*, *Klebsiella pneumoniae*, *Proteus mirabilis*, *Salmonella enterica* and *Yersinia pestis*. In intestinal lumen of CKD patients, some members of Enterobacteriaceae are considered pathobionts due to their capacity to opportunistically adhere and invade host tissues [116]. These microorganisms can translocate to the blood, increasing risk of endotoxemia [6].

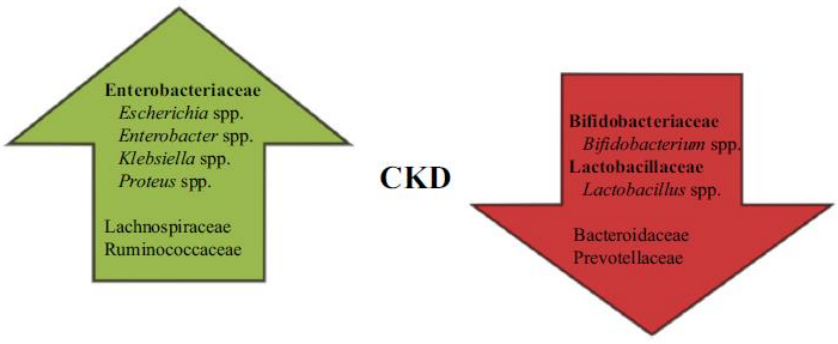


**Figure 8.** Bacterial family or genera associated to CKD. CKD is associated with higher levels of families described in the upward green arrow and with lower levels of the families described in the downward red arrow. Adapted from [6].

*E. coli* is a very common bacteria in the GIT and part of the normal microbiome. However, some *E. coli* strains are able to produce toxins that could produce serious consequences. *E. coli* has been shown to metabolize tryptophan resulting in the production of indole. Indole is subsequently absorbed and metabolized to IS, a uremic toxin, in the liver [117]. *E. coli* has a small size, approximately 1 µm in diameter and 3 µm in length [118], and shown to adhere to M cells and some strains shown to be specifically transported by these cells [66-68].

Thus, the disruption of the normal intestinal microbiome leads to intestinal dysbiosis, intestinal barrier dysfunction and bacterial translocation [119]. Uremia can increase the paracellular pathway and adversely affect barrier permeability, which leads to an ineffective nutrient absorption and a failure to prevent the translocation of luminal bacteria and their products [120-123]. In CKD, the impairment of the intestinal barrier function, caused by gut dysbiosis, may allow the translocation of intestinal microorganisms, endotoxin, antigens and other microbial products from intestinal lumen to systemic circulation, contributing to the pathogenesis of systemic inflammation, cardiovascular risk and progress of CKD (figure 9) [6].

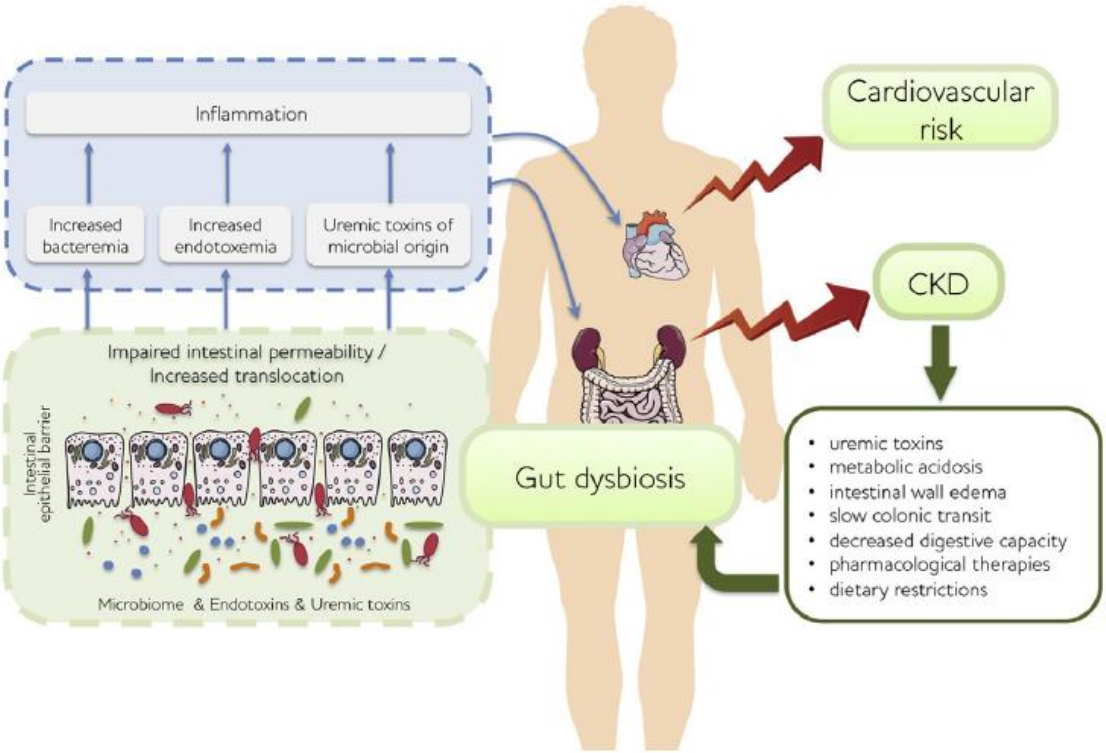


**Figure 9.** Summary of the mechanisms underlying to CKD. Adapted from [6].

## 1.3 Therapeutic approaches in chronic kidney disease

Uremic toxins may contribute to inflammation and cardiovascular risk in CKD patients. Thus, these toxins as well as the intestinal epithelial barrier could be considered important targets for treatment of these patients [24]. Restoring the integrity of the IECs and TJs proteins can reduce epithelial permeability preventing uremic toxins from entering the circulatory system [44]. The intestinal microbiome can be used as a biomarker for screening individuals with susceptibility to develop CKD [109]. Modifying the intestinal microbiome, to revert intestinal dysbiosis, may have also the potential to treatment CKD [44]. Previous studies have shown that probiotics have a therapeutic effect in maintaining the intestinal microbiome population [124]. This in turn can preventing pathogens and endotoxins from passing through the mucosa [125, 126].

Thus, therapeutic strategies in CKD can include administration of oral adsorbents to limit absorption of the toxins of microbial origin, prebiotics, probiotics, synbiotics [6], intestinal microbiome transplantation [127], phage therapy or even antibiotics [128]. The reduction of the generation of uremic toxins is crucial for the improvement of dialysis efficacy and the reversal of intestinal disfunction and dysbiosis can be target strategies to reduce complications of CKD, mainly inflammation and CVD, in CKD patients.

## 1.4 *In vitro* intestinal models

The study of absorption and translocation mechanisms can be performed using *in vitro* intestinal models. Inserts are used to facilitate the access to apical and basolateral sides creating this way two compartments, apical and basolateral, mimicking the intestinal lumen and connective tissue underlying, respectively [52]. Monocultures of Caco-2 cells and co-cultures of Caco-2/HT29-MTX/Raji B cells are examples of *in vitro* intestinal models. The use of Caco-2 and HT29-MTX cells reproducibly display several properties characteristic of differentiated intestinal cells [129].

These cell lines are out of the *in vivo* physiological environment and, therefore, the extrapolation of the data to the *in vivo* situation may be difficult and, so, the limitations of cell models must not be overlooked. Despite that, they offer the advantage of relative simplicity [52], allowing performing translocation studies [129].

### 1.4.1 Caco-2 monoculture model

Caco-2 monoculture is the most common cellular model used to perform studies of passage and transport of compounds. Caco-2 cells are derived from human colorectal adenocarcinoma and, despite their colonic origin, they are able to express in culture most of the morphological and functional characteristics of small intestinal absorptive cells, the enterocytes. They differentiate spontaneously into polarized intestinal cells possessing an apical brush border and TJs between adjacent cells, and they express hydrolases and typical microvillar transporters. Main features of Caco-2 cells are described on table 2. When grown on a semi-permeable membrane, Caco-2 cells form a differentiated and polarized monolayer after 21 days in culture [52] (figure 10).

**Table 2.** Characteristics of Caco-2 cells. Adapted from [52].

| | |
|---|---|
| Origin | Human colorectal adenocarcinoma |
| Growth in culture | Monolayer epithelial cells |
| Differentiation | 14–21 days after confluence in standard culture medium |
| Morphology | Polarised cells, with tight junctions, apical brush border |
| Electrical parameters | High electrical resistance |
| Digestive enzymes | Typical membranous peptidases and disaccharidases of the small intestine |
| Active transport | Amino acids, sugars, vitamins, hormones . . . |
| Membrane ionic transport | $Na^+/K^+$ ATPase, $H^+/K^+$ ATPase, $Na^+/H^+$ exchange, $Na^+/K^+/Cl^-$ co-transport, apical $Cl^-$ channels |
| Membrane non-ionic transporters | Permeability-glycoprotein, multidrug resistant associated protein, lung cancer associated resistance protein |
| Receptors | Vitamin $B_{12}$, vitamin $D_3$, epidermal growth factor, sugar transporters (GLUT1, GLUT3, GLUT5, GLUT2, SGLT1) |

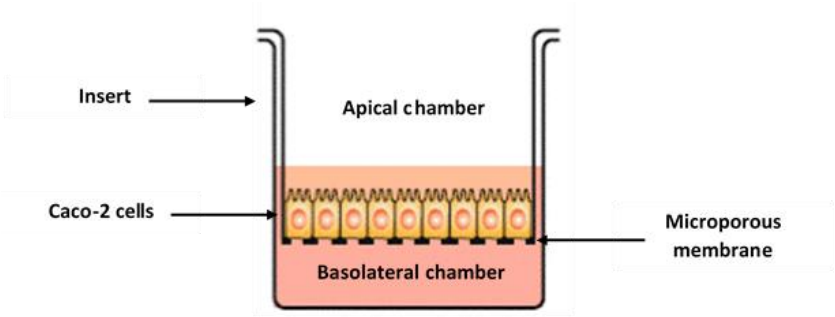


**Figure 10.** Schematic representation of Caco-2 monoculture on a microporous membrane. Image constructed on Microsoft Word.

The Caco-2 monoculture model offers several advantages to perform transport and translocation studies in intestinal epithelial barrier:

- It is comprised of human cells [52];
- It does not require the isolation of primary cells or the use of animals [62];
- Caco-2 cells behave in a similar way to the enterocytes, both functionally and structurally, resembling normal intestinal epithelium [130];
- Can be used for transport studies [52];
- Caco-2 cell line has been the most used and accepted *in vitro* cell model to study the intestinal permeability [63];
- It is a good and flexible model that mimic the physiological situation [52];
- Relatively fast and simple method [52].

However, despite of several advantages, Caco-2 monoculture has its own limitations:

- Is a static model [52];
- Cells have a tumoral origin [52];
- The model is comprised of only one cell type [52], not mimicking the complex interactions with other cells existing in human intestinal epithelium [131, 132];
- Caco-2 cells form TJs that resemble the tightness of the colon, in contrast to the looser junctions present in the small intestine [133, 134];
- Carrier-mediated compounds have lower permeability in the Caco-2 monolayers as compared to the human small intestine [133];
- Physiological factors that influence the passage are not present (mucus, bile salts, cholesterol) [52].

### 1.4.2 Caco-2/HT29-MTX/Raji B triple model

Some alternative cell cultures to mimic the human intestinal epithelium, as closely as possible, have been developed to achieve more physiological resemblance, such as the Caco-2/HT29-MTX/Raji B triple model. The triple co-culture of Caco-2/HT29-MTX/Raji B cells is an useful model to predict intestinal permeability [135].

A triple co-culture comprising Caco-2, HT29-MTX and Raji B cells mimics in a closer way the human intestinal epithelium, presenting the main cellular components in the process of absorption, namely the absorptive cells that resemble enterocytes (Caco-2), mucus-producing cells (HT29-MTX) and cells able to induce M cells phenotype in Caco-2 cells (Raji B). All the three cell lines maintain their function when cultured together [63].

The *in vitro* triple model is performed in three main steps. First, Caco-2 and HT29-MTX cells are seeded at the apical side of the inserts. The seeding ratio Caco-2:HT29-MTX of 90:10 showed to be the best to achieve physiological proportions after cells maturation and differentiation in culture [63]. Second, Raji B cells are seeded at the basolateral side of the inserts. Third, the conversion of Caco-2 cells into M cells is performed by mediators produced by Raji B cells (figure 11). The model is obtained after 21 days to fully differentiation [63] and transport experiments across the differentiated model can be carried out [62]. Thus, the triple co-culture model is a good and reliable alternative to the *in vitro* methods already existents for the study of intestinal permeability [63].

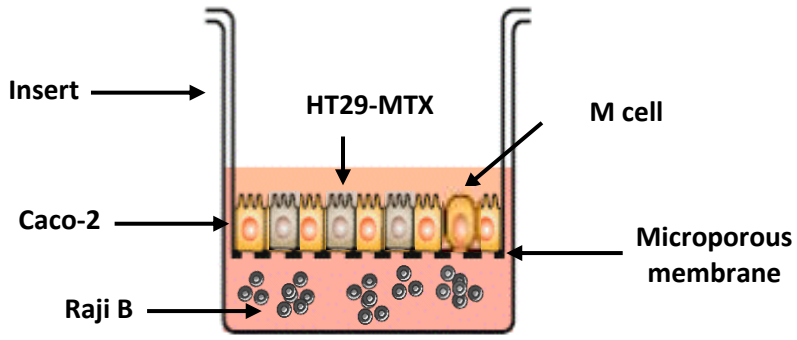


**Figure 11.** Schematic representation of Caco-2/HT29-MTX/Raji B triple model on a microporous membrane. Image constructed on Microsoft Word.

**HT29-MTX**

HT29-MTX cells, originated from human colorectal adenocarcinoma, are mucus-producing cells resemble the intestinal goblet cells [136]. HT29-MTX cell line grows in a polarized monolayer with a discrete apical brush border and microvilli, smaller than those observed in Caco-2 cells, but with similar cellular complexity [137]. HT29-MTX cells do not form TJs as tight as Caco-2 cells, so when these cells are cultured together with Caco-2 cells, they mimic the small intestine in a closer way [138, 139]. Moreover, the most important feature of these cells is the production of mucus all over the monolayer similarly what happens in the human intestinal mucosa [132, 137, 140].

Mucins are the major glycoprotein components of the mucous that coats the surfaces of cells lining the respiratory, digestive and urogenital tracts. They function to protect epithelial cells from infection, dehydration, physical or chemical injury and act as a barrier to compound absorption [141]. Mucin secretion by HT29-MTX cells is of importance because the mucus layer has been suggested to play a role in adhesion of live organisms to the epithelial surface as well as bacterial components such as LPS [142]. The intestinal mucus offers numerous ecological advantages for both resident microbiome and some pathogenic bacteria present within the lumen and intestinal epithelium. It can provide nutrients for bacterial growth, thus promoting intestinal colonization by the bacteria which have the ability to survive and multiply in the outer regions of the mucus layer [143].

**Raji B**

Raji B cells are lymphoblastoid cells, derived from human Burkitt's lymphoma, that induce M cells phenotype in Caco-2 cells [136]. The induction of M cells phenotype in Caco-2 cells is possible due to the action of mediators produced by Raji B lymphocytes [63]. These mediators are still not identified [67]. For the M cells phenotype acquisition, reorganization of cytoskeleton in Caco-2 cells occurs, losing the apical brush border and the microvilli and lacking the expression of enzymes like alkaline phosphatase [144]. The conversion of Caco-2 cells into M cells is related to the increase of bacterial adherence and translocation [62].

It was demonstrated that some pathogens are capable of efficient translocation through M cells, *in vitro* [65].

The triple model offers several advantages when performing transport and translocation studies in intestinal epithelial barrier:

- Comprises human cells [52];
- It is based on co-culture with well-established differentiated human cell lines [62];
- It does not require the isolation of primary cells or the use of animals [62];
- It is a reproducible model [62];
- Triple co-culture is a more complex model than Caco-2 monocultures and more suitable because is more physiological relevant [135].

However, despite of several advantages, triple model has some limitations, namely:

- Cells have a tumoral origin [52];
- As for other *in vitro* culturing systems the data should be interpreted with care as they do not represent the complexity found in the *in vivo* situation [145].

### 1.4.3 Assessment of intestinal models integrity

To evaluate the integrity of intestinal models in uremic conditions present in CKD, several methodologies can be performed. In the present work were used the transepithelial electrical resistance (TEER) evaluation, permeability assays using fluorescein isothiocyanate-dextran (FITC-dextran) and localization and quantification of TJs proteins.

#### 1.4.3.1 Transepithelial electrical resistance

Transepithelial/transendothelial electrical resistance (TEER) is a measurement of electrical resistance across a cellular monolayer and is a very sensitive and reliable method to confirm the integrity and permeability of the monolayer [146]. TEER is a quantitative technique, based on ohmic resistance, measured with a voltohmmeter (figure 12), to evaluate the integrity of TJs dynamics in cell culture models of endothelial and epithelial

monolayers. TEER reflects the ionic conductance of the paracellular pathway in the epithelial monolayer [147]. Thus, TEER is an instantaneous measurement for the degree of tightness, paracellular flux and capacity of transport in intestinal epithelial barrier [78].

The most acceptable TEER values for permeability experiments have a large range, between 150 and 1600 $\Omega.cm^2$ [138, 148, 149]. As it is expected, TEER values increase along time in culture, being higher in Caco-2 monocultures and lower in triple co-cultures [63]. This can be explained by the fact that TJs are very tight between enterocytes in Caco-2 monocultures [133]. In the triple model, the presence of HT29-MTX cells, which do not possess such TJs, make the TEER of the monolayer decrease [133, 140, 150, 151].

The advantages and wide use of the TEER method is because it is non-invasive and can be applied to monitor live cells during their various stages of growth and differentiation, and the measurements can be performed in real-time without cell damage [146]. Factors that can affect TEER measurements are temperature, cell passage number, cell culture medium composition and cell culture period [146].

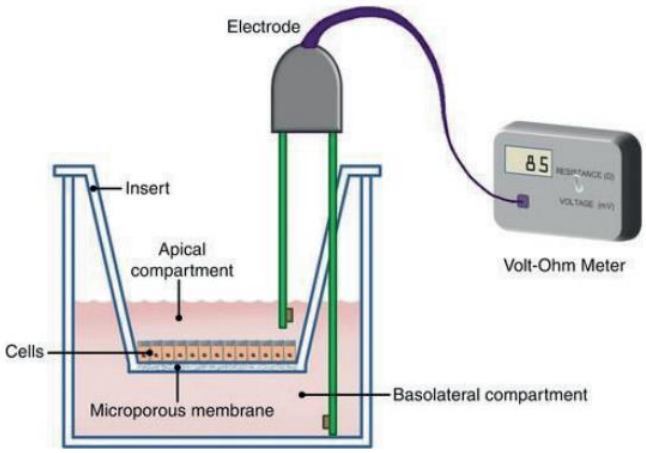


**Figure 12.** TEER measurement with a voltohmmeter. Adapted from [152]. The total resistance includes the ohmic resistance of the cell layer $R_{TEER}$, the cell culture medium $R_M$, the semipermeable membrane insert $R_I$ and the electrode medium interface $R_{EMI}$ [146].

### 1.4.3.2 Permeability assays using FITC-dextran

Permeability assays are performed to assess the integrity and permeability of *in vitro* intestinal models. FITC-dextran is one of the most used markers in paracellular permeability assays and transport studies in cells and tissues. FITC-dextran permeability assay is just relative to compounds that pass paracellularly. FITC-dextran is a polysaccharide available in MWs ranging from 4 – 70 kDa and can be used to determine solute, ion and protein permeability. The measurement with FITC-dextran 4 kDa is a useful method for studying intestinal permeability [153]. A benefit of FITC-dextran is that low concentrations of fluorescein can be measured due to the high sensitivity of fluorescence detection [154]. The excitation maximum of FITC-dextran is 490 nm. The emission maximum is 520 nm [155]. Measurements of the fluorescence provide quantitative data of the permeability of tissues and cells [156]. Passage of marker FITC-dextran is an indicator of the integrity of the TJs and of the intestinal epithelial barrier [147] (figure 13).

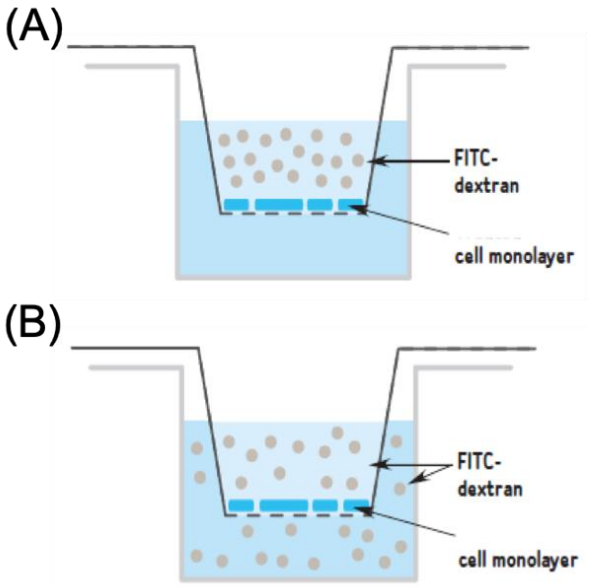


**Figure 13.** Permeability assay test principle. **(A)** FITC-dextran is added to the semi-permeable insert coated with a cell monolayer. **(B)** FITC-dextran permeates the cell monolayer into the plate well. The resulting fluorescence in the plate well is measured and used as an indicator of the extent of monolayer permeability. Adapted from [157].

### 1.4.3.3 Immunocytochemistry of tight junctions

Immunocytochemistry (ICC) is a highly reproductive method in biomedical research used to identify proteins and other macromolecules in tissues and cells [158], such as TJs. Identification and quantification of TJs is important to understand the level of tightness between adjacent cells and, therefore, the localization and quantification of TJs were performed in this work through of ICC.

ICC refers to immunostaining of cultured cell lines or primary cells. ICC offers a semi-quantitative means of analyzing the relative abundance, conformation and localization of target antigens. In ICC assays, the cellular antigens are visualized using either fluorochrome-conjugated primary antibodies (direct detection) or a two-step method (indirect detection) involving an unlabeled primary antibody followed by a fluorochrome-conjugated secondary antibody. By combining different fluorochrome-labeled antibodies, ICC can detect several antigens in the same sample. The general protocol of ICC includes sample preparation, immunostaining and image analysis (figure 14) [159].

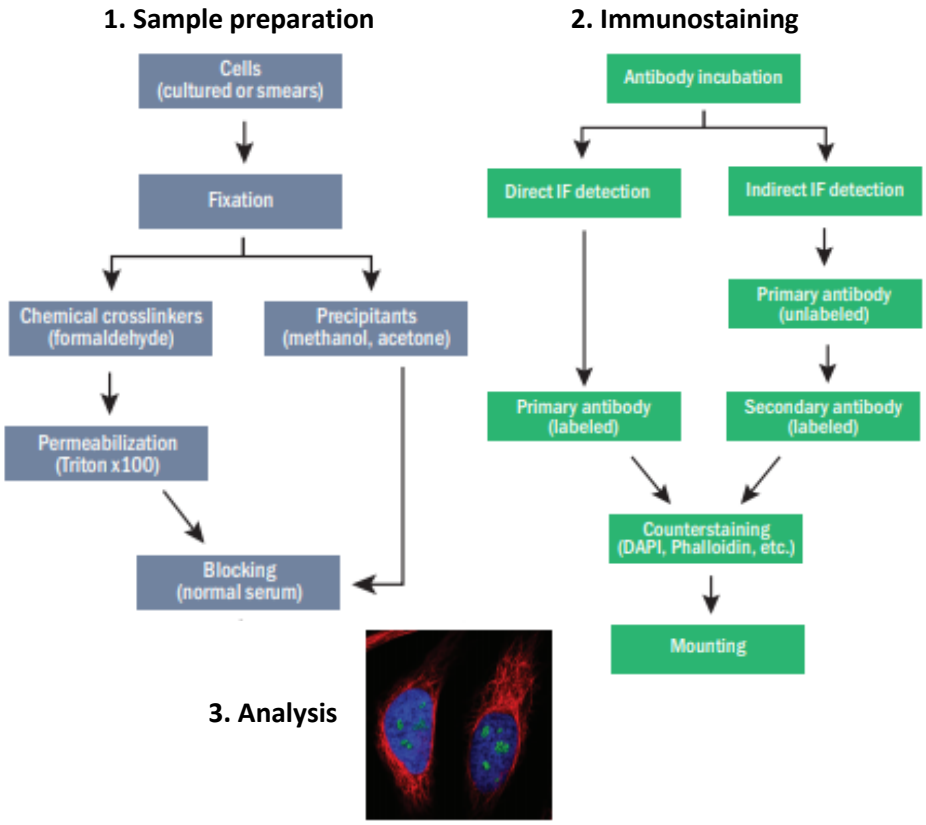


**Figure 14.** General protocol steps in an ICC assay. Adapted from [159].

### 1.4.4 Microbial translocation studies

Once this study pretends evaluate the microbial translocation in intestinal epithelial barrier in uremic conditions present in CKD, after assessment the integrity of intestinal models through the methodologies mentioned above, microbial translocation assays were performed. Microbial translocation studies can be performed through the *in vitro* intestinal models [62] and they are based on three main steps:

1) Bacteria are added to the apical compartment at an adequate multiplicity of infection (MOI). MOI represents the number of bacteria per epithelial cell. For example, a MOI of 100 represent 100 bacteria per epithelial cell. Therefore, taking in account the number of epithelial cells that comprising the intestinal model and the MOI, is possible calculate the number of bacteria to place in the apical compartment.
2) Bacteria translocate through the intestinal model into the basolateral compartment.
3) Bacteria that translocate to the basolateral compartment are quantified. Different methods may be applied, but one of the most used to quantify viable bacteria is the pour plate method [160].

In this study, the assessment of the integrity of intestinal epithelial barrier through the TEER measurement, FITC-dextran assays and ICC of TJs proteins, and the assessment of microbial translocation through microbial translocation assays were methodologies performed in the *in vitro* intestinal models. The intestinal models and methodologies described were implement in this study to evaluate the effect of uremic conditions present in CKD on integrity, permeability, localization and quantification of TJs proteins and on microbial translocation in intestinal epithelial barrier.

# AIMS

# 2 AIMS

Our main goal was to evaluate the application of two *in vitro* models of intestinal epithelial barrier for the study of microbial translocation and to evaluate the impact of different uremic conditions present in CKD on this microbial translocation. For that we analyzed the effect of plasma of CKD patients and the uremic toxin urea on microbial translocation through intestinal epithelium as well as on integrity, permeability and localization and quantity of TJs in the *in vitro* intestinal models, Caco-2 monoculture and Caco-2/HT29-MTX/Raji B triple model.

# MATERIALS AND METHODS

# 3 MATERIALS AND METHODS

## 3.1 *In vitro* intestinal models

### 3.1.1 Cell culture

Human colorectal adenocarcinoma Caco-2 clone C2BBe1 (passage 59–74) and human Burkitt's lymphoma Raji B (passage 18–30) cell lines were obtained from the American Type Culture Collection™ (ATCC, USA). Human colorectal adenocarcinoma HT29-MTX (passage 41–58) cell line was kindly provided by Dr. T. Lesuffleur (INSERM U 178, Villejuif, France). Cells have grown separately in tissue culture flasks (SPL Life Sciences, Korea) in a complete medium, consisting of Dulbecco's Modified Eagle Medium (DMEM) with 4.5 g/L glucose and ultraglutamine (BioWhittaker™, Lonza, Swiss), supplemented with 10% (v/v) of inactivated fetal bovine serum (FBS) (Biochrom, UK), 1% (v/v) of non-essential amino acids (NEAA) (Gibco™, Thermo Fisher Scientific, USA) and 1% (v/v) of penicillin/streptomycin (P/S) (Biowest, France) mixture. Cells were maintained in an incubator (Esco CelCulture™ $CO_2$ Incubators, UK) at 37°C temperature and 5% $CO_2$ in a water saturated atmosphere.

### 3.1.2 Optic microscopy

Growth and morphology of Caco-2, HT29-MTX and Raji B cells were monitored by optic microscopy (Olympus, America), over time of culture.

### 3.1.3 Cell viability

Cell viability was assessed through trypan blue exclusion test. Trypan blue (Sigma-Aldrich, USA) staining is a widely used method to identify dead cells. Only cells with intact membranes can effectively exclude the dye, so dead cells with compromised membranes become stained [161]. More than 95% of cells were viable to all cell lines used.

## 3.1.4 *In vitro* intestinal models

### 3.1.4.1 Caco-2 monoculture model

Monocultures of Caco-2 cells were grown in polyethylene terephthalate (PET) inserts with pore size of 1 µm, pore density of $2\times10^6$ pores/cm$^2$ and area of 1.1 cm$^2$ (Millicell$^{TM}$ Hanging Cell Culture Inserts, USA) in 12-well plates (VWR$^{TM}$, USA). Caco-2 cells were seeded on the apical chamber of inserts (figure 10), to a final density of $1\times10^5$ cells/cm$^2$. Cells were allowed to grow in an incubator at 37°C temperature and 5% $CO_2$ in a water saturated atmosphere, for 21 days until maturation, with medium renewal every two-three days, based on previous experiments [63, 162].

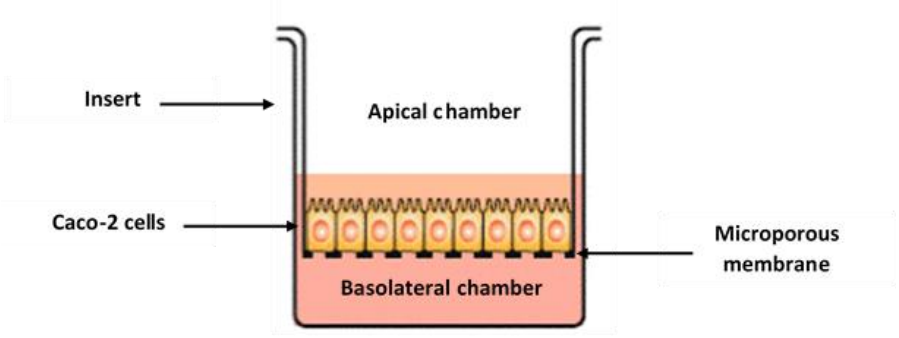


**Figure 10.** Schematic representation of Caco-2 cells on a microporous membrane. Image constructed on Microsoft Word.

### 3.1.4.2 Caco-2/HT29-MTX/Raji B triple model

Co-cultures of Caco-2/HT29MTX/Raji B were grown in PET inserts with pore size of 1 µm, pore density of $2\times10^6$ pores/cm$^2$ and area of 1.1 cm$^2$ in 12-well plates. Caco-2 and HT29-MTX cells were seeded on the apical chamber of inserts (figure 11), to a final density of $1\times10^5$ cells/cm$^2$, in a ratio of 90:10 (Caco-2:HT29-MTX), according to previous studies [63]. Cells were allowed to grow in an incubator at 37°C temperature and 5% $CO_2$ in a water saturated atmosphere, for 21 days until maturation with medium renewal every two-three days, based on previous experiments [63, 162]. Raji B cells were seeded on basolateral chamber of inserts (figure 11) on the 14$^{th}$ day of differentiation of model, to a final density equal to Caco-2 cells in each insert, to allow Caco-2 cells differentiation to M cells. After

Raji B cells seeding on basolateral chamber, the medium was changed daily only on the apical side to avoid the removal of Raji B cells from the basolateral side since these are non-adherent cells.

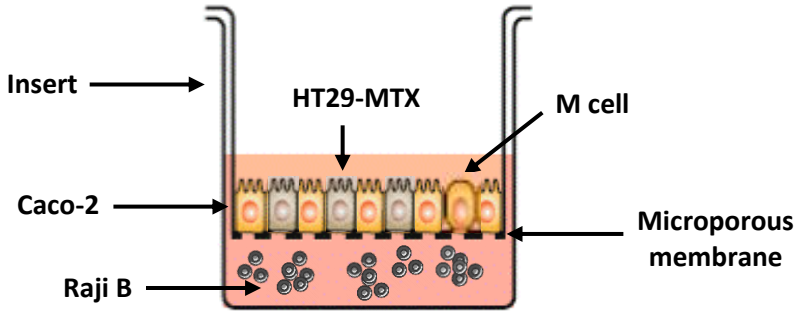


**Figure 11.** Schematic representation of Caco-2/HT29-MTX/Raji B triple model on a microporous membrane. Image constructed on Microsoft Word.

### 3.1.5 Measurement of transepithelial electrical resistance

The integrity of the intestinal barrier was assessed through TEER measurements over the 21 days of differentiation. TEER of intestinal models were measured before each medium exchange to monitor the evolution of confluence and integrity of models, using an Epithelial Voltohmmeter (EVOM, World Precision Instruments, USA) equipped with chopstick electrodes (see figure 12 section 1.4.3.1). TEER was measured on two different sites of insert and values were converted to Ohms.cm$^2$.

### 3.1.6 Cell count of mature intestinal models

Both cell models were detached from PET membrane of the inserts with trypsin-EDTA (ethylenediaminetetraacetic acid) (Sigma-Aldrich/VWR, USA) on the 22$^{nd}$ day (one day after maturation) and counted using a hemocytometer (Neubauer chamber) (Marienfeld, Germany) according to the following equation:

$$\text{Number of cells per mL} = \frac{\text{Number of cells counted}}{\text{Number of quadrants counted}} \times \text{diluition factor} \times 10^4$$

## 3.2 Exposure to uremic conditions

The effect of uremic conditions on integrity, permeability, localization and quantity of TJs proteins and microbial translocation in epithelial barrier of intestinal models was evaluated. The uremic conditions tested were plasma of CKD patients and uremic toxin urea. DSS was tested in intestinal models as a positive control, once it was described as a compound that leads to disruption of TJs leading to intestinal epithelium dysfunction [96].

### 3.2.1 Plasma of chronic kidney disease patients

Four adult CKD patients undergoing PD (thus, ESKD) and without diabetes mellitus followed up in the Nephrology Department of "Centro Hospitalar Universitário S. João", were asked to collect blood under fasting conditions in the heparinized tubes by trained nurses. Afterwards, the blood was centrifuged at 5000 rpm for 15 min and the supernatant was collected (plasma). The study protocol was approved by the local Ethics Committee and is in accordance with the 1964 Helsinki declaration and its later amendments; all recruited patients were asked to give their free written informed consent. Also, the blood of two healthy controls was collected for the same purpose. Samples were stored at -80°C until used. The healthy controls and CKD plasma samples were used on *in vitro* intestinal models, in order to understand the effect of both plasmas on the integrity of intestinal barrier and on microbial translocation.

Cells of intestinal models (Caco-2 monoculture and Caco-2/HT9-MTX/Raji B triple co-culture) were incubated with healthy and CKD plasma. Plasma of healthy individuals and CKD patients were added on the basolateral compartment (mimicking the bloodstream) of the inserts at 10% (v/v) in DMEM for 24 h, according to [47]. TEER was monitored from time 0 to 24h, to evaluate the effect of healthy and CKD plasma on the integrity of intestinal barrier.

### 3.2.2 Urea

Urea (Sigma-Aldrich, USA) at concentrations 20 mg/dL and 150 mg/dL with and without urease (Sigma-Aldrich, USA) at concentration 0.63 mg/mL were added to the intestinal models (Caco-2 monoculture and Caco-2/HT9-MTX/Raji B triple co-culture). The urea

solutions were prepared in DMEM. Samples were added to the apical compartment of the insert (mimicking the intestinal lumen, where uremic toxins like urea are converted to ammonia by microbial urease) for 24 h. Afterwards, the effect of normal (20 mg/dL) and uremic (150 mg/dL) concentrations of urea in the presence or not of urease was evaluated. The effect of urease in intestinal barrier was also tested, serving as a toxicity control. TEER was monitored from time 0 to 24h, to evaluate the effect of different conditions on the integrity of intestinal barrier.

### 3.2.3 Dextran sodium sulfate

Cells of intestinal models (Caco-2 monoculture and Caco-2/HT9-MTX/Raji B) were incubated with 2% DSS (pK Chemicals, Denmark) in DMEM on the apical compartment of the insert for 3h, according to [96]. The addition of DSS served as positive control since, according to previous studies [97], DSS is associated with disruption of TJs. TEER was measured after incubation, to evaluate the effect of DSS on integrity of intestinal barrier.

## 3.3 Assessment of the effect of uremic conditions on transepithelial electrical resistance

The integrity of intestinal barrier was assessed through TEER measurements after exposure to uremic conditions. TEER was monitored from time 0 to 24h, to evaluate the effect of plasma of CKD patients, urea and DSS on the integrity of intestinal barrier. TEER was measured on two different sites of insert and values were converted to Ohms.cm$^2$.

## 3.4 Assessment of the effect of uremic conditions on permeability

Permeability studies were performed using 4 kDa FITC-dextran (Sigma-Aldrich, Portugal) as a marker of paracellular pathway [163].

To perform the assay, a solution of FITC-dextran was prepared in Hank's Balanced Salt Solution (HBSS) (Gibco$^{TM}$, Thermo Fisher Scientific, USA) at a concentration of 200 or

1000 µg/mL. Then, TEER of mature intestinal models was measured, the culture medium was removed from the compartments of the inserts and cells were washed twice with pre-warmed phosphate-buffered saline 1× (PBS 1×). PBS 1× was then replaced by HBSS. HBSS was allowed to equilibrate for 30 min at 37°C with agitation at 100 rpm in an orbital shaker oven (Ika™, Germany). After 30 min, HBSS was removed from the apical side and the sample of FITC-dextran diluted in HBSS (200 or 1000 µL/mL) was added. TEER was measured in the instant after adding the sample (t = 0 min). The plate was placed at 37°C with agitation at 100 rpm. At pre-determined time-points (15, 30, 45, 60, 90, 120, 180 and 240 min), TEER was measured and a sample of 200 µL was taken from the basolateral side and placed on black 96-well plate (Greiner Bio-One, Austria) and respective fluorescence was readen by fluorescence spectrophotometry through of Synergy™ MX microplate reader (Biotek Instruments™, USA), at an excitation wavelength of 490 nm and an emission wavelength of 520 nm. 200 µL of new HBSS was replaced to the basolateral side and the plate was placed again on the stove at 37°C with agitation at 100 rpm. At the end of the experiment, 200 µL were removed from the apical compartment to analyze the quantity of FITC-dextran that remained on the apical side. The values of concentration of FITC-dextran were calculated from a standard curve obtained with known concentrations. The permeability results were expressed in percentage of permeability (% of FITC-dextran that passed to the basolateral side).

## 3.5 Assessment of the effect of uremic conditions on tight junctions

### 3.5.1 Immunocytochemistry

ICC was performed to evaluate membrane integrity and detection of TJs. ICC encompassed fixing, permeabilization, blocking, staining and mounting, described in detail hereafter.

The medium was removed from inserts and cells were washed with PBS 1×. Cells were fixed using paraformaldehyde (PFA) (Electron Microscopy Sciences, UK) at 2% during 30

min at room temperature (RT) and after, cells were washed three times for 5 min with 0.05% (v/v) Tween™ 20 (Sigma-Aldrich, USA) in PBS (PBS-T). The membranes of inserts were detached and placed on 24-well plate wells (Falcon™, USA). Cells were permeabilized with 0.05% (v/v) Triton™ X-100 (Sigma-Aldrich, USA) in PBS for 10 min. Then, cells were washed three times for 5 min with PBS-T. In order to prevent non-specific binding, cells were incubated with blocking solution, PBS-T with 1.5% bovine serum albumin (BSA) (VWR™, USA) and 5% FBS, for 1h. Primary antibodies to TJs were diluted on blocking solution at the following dilutions: rabbit anti-OCLN (Thermo Fisher Scientific, USA) 1:250, rabbit anti-CLDN1 (Thermo Fisher Scientific, USA) 1:200, mouse anti-CLDN2 (Thermo Fisher Scientific, USA) 1:50 and rat anti-ZO1 coupled to Alexa Fluor 488 (Santa Cruz Biotechnology™, USA) 1:50. Primary antibodies were incubated overnight on a humidified chamber at 4°C. Then, cells were washed three times for 5 min with PBS-T. Secondary antibodies, goat anti-rabbit Alexa Fluor 488 (Invitrogen™, USA) to anti-OCLN primary antibody, donkey anti-rabbit Alexa Fluor 594 (Abcam™, UK) to anti-CLDN1 and goat anti-mouse Alexa Fluor 594 (Invitrogen™, USA) to anti-CLDN2 were diluted on blocking solution at a dilution 1:500. Secondary antibodies were incubated during 1h. Then, cells were washed three times for 5 min with PBS-T. The solutions 4',6-diamidino-2-phenylindole (DAPI) (Sigma-Aldrich, USA) at concentration of 0.5 µL/mL, to stain nuclei, and CellMask™ deep red plasma membrane Cy5 647 (Molecular Probes™, USA), at concentration of 0.5 µL/mL, to stain plasma membrane, were incubated together during 15 min. After 15 min, cells were washed twice for 5 min with PBS-T and, then, once with PBS 1×. The membranes were mounted using fluorescence mounting medium (Dako, USA). Slides were stored at 4°C in a dark box until further use.

### 3.5.2 High-throughput widefield fluorescence microscopy image acquisition and analysis

The localization of TJs proteins was assessed in the different conditions by immunofluorescence using the equipment IN Cell Analyzer 2000 (GE Healthcare, USA). IN Cell Analyzer 2000 high-content analysis provides multiplexed, quantitative data based on automated cell imaging, allowing to answer complex questions rapidly, in a true biological

context [164]. Fluorescence images were obtained using a Nikon 20X/0.45 NA Plan Fluor objective, 2 × 2 binning and the 2.5D acquisition mode with a Z section of 5 µm to allow focusing in all planes. 25 fields were obtained per sample, enabling the acquisition of thousands of cells. Exposure times were maintained for all samples within experiments and for all experiments.

All images were further treated and processed using Ilastik software version 1.3.2 [165], CellProfiler software version 3.1.5 [166] and Image J/Fiji software [167].

### 3.5.3 Quantification of tight junctions

Nuclei and plasma membrane were identified using Ilastik [165], machine learning algorithms to easily segment, classify, track and count cells or other experimental data. The resulting segmented images were used to quantify fluorescence intensity on the TJs using the image analysis software CellProfiler [166]. Briefly, upon uneven illumination correction and plasma membrane segmentation, the mean fluorescence intensity of each TJ antibody (anti-OCLN, anti-ZO1, anti-CLDN1 and anti-CLDN2) was quantified (see supplementary figure 1). The results of quantification of TJs were represented as mean intensity of Alex Fluor 488, corresponding to OCLN and ZO1 TJs, and mean intensity of Alex Fluor 594, corresponding to CLDN1 and CLDN2 TJs.

## 3.6 Assessment of the effect of uremic conditions on microbial translocation

### 3.6.1 Identification of bacteria

Bacterial isolates from CKD patients were identified by matrix assisted laser desorption ionization-time of flight mass spectrometry (MALDI-TOF MS) (Bruker MALDI Biotyper$^{TM}$, USA). MALDI-TOF MS has emerged as a potential tool for microbial identification and diagnosis. During the MALDI-TOF MS process, microbes are identified using either intact cells or cell extracts [168]. A fecal isolate from a CKD patient stool was well identified by MALDI-TOF MS as *E.* coli (figure 15), with an identification score value higher than 2.0.

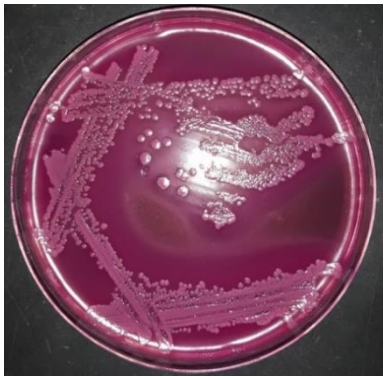

**Figure 15.** *E. coli* isolated from feces of a CKD patient, cultured in MacConkey Agar (Sigma-Aldrich, USA).

### 3.6.2 Bacterial translocation assay

*E. coli* isolated from feces of a CKD patient, identified by MALDI-TOF MS, was used in the present study (figure 15). Calibration curve for different optical density at 600 nm ($O.D_{600\ nm}$) of *E. coli* diluted in HBSS was obtained by quantifying the bacteria by the pour plate method counting the colony forming units (CFU) formed in Brain Heart Infusion (BHI) Agar (Biolab Zrt., Hungary) (figure 16).

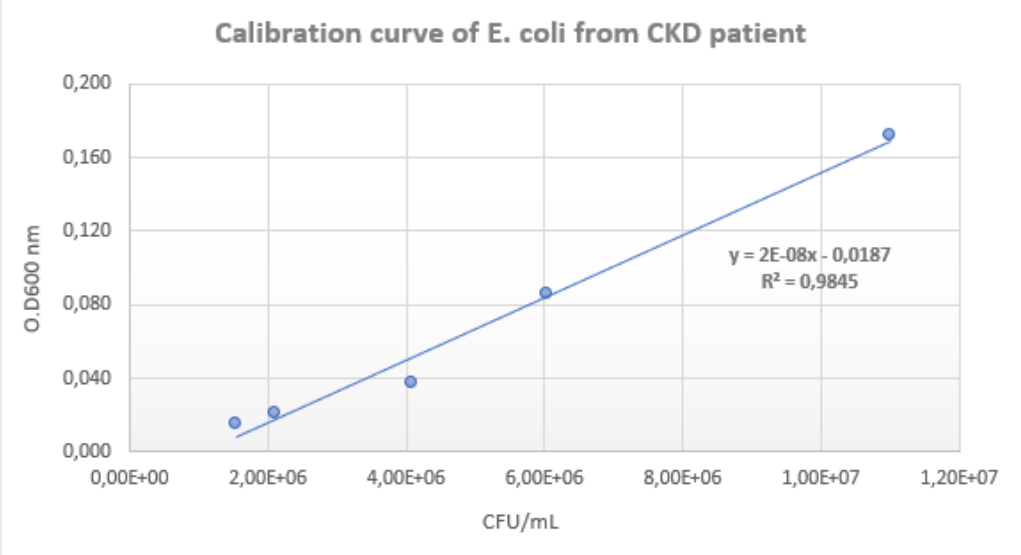


**Figure 16.** Calibration curve of *E. coli* from CKD patient.

Bacterial translocation assay was performed in both Caco-2 monoculture and Caco-2/HT29-MTX/Raji B triple model after exposure to uremic conditions. In sum, after

overnight incubation of *E. coli* in BHI Broth (Liofilchem™, Italy) at 37°C and 160 rpm, the *E. coli* suspension was centrifuged at 12 300 g during 3 min. Then, the supernatant was removed, the pellet was resuspended in HBSS (this last step was performed twice). For each translocation experiment, the MOI was adjusted to 5. The number of epithelial cells in each insert of Caco-2 monocultures and Caco-2/HT29-MTX/Raji B triple models was counted (table 3), as described in the section 3.1.6.

**Table 3.** Number of epithelial cells at 22nd day of maturation in both Caco-2 monoculture and triple model. Values are expressed in cells/$cm^2$ as mean ± SD of three replicates.

| **Intestinal models** | **Mean (cells/$cm^2$) ± SD** |
|---|---|
| Caco-2 monoculture | $3.8 \times 10^5 \pm 8.9 \times 10^4$ |
| Caco-2/HT29-MTX/Raji B | $3.7 \times 10^5 \pm 1.8 \times 10^5$ |

The number of CFU of *E. coli* to use was calculate as follows: number of CFU = MOI × number of epithelial cells in insert. This number of CFU was converted to a concentration value (CFU/mL) and, through of calibration curve of *E. coli* from CKD patient, the value of $O.D_{600\,nm}$ corresponding to the concentration value is calculated. Thus, it is possible to know the number of bacteria (CFU) to use on the apical compartment (mimicking the intestinal lumen) on bacterial translocation assay.

At each microbial translocation experiment the cell medium was replaced by HBSS, after washing twice the cells with pre-warmed PBS 1 ×. After 30 min of stabilization, at 37°C at 100 rpm, the HBSS of the apical chamber was replaced by HBSS with *E. coli* at MOI=5. At pre-determined time-points, a sample of 50 µL was taken out of the basolateral side and seeded on BHI Agar plates (in duplicated). All basolateral medium was removed at each time point and replaced by new HBSS. At the end, 20 µL were removed from the apical compartment and seeded on BHI Agar plates (in duplicated), to know the quantity of bacteria that remain on the apical side. Plates were incubated 24h at 37°C with 5% $CO_2$. The next day, CFU of all time-points and conditions were counted. The results of bacterial translocation were represented as $\log_{10}$(CFU) vs time.

## 3.7 Statistical analysis

All the results were represented as mean ± standard deviation (SD) or in percentage (%). Results were analyzed using ANOVA test for multiple comparisons followed by *t*-student test using GraphPad Prism™ software (version 8.0.2.263). Statistical significance was assumed when p values were less than 0.05. $p < 0.05$ was denoted as (*) and $p < 0.01$ as (**).

## 3.8 Scheme of methodology

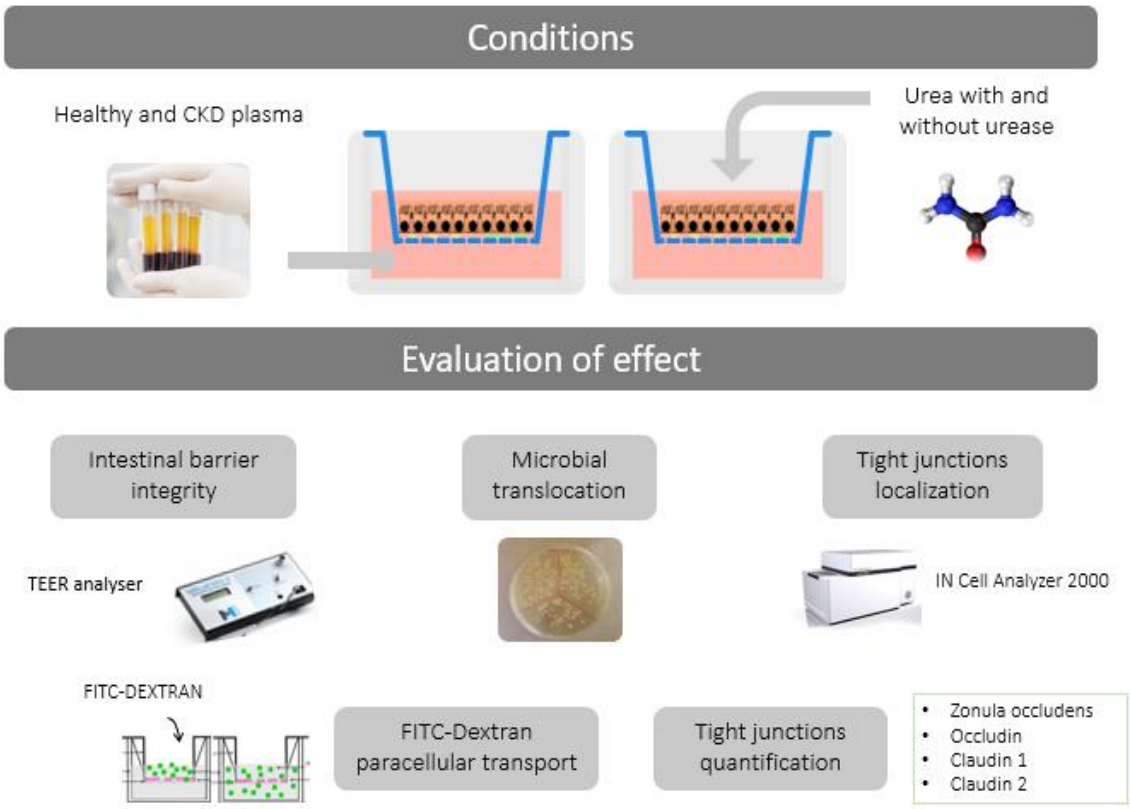


**Figure 17.** Schematic representation of the methodology. In sum, the effect of uremic conditions was evaluated in the intestinal barrier integrity, permeability (FITC-Dextran paracellular transport), localization and quantity of TJs proteins, and in the microbial translocation in intestinal epithelium of Caco-2 monoculture and triple model.

# RESULTS

# 4 RESULTS

## 4.1 Morphology of cell lines of intestinal models

Since this study aimed to evaluate the effect of uremic conditions on the integrity of intestinal epithelial barrier and microbial translocation, two intestinal models were implemented, Caco-2 monoculture and Caco-2/HT29-MTX/Raji B triple model. The optic microscopy shows the aspect of cell lines used to establish the two intestinal models (figure 18). In culture, Caco-2 and HT29-MTX epithelial cells grow in a cell monolayer. In Caco-2/HT29-MTX/Raji B triple model, Caco-2 and HT29-MTX cells establish intercellular contacts between them forming an intact cell barrier, growing attached to the insert membrane, in the apical side. Raji B cells have a lymphoblastoid morphology and grow like clumps in suspension in the basolateral side, and their function is to induce M cells phenotype in Caco-2 cells [136].

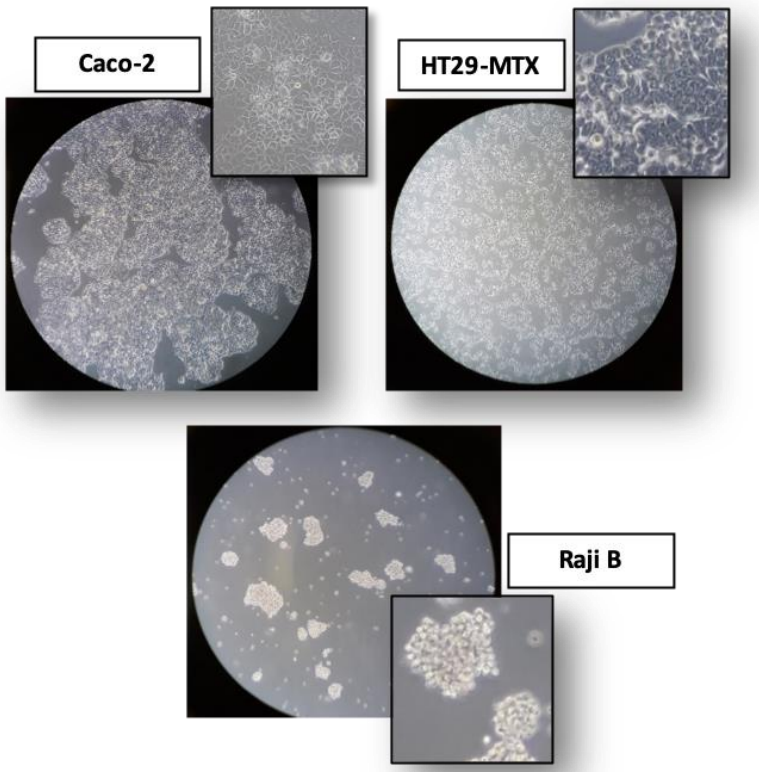


**Figure 18. Morphology of cell lines used in intestinal models.** Images were obtained by optic microscopy, at 400× magnification, and demonstrate epithelial cells growing in monolayer (Caco-2 and HT29-MTX) and lymphocytes B in suspension (Raji B).

## 4.2 Integrity of intestinal epithelial barrier

### 4.2.1 Transepithelial electrical resistance

To evaluate the integrity of the epithelial barrier of intestinal models, the TEER was monitored. Monocultures of Caco-2 and triple co-cultures of Caco-2/HT29MTX/Raji B have grown for 21 days until maturation, as described in section 3.1.4. The integrity of intestinal barrier was assessed through TEER throughout the differentiation process (figure 19). The results show that the TEER values of Caco-2 monoculture range from 1500 Ω.cm$^2$ to 3600 Ω.cm$^2$ and that TEER values of triple model range from 115 Ω.cm$^2$ to 390 Ω.cm$^2$ over 24 days. It is possible observe that TEER values of Caco-2 monoculture are higher than values in triple model, which is in accordance with the literature [63]. In triple model, the addition of Raji B cells to the model at 14$^{th}$ day leads to a decrease of TEER, as show the graph.

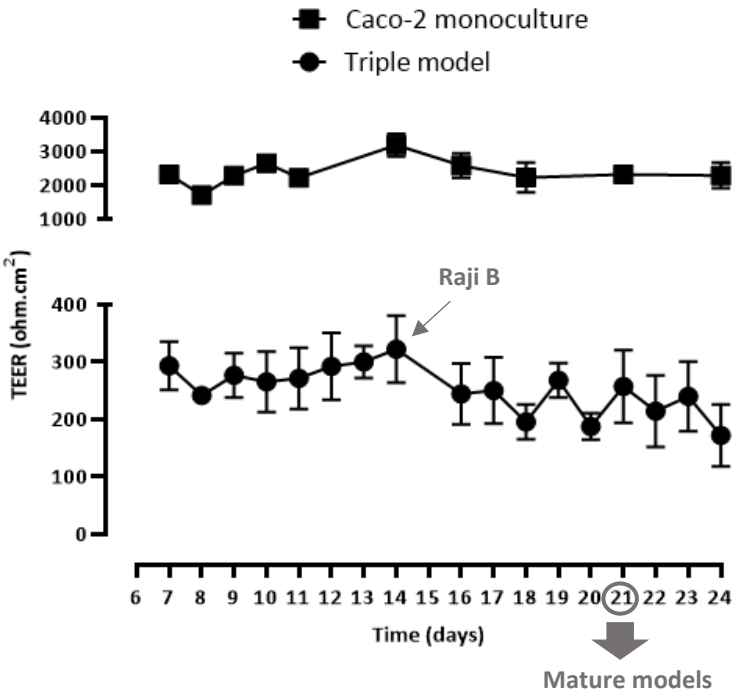


**Figure 19. TEER variation over 24 days on both Caco-2 monoculture and triple model.** TEER values are expressed in ohm.cm$^2$ as mean ± SD of eight independent Caco-2 monoculture models and fourteen independent triple culture models. The larger arrow represents the day of maturation (21$^{st}$ day). The smaller arrow represents the addition of Raji B cells at 14$^{th}$ day of differentiation of the triple model.

### 4.2.2 Paracellular permeability of intestinal epithelial barrier

Since transepithelial resistance is directly related with paracellular permeability and low TEER values may be related with higher paracellular permeability, this permeability was assessed on the triple model after maturation, to evaluate the integrity of the intestinal epithelial barrier.

Paracellular permeability of the intestinal epithelium was assessed through FITC-dextran permeability assay. Permeability assays were performed in three different days after maturation (21st, 23rd and 25th day) (figure 20), as described before in section 3.4. The results show that permeability increase from 21st to 25th day. In the end of the permeability assay (time 240 min), the percentage of permeability (% FITC-dextran that passed to the basolateral compartment) at 21st day was in mean 20%, at 23rd day was in mean 34% and at 25th day was in mean 50%. Thereby, the results show that the paracellular permeability of the intestinal triple model increased after the 21st day of maturation.

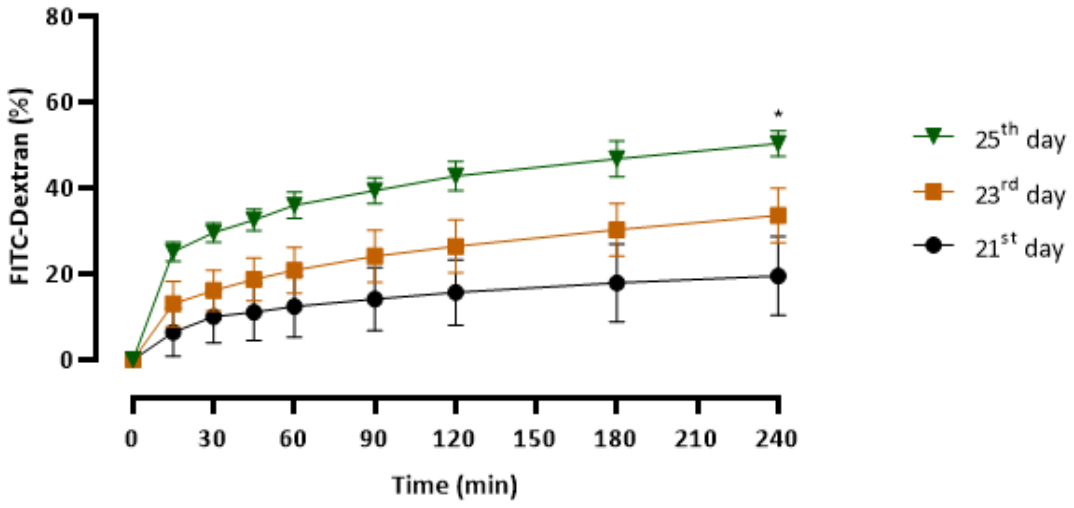


**Figure 20. Paracellular permeability increased from 21st to 25th days in triple model.** FITC-dextran permeability assay was performed at three different days after maturation (21st, 23rd and 25th day) with a concentration of 1000 µg/mL of FITC-dextran used on apical compartment of triple model. The graph shows the percentage of FITC-dextran that passed to the basolateral compartment in the three different days in eight time points. The results are expressed as mean ± SD of four replicates at 21st day, three replicates at 23rd day and four replicates at 25th day. Statistically significant differences are signed as (*) $p < 0.05$ compared with 21st day.

## 4.3 Microbial translocation in intestinal epithelial barrier

To understand the translocation of bacteria in both Caco-2 monoculture and triple model, *E. coli* translocation assays were performed to evaluate the ability of bacteria to cross the intestinal barrier. The MOI used in apical side was 5 and the quantification of CFU that passed to the basolateral side of models was performed 24h after incubation of plates. The results of bacterial translocation show that *E. coli* translocation in Caco-2 monoculture was higher than in triple model (figure 21).

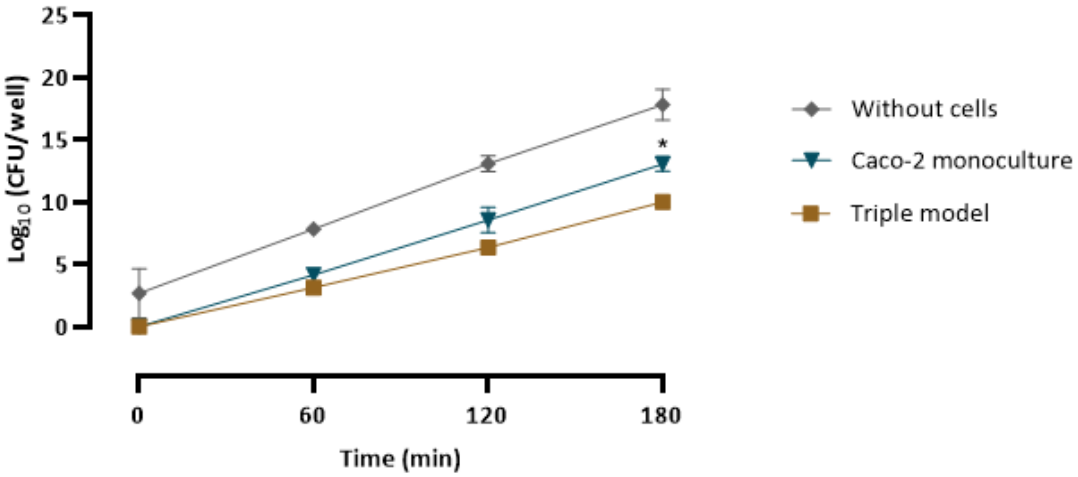


**Figure 21. *E. coli* translocation was higher in Caco-2 monoculture than in triple model.** Bacterial translocation assay was performed for 180 min, using MOI=5. The results are represented as $log_{10}$(CFU/well) vs time and are the mean ± SD of five independent experiments. Statistically significant differences are signed as (*) $p < 0.05$ compared with triple model.

## 4.4 Effect of uremic conditions on transepithelial electrical resistance

To evaluate the integrity of models after exposure to uremic conditions, the resistance of intestinal epithelial barrier was assessed. The TEER was assessed after exposure to plasma of CKD patients, urea (with or without urease) and DSS. The results are expressed in ohm.cm$^2$ and show the implication of uremic conditions on TEER in both Caco-2 monocultures and Caco-2/HT29-MTX/Raji B triple models.

### 4.4.1 Effect of plasma of chronic kidney disease patients

Healthy and CKD plasma were added at the basolateral compartment (mimicking the bloodstream) of Caco-2 monoculture and triple model during 24h, and the TEER was monitored during this period, to evaluate the effect of healthy and CKD plasma on intestinal barrier integrity. The results in Caco-2 monoculture show that healthy plasma did not induce significant alterations on TEER and that CKD plasma decreased the TEER, 24h after exposure (figure 22A). The results in triple model show that healthy and CKD plasma did not induce significant alterations on TEER, 24h after exposure (figure 22B).

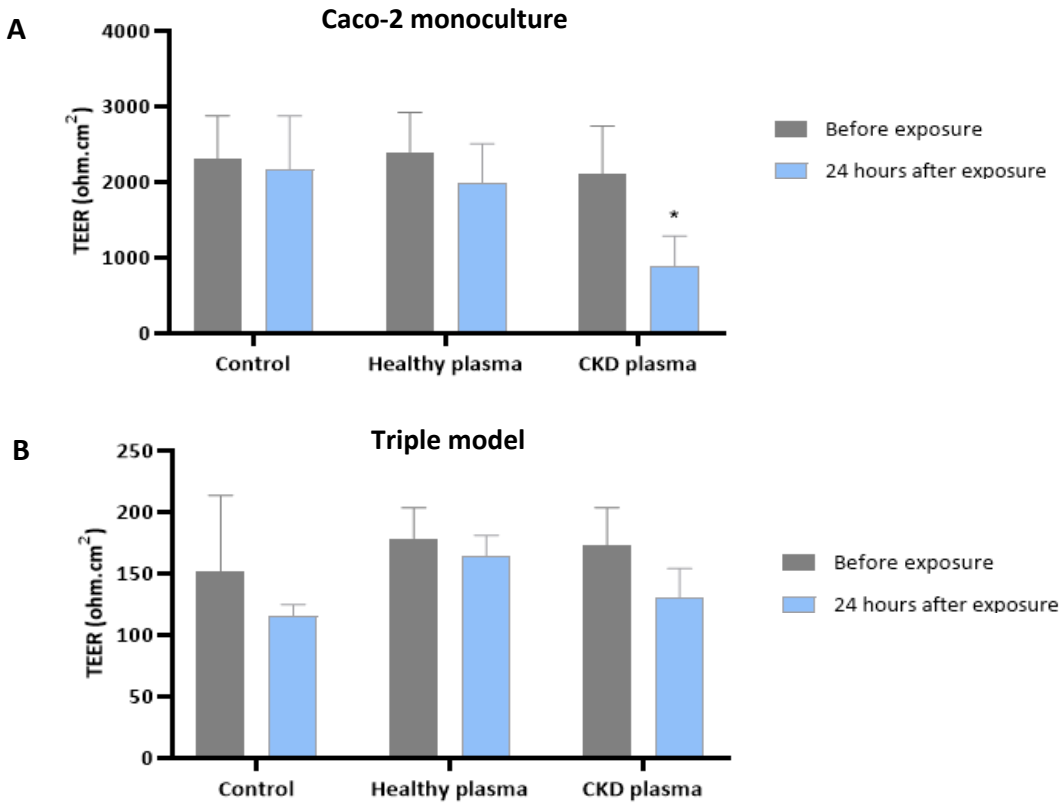


**Figure 22. Effect of CKD plasma on TEER. (A) CKD plasma decreased the TEER in Caco-2 monoculture.** The graph shows the TEER values 24h after exposure to healthy and CKD plasma in Caco-2 monoculture. Results are expressed as mean ± SD of three independent experiments. Statistically significant differences are signed as (*) $p < 0.05$ compared with 0 hours (before exposure). **(B) CKD plasma did not induce significant alteration on TEER in triple model.** The graph shows the TEER values 24h after exposure to healthy and CKD plasma in triple model. Results are expressed as mean ± SD of six independent experiments.

### 4.4.2 Effect of urea

Urea at a concentration of 20 mg/dL ("healthy" concentration) with urease, urea at a concentration of 150 mg/dL (uremic concentration) with urease, urea at a concentration of 150 mg/dL (uremic concentration) without urease and urease were added at the apical compartment (mimicking the intestinal lumen where uremic toxins like urea are converted to ammonia by microbial urease) of Caco-2 monoculture and triple model during 24h, and the TEER was monitored in this period, to evaluate the effect of the different conditions on intestinal barrier integrity. The results in Caco-2 monoculture show that urea at a concentration of 20 mg/dL (normal concentration) with urease, urea at a concentration of 150 mg/dL (uremic concentration) without urease and urease did not induce significant alterations of the TEER, and that urea at a concentration of 150 mg/dL (uremic concentration) with urease decreased the TEER, 24h after exposure (figure 23A). The results in triple model show that there were no differences on TEER in the different conditions tested, 24h after exposure (figure 23B).

**A**

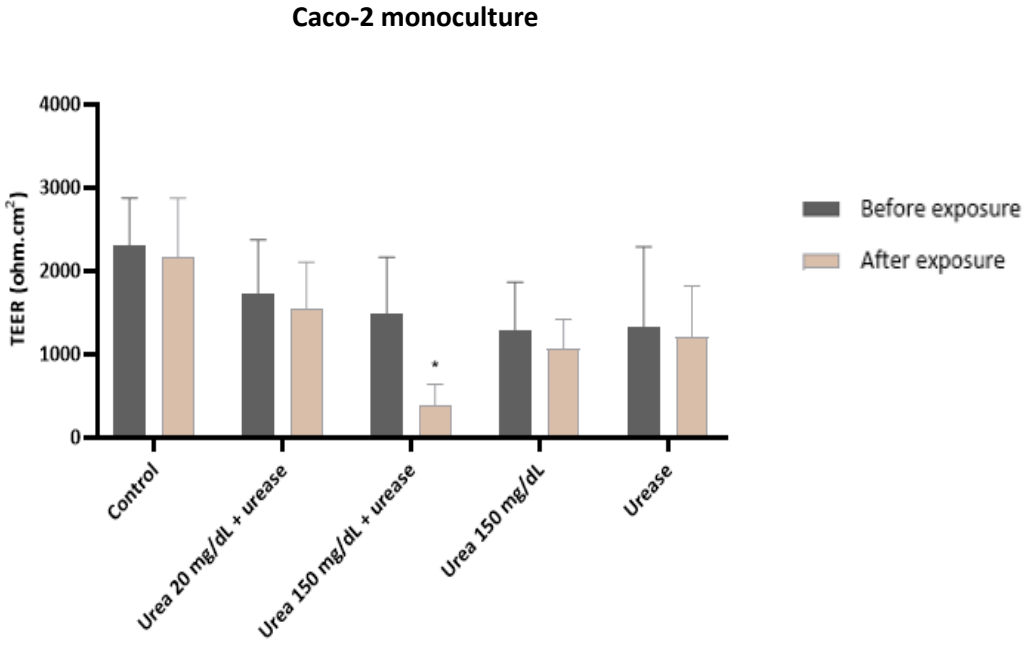

**B**

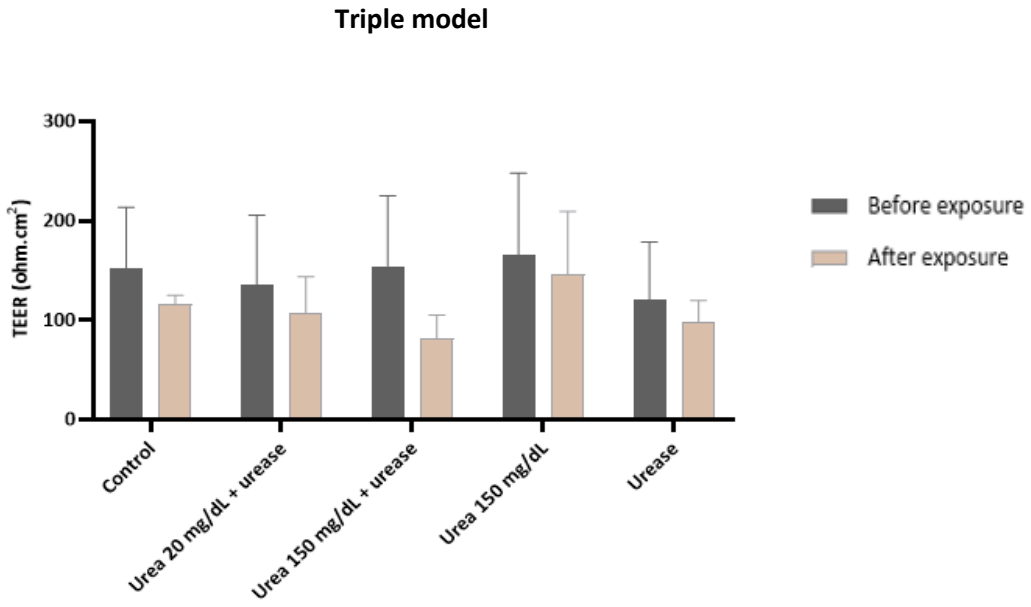


**Figure 23. Effect of urea on TEER. (A) Uremic concentration of urea in the presence of urease decreased the TEER in Caco-2 monoculture.** The graph shows the TEER values 24h after exposure to urea 20 mg/dL plus urease, urea 150 mg/dL plus urease, urea 150 mg/dL without urease and urease in Caco-2 intestinal model. Results are expressed as mean ± SD of three independent experiments. Statistically significant differences are signed as (*) $p < 0.05$ compared with 0 hours (before exposure). **(B) Urea did not induce significant alteration on TEER in triple model.** The graph shows the TEER values 24h after exposure to urea 20 mg/dL plus urease, urea 150 mg/dL plus urease, urea 150 mg/dL without urease and urease in triple intestinal model. Results are expressed as mean ± SD of three independent experiments.

### 4.4.3 Effect of dextran sodium sulfate

According to previous studies [97], DSS is associated with disruption of TJs and, since the presence of TJs at the intestinal epithelial barrier is important to maintain the integrity of the barrier, the effect of DSS on the transepithelial resistance of Caco-2 monoculture and triple model was assessed. DSS at 2% concentration was added at the apical compartment (mimicking the intestinal lumen) of intestinal models during 3h, and the TEER was measured at the end of 3h to evaluate the effect of the DSS on integrity of intestinal barrier. The results in Caco-2 monoculture show that DSS decreased the TEER, 3h after exposure (figure 24A). The results in triple model show that DSS did not induce significant alteration on TEER, 3h after exposure (figure 24B).

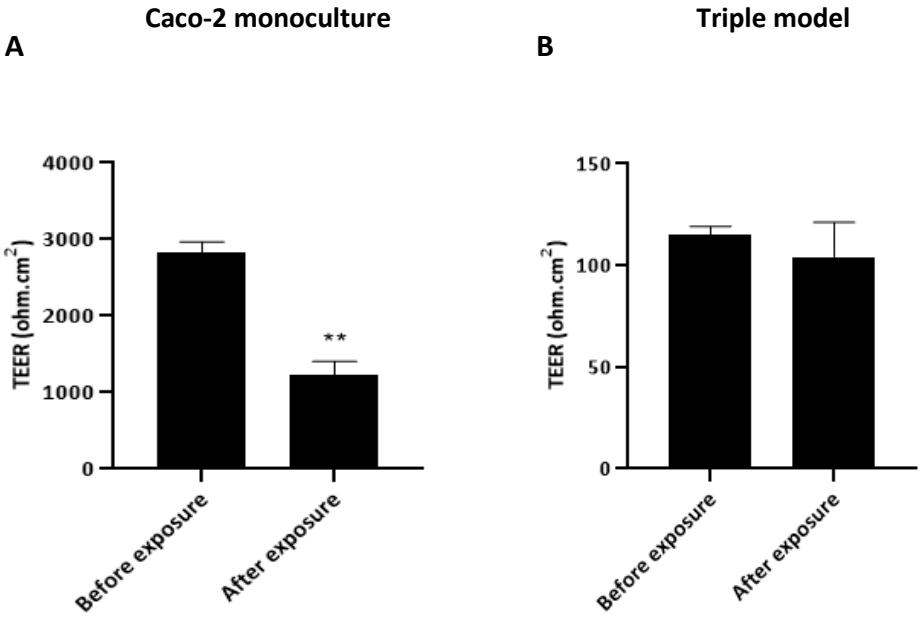


**Figure 24. Effect of DSS on TEER. (A) DSS decreased the TEER in Caco-2 monoculture.** The graph shows the TEER values 3h after exposure to DSS in Caco-2 intestinal model. Results are expressed as mean ± SD of three replicates. Statistically significant differences are signed as (**) $p < 0.01$ compared with 0 hours (before exposure). **(B) DSS did not induce significant alteration on TEER in triple model.** The graph shows the TEER values 3h after exposure to DSS in triple intestinal model. Results are expressed as mean ± SD of three replicates.

## 4.5 Effect of uremic conditions on permeability

To evaluate the integrity of models after exposure to uremic conditions, the permeability was assessed with FITC-dextran, a marker of paracellular pathway [163]. The FITC-dextran permeability assay was assessed after exposure to plasma of CKD patients and urea (with or without urease). The results were expressed in percentage of FITC-dextran that passed from apical side (mimicking the intestinal lumen) to basolateral side (mimicking the bloodstream) and show the implication of uremic conditions on permeability in both Caco-2 monoculture and Caco-2/HT29-MTX/Raji B triple model.

### 4.5.1 Effect of plasma of chronic kidney disease patients

The permeability of Caco-2 monoculture and triple model was performed by FITC-dextran assay 24h after exposure to healthy and CKD plasma. FITC-dextran was added to the apical side (mimicking the intestinal lumen) at 200 µg/mL and the content that passed to the basolateral side (mimicking the bloodstream) was quantified by fluorescence spectrophotometry. The values of concentration of FITC-dextran were calculated from a standard curve obtained with known concentrations. The permeability results were expressed in percentage of FITC-dextran that passed to basolateral compartment and show that healthy and CKD plasma did not induce significant alterations on permeability in Caco-2 monoculture and triple model (figure 25).

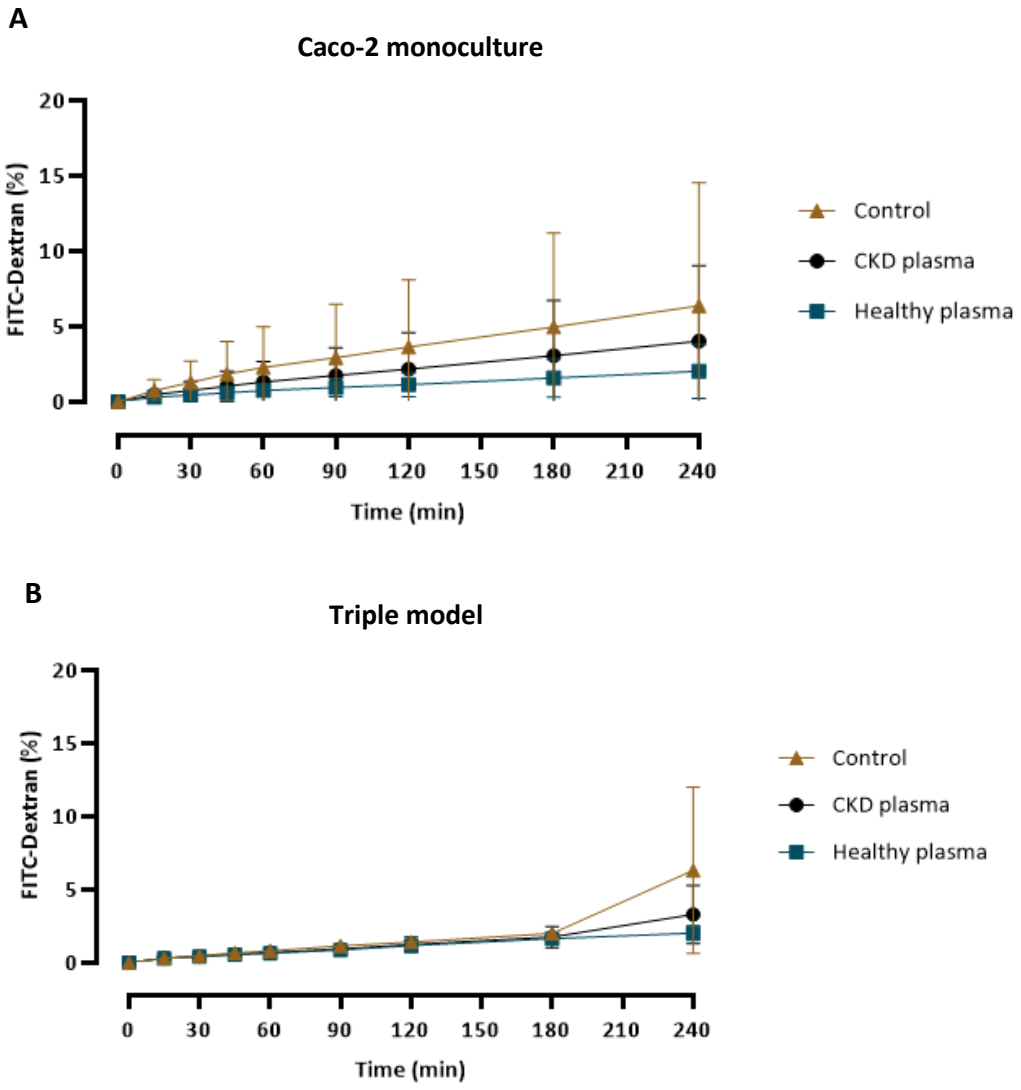

**Figure 25. Effect of CKD plasma on permeability. CKD plasma did not induce significant alteration on permeability in (A) Caco-2 monoculture and (B) triple model.** FITC-dextran permeability assay was performed 24h after incubation with healthy and CKD plasma, with a concentration of 200 µg/mL of FITC-dextran used on apical compartment of intestinal model. The graphs show the percentage of FITC-dextran that passed to the basolateral compartment in eight time points. The results are expressed as mean ± SD of three replicates.

### 4.5.2 Effect of urea

The permeability of the triple model 24h after exposure to normal concentration of urea (20 mg/dL) with urease, uremic concentration of urea (150 mg/dL) with urease, uremic concentration of urea (150 mg/dL) without urease and urease was performed using FITC-dextran. FITC-dextran was added to apical side (mimicking the intestinal lumen) at 200 µg/mL and the content that passed to basolateral side (mimicking the bloodstream) was quantified by fluorescence spectrophotometry. The values of concentration of FITC-dextran were calculated from a standard curve obtained with known concentrations. The permeability results were expressed in percentage of FITC-dextran that passed to basolateral compartment and show that normal concentration of urea (20 mg/dL) in the presence of urease, uremic concentration of urea (150 mg/mL) without urease and urease did not induce significant alterations on permeability and that uremic concentration of urea (150 mg/mL) in the presence of urease increased the permeability in triple model (figure 26).

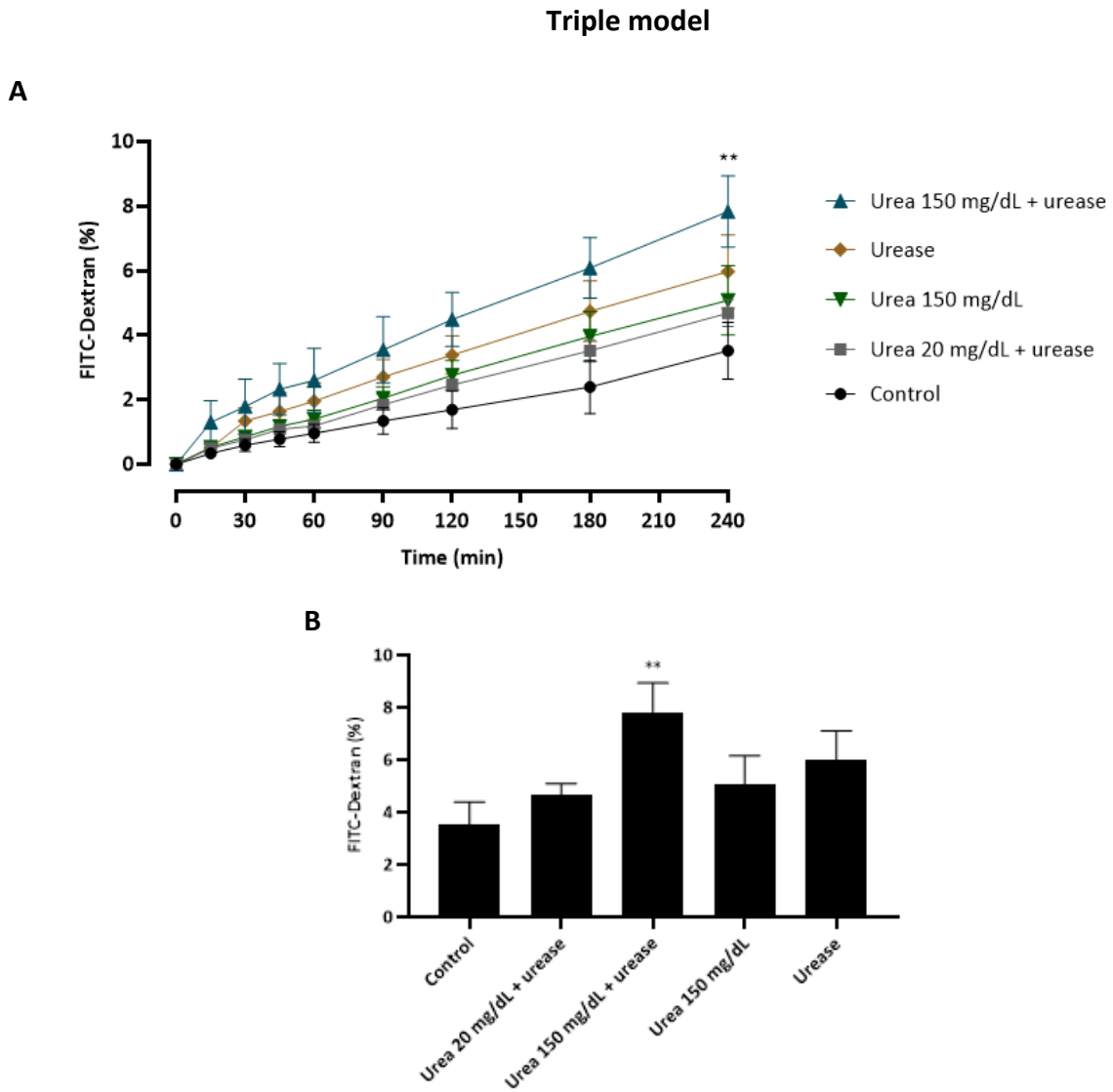


**Figure 26. Uremic concentration of urea in the presence of urease increased the permeability in triple model.** FITC-dextran permeability assay was performed 24h after exposure to urea 20 mg/dL plus urease, urea 150 mg/dL plus urease, urea 150 mg/dL without urease and urease, with a concentration of 200 µg/mL of FITC-dextran used on apical compartment of intestinal model. **(A)** The graph shows the percentage of FITC-dextran that passed to the basolateral compartment in eight time points. **(B)** Percentage of FITC-dextran that passed to the basolateral compartment at the end of experiment (time 240 min). All results are expressed as mean ± SD of three replicates. Statistically significant differences are signed as (**) $p < 0.01$ compared with control.

## 4.6 Effect of uremic conditions on quantity of tight junctions

The permeability of intestinal barrier is regulated by the integrity of cellular plasma membranes and TJs [75] and, therefore, the presence of TJs in intestinal epithelium is crucial to the maintenance of an integrated barrier. Thus, it is important to assess the effect of uremic conditions on integrity, quantity and localization of TJs in intestinal barrier. For this, four TJs proteins that constitute the intestinal epithelium, ZO1, OCLN, CLDN1 and CLDN2, already described in section 1.2.2, were evaluated. The localization and quantity of ZO1, OCLN, CLDN1 and CLDN2 was performed after exposure to healthy and CKD plasma and DSS in both Caco-2 monoculture and triple model. The localization of TJs was assessed by immunofluorescence and the mean fluorescence intensity of each TJ antibody was quantified. The results of quantification of TJs were represented as mean intensity of Alexa Fluor 488, corresponding to OCLN and ZO1 TJs, and mean intensity of Alexa Fluor 594, corresponding to CLDN1 and CLDN2 TJs.

### 4.6.1 Effect of plasma of chronic kidney disease patients and dextran sodium sulfate

The location of ZO1, OCLN, CLDN1 and CLDN2 was assessed after exposure to uremic conditions in Caco-2 monoculture and triple model. Relatively to ZO1, an adapter protein linking the transmembrane proteins to cytoplasmic proteins such as actin filaments [88, 89], the results show that its localization was not specific to the membrane cell in both intestinal models, once these proteins are presented intracellularly close to the cell membrane and not at transmembrane site. Relatively to OCLN, CLDN1 and CLDN2, all transmembrane proteins [45], the results show that the location was specific to the cell membrane in both intestinal models (figures 27 and 29).

The results of quantification show that there were no differences between the different groups tested to each TJ. However, the mean fluorescence intensity of Alexa Fluor 488 (ZO1 and OCLN) was lower than the mean fluorescence intensity of Alexa Fluor 594 (CLDN1 and CLDN2) to all conditions tested for both Caco-2 monoculture and triple model (figures 28 and 30).

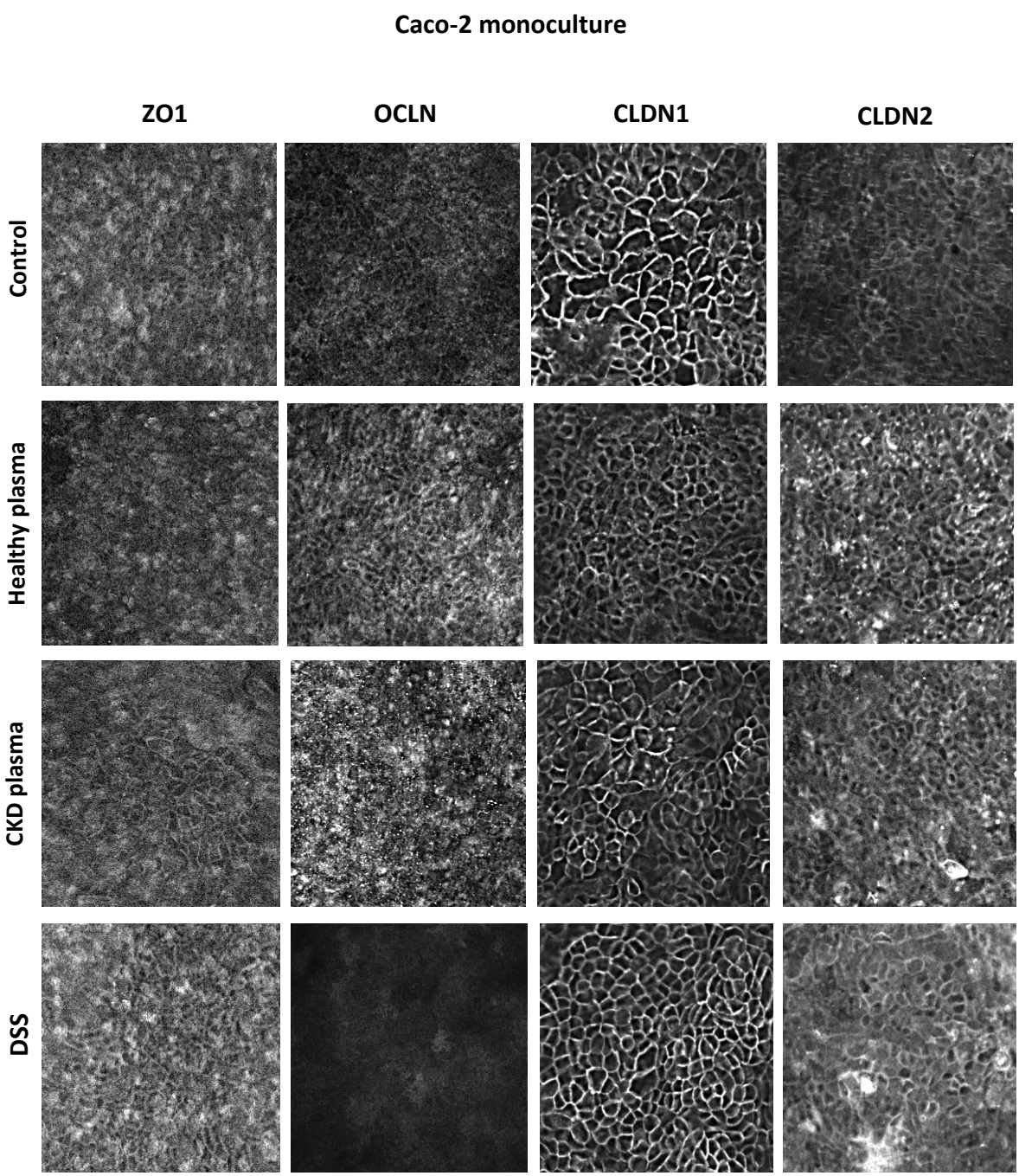


**Figure 27. Localization of TJs ZO1, OCLN, CLDN1 and CLDN2 in different conditions in Caco-2 monoculture.** Images representative of localization of TJs ZO1, OCLN, CLDN1 and CLDN2 24h after exposure to healthy plasma and CKD plasma, and 3h after exposure to DSS.

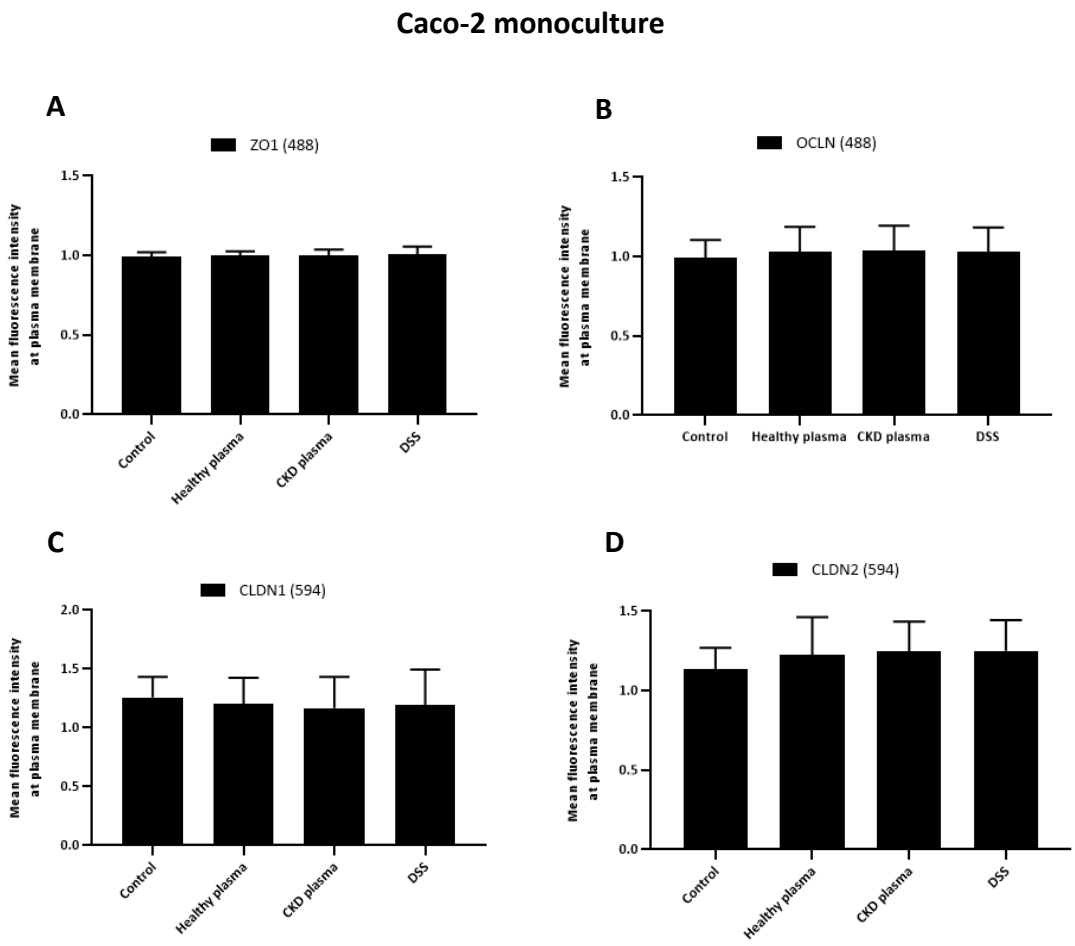


**Figure 28. CKD plasma and DSS did not induce significant alterations on quantity of TJs in Caco-2 monoculture.** Quantification of TJs represented in figure 27. Mean fluorescence intensity of **(A)** ZO1 (Alexa Fluor 488), **(B)** OCLN (Alexa Fluor 488), **(C)** CLDN1 (Alexa Fluor 594) and **(D)** CLDN2 (Alexa Fluor 594) at plasma membrane. All results are expressed as mean fluorescence intensity ± SD, normalized to fluorescence measured at the membrane without antibodies, obtained in three independent experiments.

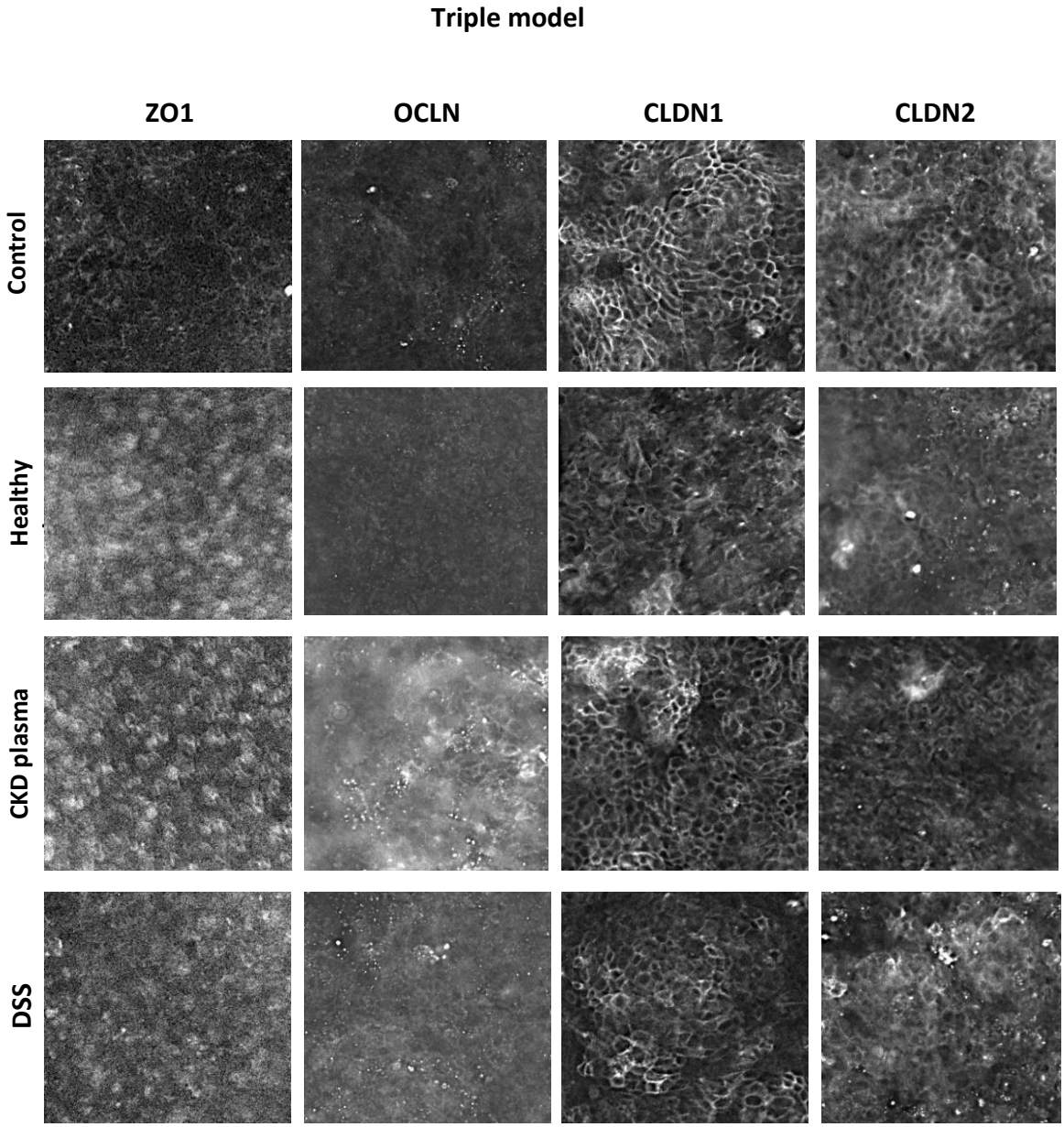


**Figure 29. Localization of TJs ZO1, OCLN, CLDN1 and CLDN2 in different conditions in triple model.** Images representative of localization of TJs ZO1, OCLN, CLDN1 and CLDN2 24h after exposure to healthy plasma and CKD plasma, and 3h after exposure to DSS.

**Triple model**

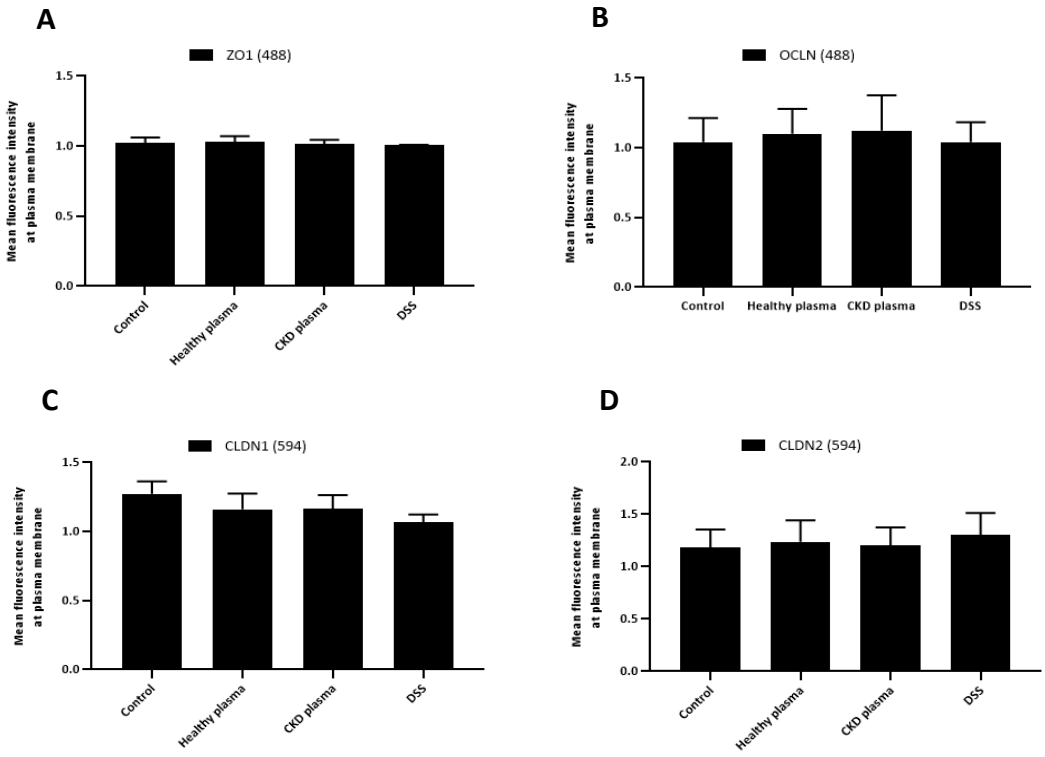


**Figure 30. CKD plasma and DSS did not induce significant alterations on quantity of TJs in triple model.** Quantification of TJs represented in figure 29. Mean fluorescence intensity of **(A)** ZO1 (Alexa Fluor 488), **(B)** OCLN (Alexa Fluor 488), **(C)** CLDN1 (Alexa Fluor 594) and **(D)** CLDN2 (Alexa Fluor 594) at plasma membrane. All results are expressed as mean fluorescence intensity ± SD, normalized to fluorescence measured at the membrane without antibodies, obtained in three independent experiments.

## 4.7 Effect of uremic conditions on microbial translocation

### 4.7.1 Effect of plasma of chronic kidney disease patients and dextran sodium sulfate

Bacterial translocation assay of *E. coli* isolate from CKD patient was performed in Caco-2 monoculture and triple model after exposure to healthy and CKD plasma as well to DSS. The results of bacterial translocation show that healthy and CKD plasma and DSS did not induce significant alterations in *E. coli* translocation in both Caco-2 monoculture and triple model (figure 31).

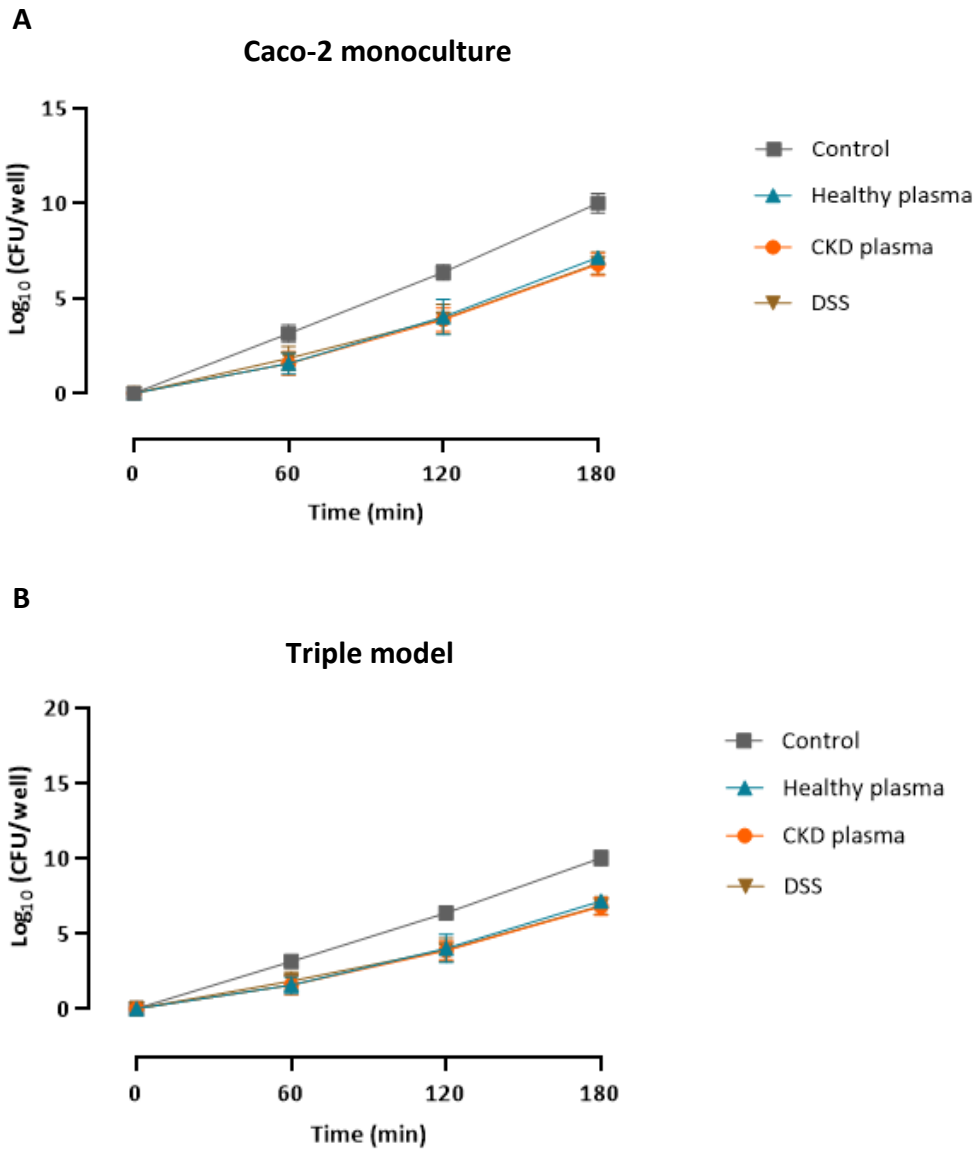


**Figure 31. Effect of CKD plasma and DSS on microbial translocation. CKD plasma and DSS did not induce significant alterations in *E. coli* translocation in (A) Caco-2 monoculture and (B) triple model.** Bacterial translocation assay was performed 24h after exposure to healthy and CKD plasma and 3h after exposure to DSS, for 180 min with a MOI=5. The results were represented as $\log_{10}$(CFU/well) vs time and are the mean ± SD of five independent experiments.

### 4.7.2 Effect of urea

Bacterial translocation assay of *E. coli* isolate from CKD patient was performed in Caco-2 monoculture and triple model after exposure to urea 20 mg/dL and urea 150 mg/dL in the presence of urease, urea 150 mg/dL without urease and urease. The MOI used in apical side was 5. The results of bacterial translocation are represented as $\log_{10}$(CFU/well) vs time and show that there were no differences between the different conditions tested in *E. coli* translocation in Caco-2 monoculture and triple model (figure 32).

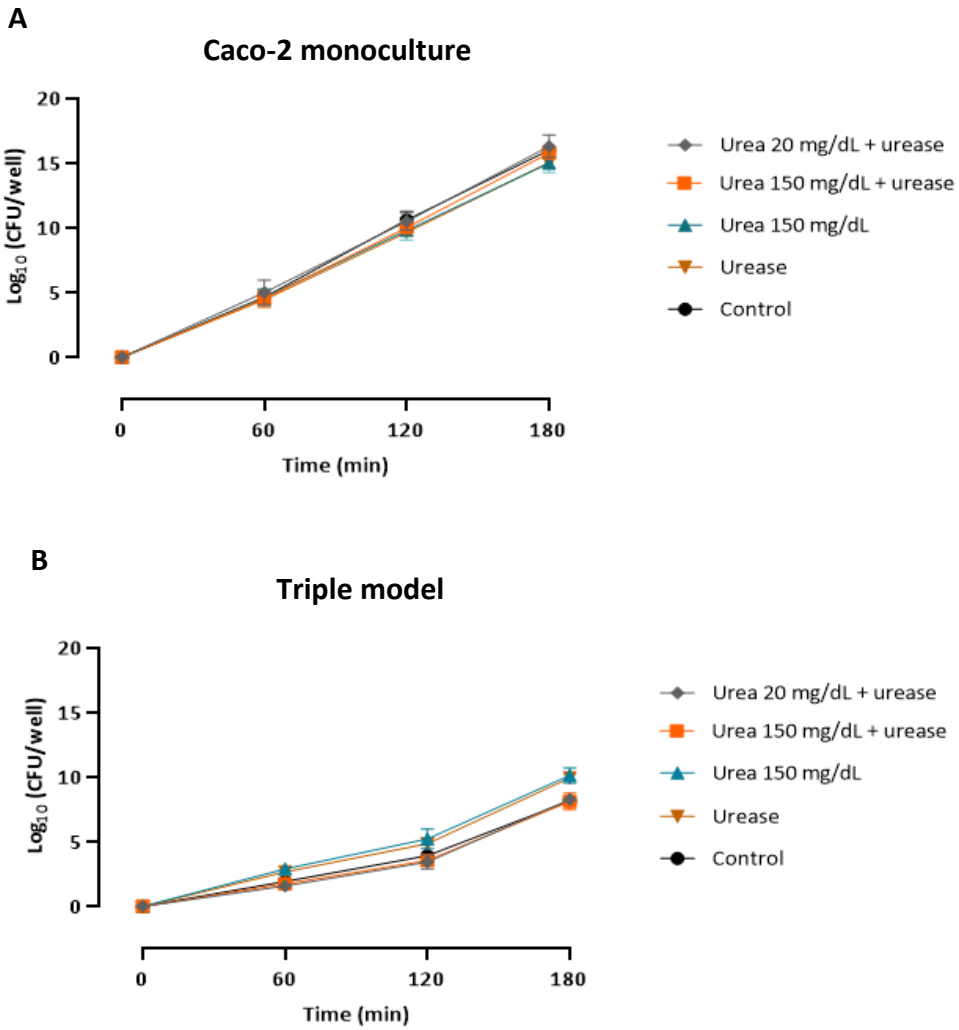


**Figure 32. Effect of urea on microbial translocation. Urea did not induce significant alteration in *E. coli* translocation in (A) Caco-2 monoculture and (B) triple model.** Bacterial translocation assay was performed 24h after exposure to urea 20 mg/dL plus urease, urea 150 mg/dL plus urease, urea 150 mg/dL without urease and urease, for 180 min with a MOI=5. The results were represented as $\log_{10}$(CFU/well) vs time and are the mean ± SD of one independent experiment with 3 replicates.

# DISCUSSION

# 5 DISCUSSION

**The main goal of this investigation was to evaluate the application of two stablished *in vitro* models of intestinal epithelial barrier for the study of microbial translocation and to evaluate the impact of different uremic conditions present in CKD on this microbial translocation. It was indeed possible to study the microbial translocation through intestinal epithelial barrier, although with some methodological limitations that should be improved in the future. Microbial translocation was higher in Caco-2 monoculture than in triple model, suggesting that the triple model creates a more effective barrier and, therefore, apparently is a more robust intestinal model for what happens in the human intestine. The experimental uremic conditions simulated in this study did not potentiate the microbial translocation through the *in vitro* intestinal epithelial barrier models, Caco-2 monoculture and Caco-2/HT29-MTX/Raji B triple model, although interfered at some extent with the integrity and the permeability of intestinal epithelial barrier models.**

The results of intestinal barrier transepithelial resistance in both Caco-2 monoculture and Caco-2/HT9-MTX/Raji B triple model throughout the maturation process, that is, during the 21 days, showed that the TEER was significantly higher in Caco-2 monoculture than in triple model, which is in accordance with the literature [63]. This difference can be explained by the fact that the TJs are very tight between Caco-2 cells in Caco-2 monocultures [133]. On the other hand, in triple model, the presence of HT29-MTX cells influences the tightness level of the epithelium due to the fact that the HT29-MTX attachment to Caco-2 cells is done by TJs that are not as tight as in Caco-2 monoculture [133, 140, 150, 151] and, therefore, more intercellular space exist.

Considering what was mentioned above, a higher microbial translocation would be expected in triple model. Also, the presence of Raji B cells in triple model allows the differentiation of Caco-2 cells into M cells [63], and M cells are able to translocate microorganisms through transcellular pathway [62]. However, the results comparing the microbial translocation between models demonstrated that this microbial translocation is higher in Caco-2 monoculture than in triple model. The HT29-MTX cells that integrate the

triple model are mucus-producing cells [136], that coats the surface of intestinal epithelial barrier and play an important role in adhesion of live organisms as well as bacterial components, such as LPS [142]. Given these facts, the lower microbial translocation verified in triple model may be explained by the presence of this mucus layer that restricts the microbial translocation, once the bacteria adhere to the mucus and, therefore, do not translocate easily through the intestinal epithelial barrier. Moreover, only a small percentage of Caco-2 cells may differentiate into M cells [64] and only a few strains of *E. coli* have the capacity to translocate M cells [66-68]. Therefore, in our experimental setting, the *E. coli* strain used may have not translocate through M cells.

The assessment of the effect of uremic conditions in transepithelial resistance demonstrates that the plasma of CKD patients, uremic concentrations of urea in the presence of urease and DSS decreased the TEER of the intestinal epithelial barrier of Caco-2 monocultures but not of triple model. This absence of changes on TEER values in response to CKD plasma, uremic concentrations of urea in the presence of urease and DSS in the triple model may be due to the fact that, in this model, the TEER values are quite low and, therefore, the effect of these uremic conditions in intestinal epithelial barrier cannot be noticeable. As so, TEER evaluation may not be the best methodology to assess the integrity of the epithelial barrier in triple model.

Recent studies associated the uremic plasma of CKD patients to damage of intestinal epithelial barrier function and to depletion of TJs proteins [47]. The results of the effect of CKD plasma on TEER showed that CKD plasma decreased the TEER values in Caco-2 monocultures. These effects may be explained by the fact that uremic plasma of CKD patients has uremic toxins and metabolites capable of exerting damage on epithelial barrier function [47]. The same authors , in other studies, suggested that the disruption of TJs and of intestinal epithelial barrier function in uremic conditions is mediated by ammonia, a product of urea metabolization by urease of microbial origin [102, 106, 107]. In agreement, the results of this study showed that the effect of urea in decreased TEER values in Caco-2 monoculture is only significant in the presence of elevated concentrations of urea (uremic concentrations) when incubated with urease. Thus, urea by itself does not influence the intestinal epithelium integrity, but when in high concentrations and in the concomitant

presence of microbial urease in intestinal lumen, urea is transformed to another uremic toxin, ammonia, that will exert negative effects on the epithelial barrier. It was described that DSS leads to disruption of TJs and consequent intestinal epithelial barrier disfunction [96]. In agreement with this view are the results of our study demonstrating that DSS decrease the TEER in Caco-2 monocultures, that will be associated with barrier function damage. In sum, it was demonstrated that the exposure to plasma of CKD patients, uremic concentrations of urea in the presence of urease and DSS leads to decrease the transepithelial resistance and consequently integrity of Caco-2 monocultures.

Although the plasma of CKD patients altered the TEER in Caco-2 monocultures, there was no effect on the paracellular transport of FITC-dextran as well on the TJs proteins expression in Caco-2 monocultures and triple models. These results could be explained by the fact that, despite the plasma of CKD patients decrease the resistance and integrity of intestinal barrier, this effect cannot be enough to potentiate the passage of FITC-dextran used in the permeability assay, once the decrease of integrity cannot be associated with depletion of TJs. Other reason could be that the time of exposure of the intestinal epithelial models to uremic plasma may have not been enough to allow the disruption of TJs and, therefore, the permeability may not be affected.

On the other hand, uremic concentrations of urea in the presence of urease demonstrated to interfere in FITC-dextran permeability in triple model. These results were interesting once one would expect the same effect on permeability that occurred in the presence of plasma of CKD patients. This increase of permeability in uremic concentrations of urea in the presence of urease can be explained by the fact that the exposure to elevated concentrations of urea allows the action of microbial urease and production of large amounts of ammonia, this last one with negative effects in intestinal barrier, effects already reported and associated with CKD, such as depletion of TJs proteins [102, 106, 107], which is associated with an increase of permeability in intestinal epithelial barrier. The plasma of CKD patients, although contains several uremic toxins, as urea, in high concentration, may lack the local factors “given” by the intestinal microbiome that have effect on the epithelial intestinal barrier, such as microbial urease and other microbial uremic toxins and, therefore, the exposure to CKD plasma did not influence the permeability in both Caco-2

monoculture and triple model, unlike exposure to uremic concentrations of urea in the presence of urease in triple model. However, the absence of altered permeability due to uremic concentrations of urea in the presence of urease in Caco-2 monoculture model is hard to explain. More replicates of this experience should be made but, this may be explained by the presence of only one type of cells that are very tight between them, that is, Caco-2 cells [133]. Given these facts, it was expectable that, in Caco-2 monoculture, the presence of very tight TJs would limit the paracellular transport, more than in triple model and, therefore, the permeability in Caco-2 monoculture will be lower, even under uremic conditions.

Our study also assessed the TJs proteins of intestinal epithelial barrier models. The assessment of TJs proteins is complex. Several factors may influence the function of TJs and, therefore, researchers should evaluate not only the *in situ* protein expression or the produced quantity of mRNA but also proteins phosphorylation, folding, localization or interprotein binding [92, 93]. Our study only evaluated the *in situ* protein expression by ICC of the following TJs proteins: ZO1, OCLN, CLDN1 and CLDN2. The evaluation of the effect of uremic conditions on quantity of TJs showed that neither plasma of CKD patients nor DSS interfere on quantity of TJs in intestinal epithelium in both Caco-2 monoculture and triple model. Therefore, we could hypothesize that the absence of differences on the expression of TJs proteins could be because uremic toxins present in CKD plasma and DSS do not interfere on quantity of TJs proteins, but may influence the phosphorylation and folding of TJs proteins and also the localization of TJs, factors that the quantification of TJs do not consider. However, other studies found changes in TJs protein expression induced by plasma of CKD patients and in CKD rats [47, 106]. Several reasons may account for the contradictory results like the use of different cells, the quantifications of TJs proteins by Western Blot and the use of animal models, that should be considered when comparing studies. The effect of urea with and without urease on TJs expression will be done in the future.

The main goal of this study was to comprehend if uremic conditions present in CKD influence the microbial translocation through the intestinal epithelial barrier. The results of this study demonstrate that the exposure to uremic plasma, uremic concentrations of

urea and DSS in the tested experimental setting do not influence the *E. coli* translocation through the intestinal epithelial barrier in both Caco-2 monoculture and triple model. These results can be explained using the same arguments applied when discussing the results of permeability. That is, CKD plasma, uremic concentrations of urea and DSS have an impact on the transepithelial resistance and integrity of intestinal epithelium but this impact is not enough to allow an increase of bacterial translocation. Also, the results of localization of TJs proteins performed by ICC agree with these results, since the localization of TJs proteins in the presence of CKD plasma and DSS is specific to the cell plasma membrane and show that these TJs proteins are binding adjacent cell membranes and closing the gaps, like it is possible visualize in CLDN1 protein in both Caco-2 monoculture and triple model. CLDN1 protein is associated with sealing pores between adjacent cell membranes and decreased the permeability in epithelial barrier [81-83]. Hence, if the translocation of the *E. coli* used in this study through epithelial barrier is limited to paracellular pathway, it was expected that *E. coli* translocation in the presence of CKD plasma and DSS did not increase. Together with what has already been mentioned, the presence of mucus in triple model and the presence of Caco-2 cells that are very tight between them in Caco-2 monoculture could limit the microbial translocation through intestinal epithelial barrier, even under uremic conditions.

In sum, the mechanisms by which bacteria translocate through the intestinal epithelium are quite complex and, therefore, the study of the bacterial translocation may require different or more complex methodological settings. Despite that, these intestinal models allowed the study of the influence of uremic conditions in intestinal epithelial barrier integrity and microbial translocation, increasing knowledge about the pathophysiological processes related with CKD.

# FINAL REMARKS

# 6 FINAL REMARKS

Applying the present experimental settings, it was possible to study the microbial translocation through intestinal epithelial barrier, although with some methodological limitations that should be improved in the future. Microbial translocation is higher in Caco-2 monoculture than in triple model, suggesting that the triple model creates a more effective barrier and, therefore, apparently is a more robust intestinal model for what happens in the human intestine. This study allowed to conclude that the uremic state influences the integrity of intestinal barrier, but this influence could not be translated in an increase in the microbial translocation through the intestinal epithelium. This study further contributes to the understanding of the impact of CKD in intestinal epithelial barrier, relating the uremic conditions to the intestinal epithelium dysfunction.

Future studies may explore mechanisms used by bacteria to translocate through the epithelial barrier in human intestine and further understand uremia factors that may impact this microbial translocation. Also, the use of other intestinal models may allow a better understanding of the host-microbiome interactions in CKD. A possible future target may be the use of gastrointestinal organoids. Culture of organotypic intestinal tissue derived from human have shown the potential to understanding effectively of host-microbe interactions [169, 170] and, for that, these *in vitro* culture systems may be an alternative to the *in vitro* intestinal epithelial barrier models already existing. Also, the use of animal models may be a possible future methodological approach, allowing the study of the *in vivo* situation. The use of these alternative *in vitro* or *in vivo* models that resemble the structural and functional complexity of the human intestine will provide knowledge in intestinal physiology and pathophysiology and how host responds to gut microbial population, allowing, in the future, the assessment of the effect of uremic conditions present in CKD on microbial translocation through intestinal epithelial barrier more effectively.

# REFERENCES

# 7 REFERENCES

[1] B. Meijers, R. Farre, S. Dejongh, M. Vicario, P. Evenepoel, Intestinal Barrier Function in Chronic Kidney Disease, Toxins (Basel) 10(7) (2018).

[2] H.C. Rayner, M. Thomas, D. Milford, Understanding Kidney Diseases, 2016.

[3] https://www.kcuk.org.uk/kidneycancer/symptoms-and-diagnosis/structure-and-function-of-the-kidneys/.

[4] C.P. Wen, T.Y. Cheng, M.K. Tsai, Y.C. Chang, H.T. Chan, S.P. Tsai, P.H. Chiang, C.C. Hsu, P.K. Sung, Y.H. Hsu, S.F. Wen, All-cause mortality attributable to chronic kidney disease: a prospective cohort study based on 462 293 adults in Taiwan, Lancet 371(9631) (2008) 2173-82.

[5] A.S. Levey, J. Coresh, Chronic kidney disease, Lancet 379(9811) (2012) 165-80.

[6] B. Sampaio-Maia, L. Simoes-Silva, M. Pestana, R. Araujo, I.J. Soares-Silva, The Role of the Gut Microbiome on Chronic Kidney Disease, Adv Appl Microbiol 96 (2016) 65-94.

[7] F. National Kidney, K/DOQI clinical practice guidelines for chronic kidney disease: evaluation, classification, and stratification, Am J Kidney Dis 39(2 Suppl 1) (2002) S1-266.

[8] https://www.cdc.gov/kidneydisease/prevention-risk.html.

[9] https://www.niddk.nih.gov/.

[10] https://www.kidneyfund.org/.

[11] https://www.urologyhealth.org/.

[12] V. Jha, G. Garcia-Garcia, K. Iseki, Z. Li, S. Naicker, B. Plattner, R. Saran, A.Y.-M. Wang, C.-W. Yang, Chronic kidney disease: global dimension and perspectives, The Lancet 382(9888) (2013) 260-272.

[13] K.T. Mills, Y. Xu, W. Zhang, J.D. Bundy, C.S. Chen, T.N. Kelly, J. Chen, J. He, A systematic analysis of worldwide population-based data on the global burden of chronic kidney disease in 2010, Kidney Int 88(5) (2015) 950-7.

[14] T.W. Meyer, Hostetter, T. H., The pathophysiology of Uremia, 2012.

[15] M.T. Velasquez, P. Centron, I. Barrows, R. Dwivedi, D.S. Raj, Gut Microbiota and Cardiovascular Uremic Toxicities, Toxins (Basel) 10(7) (2018).

[16] R.T. Gansevoort, R. Correa-Rotter, B.R. Hemmelgarn, T.H. Jafar, H.J. Heerspink, J.F. Mann, K. Matsushita, C.P. Wen, Chronic kidney disease and cardiovascular risk: epidemiology, mechanisms, and prevention, Lancet 382(9889) (2013) 339-52.

[17] R.N. Foley, P.S. Parfrey, M.J. Sarnak, Epidemiology of cardiovascular disease in chronic renal disease, J Am Soc Nephrol 9(12 Suppl) (1998) S16-23.

[18] K. Iseki, K. Fukiyama, Long-term prognosis and incidence of acute myocardial infarction in patients on chronic hemodialysis. The Okinawa Dialysis Study Group, Am J Kidney Dis 36(4) (2000) 820-5.

[19] J. Harlos, A. Heidland, Hypertension as cause and consequence of renal disease in the 19th century, Am J Nephrol 14(4-6) (1994) 436-42.

[20] I. Watanabe, J. Tatebe, S. Namba, M. Koizumi, J. Yamazaki, T. Morita, Activation of aryl hydrocarbon receptor mediates indoxyl sulfate-induced monocyte chemoattractant protein-1 expression in human umbilical vein endothelial cells, Circ J 77(1) (2013) 224-30.

[21] M. Rossi, K.L. Campbell, D.W. Johnson, T. Stanton, D.A. Vesey, J.S. Coombes, K.S. Weston, C.M. Hawley, B.C. McWhinney, J.P. Ungerer, N. Isbel, Protein-bound uremic toxins, inflammation and oxidative stress: a cross-sectional study in stage 3-4 chronic kidney disease, Arch Med Res 45(4) (2014) 309-17.

[22] Z. Tumur, H. Shimizu, A. Enomoto, H. Miyazaki, T. Niwa, Indoxyl sulfate upregulates expression of ICAM-1 and MCP-1 by oxidative stress-induced NF-kappaB activation, Am J Nephrol 31(5) (2010) 435-41.

[23] S. Ito, M. Osaka, Y. Higuchi, F. Nishijima, H. Ishii, M. Yoshida, Indoxyl sulfate induces leukocyte-endothelial interactions through up-regulation of E-selectin, J Biol Chem 285(50) (2010) 38869-75.

[24] N.A. Borges, A.F. Barros, L.S. Nakao, C.J. Dolenga, D. Fouque, D. Mafra, Protein-Bound Uremic Toxins from Gut Microbiota and Inflammatory Markers in Chronic Kidney Disease, J Ren Nutr 26(6) (2016) 396-400.

[25] K. Andersen, M.S. Kesper, J.A. Marschner, L. Konrad, M. Ryu, S. Kumar Vr, O.P. Kulkarni, S.R. Mulay, S. Romoli, J. Demleitner, P. Schiller, A. Dietrich, S. Muller, O. Gross, H.J. Ruscheweyh, D.H. Huson, B. Stecher, H.J. Anders, Intestinal Dysbiosis, Barrier Dysfunction, and Bacterial Translocation Account for CKD-Related Systemic Inflammation, J Am Soc Nephrol 28(1) (2017) 76-83.

[26] J.J. Carrero, P. Stenvinkel, Inflammation in end-stage renal disease--what have we learned in 10 years?, Semin Dial 23(5) (2010) 498-509.

[27] R. Vanholder, R. De Smet, C. Hsu, P. Vogeleere, S. Ringoir, Uremic toxicity: the middle molecule hypothesis revisited, Semin Nephrol 14(3) (1994) 205-18.

[28] D.S.R. Vanholder R, Vogeleere P, Hsu C, Ringoir S, The uraemic syndrome. In: Replacement of Renal Function by Dialysis, (1996).

[29] R. Vanholder, A. Van Loo, A.M. Dhondt, G. Glorieux, R. De Smet, S. Ringoir, Second symposium on uraemic toxicity. Summary of a symposium held in Gent, Belgium, 22-24 September 1994, Nephrol Dial Transplant 10(3) (1995) 414-8.

[30] R. Vanholder, R. De Smet, Pathophysiologic Effects of Uremic Retention Solutes, Journal of the American Society of Nephrology 10(8) (1999) 1815-1823.

[31] R. Vanholder, R. De Smet, G. Glorieux, A. Argiles, U. Baurmeister, P. Brunet, W. Clark, G. Cohen, P.P. De Deyn, R. Deppisch, B. Descamps-Latscha, T. Henle, A. Jorres, H.D. Lemke, Z.A. Massy, J. Passlick-Deetjen, M. Rodriguez, B. Stegmayr, P. Stenvinkel, C. Tetta, C. Wanner, W. Zidek, G.

European Uremic Toxin Work, Review on uremic toxins: classification, concentration, and interindividual variability, Kidney Int 63(5) (2003) 1934-43.

[32] P. Evenepoel, B.K. Meijers, B.R. Bammens, K. Verbeke, Uremic toxins originating from colonic microbial metabolism, Kidney Int Suppl (114) (2009) S12-9.

[33] Y.T. Lee, Urea concentration in intestinal fluids in normal and uremic dogs, J Surg Oncol 3(2) (1971) 163-8.

[34] W.F. Owen, Jr., N.L. Lew, Y. Liu, E.G. Lowrie, J.M. Lazarus, The urea reduction ratio and serum albumin concentration as predictors of mortality in patients undergoing hemodialysis, N Engl J Med 329(14) (1993) 1001-6.

[35] F.A. Gotch, The current place of urea kinetic modelling with respect to different dialysis modalities, Nephrol Dial Transplant 13 Suppl 6 (1998) 10-4.

[36] T. Masud, A. Manatunga, G. Cotsonis, W.E. Mitch, The precision of estimating protein intake of patients with chronic renal failure, Kidney Int 62(5) (2002) 1750-6.

[37] J. Lim, C. Gasson, D.M. Kaji, Urea inhibits NaK2Cl cotransport in human erythrocytes, J Clin Invest 96(5) (1995) 2126-32.

[38] M. Baudouin-Legros, L. Asdram, D. Tondelier, M. Paulais, T. Anagnostopoulos, Extracellular urea concentration modulates cAMP production in the mouse MTAL, Kidney Int 50(1) (1996) 26-33.

[39] E.W. Sutherland, T.W. Rall, Fractionation and characterization of a cyclic adenine ribonucleotide formed by tissue particles, J Biol Chem 232(2) (1958) 1077-91.

[40] J.P. Monti, P.J. Brunet, Y.F. Berland, D.C. Vanuxem, P.A. Vanuxem, A.D. Crevat, Opposite effects of urea on hemoglobin-oxygen affinity in anemia of chronic renal failure, Kidney Int 48(3) (1995) 827-31.

[41] Z.G. Prabhakar SS, Montoya M, Leonard C, Urea inhibits inducible nitric oxide synthesis in murine macrophages at a post-transcriptional level [Abstract], J Am Soc Nephrol 8 (1997) 24A.

[42] W.L. Lau, N.D. Vaziri, Urea, a true uremic toxin: the empire strikes back, Clin Sci (Lond) 131(1) (2017) 3-12.

[43] https://www.vectorstock.com/royalty-free-vector/urea-molecule-vector-5081076.

[44] D. Briskey, P. Tucker, D.W. Johnson, J.S. Coombes, The role of the gastrointestinal tract and microbiota on uremic toxins and chronic kidney disease development, Clin Exp Nephrol 21(1) (2017) 7-15.

[45] A. Nusrat, J.R. Turner, J.L. Madara, Molecular physiology and pathophysiology of tight junctions. IV. Regulation of tight junctions by extracellular stimuli: nutrients, cytokines, and immune cells, Am J Physiol Gastrointest Liver Physiol 279(5) (2000) G851-7.

[46] J.R. Pappenheimer, K.Z. Reiss, Contribution of solvent drag through intercellular junctions to absorption of nutrients by the small intestine of the rat, J Membr Biol 100(2) (1987) 123-36.

[47] N.D. Vaziri, N. Goshtasbi, J. Yuan, S. Jellbauer, H. Moradi, M. Raffatellu, K. Kalantar-Zadeh, Uremic plasma impairs barrier function and depletes the tight junction protein constituents of intestinal epithelium, Am J Nephrol 36(5) (2012) 438-43.

[48] J.N. Rao, J.Y. Wang, Regulation of Gastrointestinal Mucosal Growth, San Rafael (CA), 2010.

[49] M.H. van Nuenen, R.A. de Ligt, R.P. Doornbos, J.C. van der Woude, E.J. Kuipers, K. Venema, The influence of microbial metabolites on human intestinal epithelial cells and macrophages in vitro, FEMS Immunol Med Microbiol 45(2) (2005) 183-9.

[50] G.R. Davis, C.A. Santa Ana, S.G. Morawski, J.S. Fordtran, Permeability characteristics of human jejunum, ileum, proximal colon and distal colon: results of potential difference measurements and unidirectional fluxes, Gastroenterology 83(4) (1982) 844-50.

[51] J. Pacha, Development of intestinal transport function in mammals, Physiol Rev 80(4) (2000) 1633-67.

[52] E. Le Ferrec, C. Chesne, P. Artusson, D. Brayden, G. Fabre, P. Gires, F. Guillou, M. Rousset, W. Rubas, M.L. Scarino, In vitro models of the intestinal barrier. The report and recommendations of ECVAM Workshop 46. European Centre for the Validation of Alternative methods, Altern Lab Anim 29(6) (2001) 649-68.

[53] T. Foitzik, M. Kruschewski, A. Kroesen, H.J. Buhr, Does microcirculation play a role in the pathogenesis of inflammatory bowel diseases? Answers from intravital microscopic studies in animal models, Int J Colorectal Dis 14(1) (1999) 29-34.

[54] L. Eckmann, M.F. Kagnoff, J. Fierer, Intestinal epithelial cells as watchdogs for the natural immune system, Trends Microbiol 3(3) (1995) 118-20.

[55] A. Wachtershauser, J. Stein, Rationale for the luminal provision of butyrate in intestinal diseases, Eur J Nutr 39(4) (2000) 164-71.

[56] D. Haller, C. Bode, W.P. Hammes, A.M. Pfeifer, E.J. Schiffrin, S. Blum, Non-pathogenic bacteria elicit a differential cytokine response by intestinal epithelial cell/leucocyte co-cultures, Gut 47(1) (2000) 79-87.

[57] G. Schurmann, M. Bruwer, A. Klotz, K.W. Schmid, N. Senninger, K.P. Zimmer, Transepithelial transport processes at the intestinal mucosa in inflammatory bowel disease, Int J Colorectal Dis 14(1) (1999) 41-6.

[58] J.R. Turner, Intestinal mucosal barrier function in health and disease, Nat Rev Immunol 9(11) (2009) 799-809.

[59] M.R. Neutra, E. Pringault, J.P. Kraehenbuhl, Antigen sampling across epithelial barriers and induction of mucosal immune responses, Annu Rev Immunol 14 (1996) 275-300.

[60] F. Niedergang, J.P. Kraehenbuhl, Much ado about M cells, Trends Cell Biol 10(4) (2000) 137-41.

[61] L.J. Hathaway, J.P. Kraehenbuhl, The role of M cells in mucosal immunity, Cell Mol Life Sci 57(2) (2000) 323-32.

[62] A. Beloqui, D.J. Brayden, P. Artursson, V. Preat, A. des Rieux, A human intestinal M-cell-like model for investigating particle, antigen and microorganism translocation, Nat Protoc 12(7) (2017) 1387-1399.

[63] F. Araujo, B. Sarmento, Towards the characterization of an in vitro triple co-culture intestine cell model for permeability studies, Int J Pharm 458(1) (2013) 128-34.

[64] J. Wang, V. Gusti, A. Saraswati, D.D. Lo, Convergent and divergent development among M cell lineages in mouse mucosal epithelium, J Immunol 187(10) (2011) 5277-85.

[65] S. Corr, C. Hill, C.G. Gahan, An in vitro cell-culture model demonstrates internalin- and hemolysin-independent translocation of Listeria monocytogenes across M cells, Microb Pathog 41(6) (2006) 241-50.

[66] M.A. Jepson, M.A. Clark, Studying M cells and their role in infection, Trends Microbiol 6(9) (1998) 359-65.

[67] S. Kerneis, A. Bogdanova, J.P. Kraehenbuhl, E. Pringault, Conversion by Peyer's patch lymphocytes of human enterocytes into M cells that transport bacteria, Science 277(5328) (1997) 949-52.

[68] L.R. Inman, J.R. Cantey, Specific adherence of Escherichia coli (strain RDEC-1) to membranous (M) cells of the Peyer's patch in Escherichia coli diarrhea in the rabbit, J Clin Invest 71(1) (1983) 1-8.

[69] S. Kohbata, H. Yokoyama, E. Yabuuchi, Cytopathogenic effect of Salmonella typhi GIFU 10007 on M cells of murine ileal Peyer's patches in ligated ileal loops: an ultrastructural study, Microbiol Immunol 30(12) (1986) 1225-37.

[70] A. Grutzkau, C. Hanski, H. Hahn, E.O. Riecken, Involvement of M cells in the bacterial invasion of Peyer's patches: a common mechanism shared by Yersinia enterocolitica and other enteroinvasive bacteria, Gut 31(9) (1990) 1011-5.

[71] H.M. Amerongen, G.A. Wilson, B.N. Fields, M.R. Neutra, Proteolytic processing of reovirus is required for adherence to intestinal M cells, J Virol 68(12) (1994) 8428-32.

[72] P. Sicinski, J. Rowinski, J.B. Warchol, Z. Jarzabek, W. Gut, B. Szczygiel, K. Bielecki, G. Koch, Poliovirus type 1 enters the human host through intestinal M cells, Gastroenterology 98(1) (1990) 56-8.

[73] H.M. Amerongen, R. Weltzin, C.M. Farnet, P. Michetti, W.A. Haseltine, M.R. Neutra, Transepithelial transport of HIV-1 by intestinal M cells: a mechanism for transmission of AIDS, J Acquir Immune Defic Syndr 4(8) (1991) 760-5.

[74] http://www.vivo.colostate.edu/hbooks/pathphys/digestion/smallgut/mcells.html.

[75] L. Wang, C. Llorente, P. Hartmann, A.M. Yang, P. Chen, B. Schnabl, Methods to determine intestinal permeability and bacterial translocation during liver disease, J Immunol Methods 421 (2015) 44-53.

[76] S. Aijaz, M.S. Balda, K. Matter, Tight junctions: molecular architecture and function, Int Rev Cytol 248 (2006) 261-98.

[77] W.A. Awad, C. Hess, M. Hess, Enteric Pathogens and Their Toxin-Induced Disruption of the Intestinal Barrier through Alteration of Tight Junctions in Chickens, Toxins (Basel) 9(2) (2017).

[78] M.S. Balda, J.A. Whitney, C. Flores, S. Gonzalez, M. Cereijido, K. Matter, Functional dissociation of paracellular permeability and transepithelial electrical resistance and disruption of the apical-basolateral intramembrane diffusion barrier by expression of a mutant tight junction membrane protein, J Cell Biol 134(4) (1996) 1031-49.

[79] L. Shen, C.R. Weber, J.R. Turner, The tight junction protein complex undergoes rapid and continuous molecular remodeling at steady state, J Cell Biol 181(4) (2008) 683-95.

[80] G. Krause, L. Winkler, S.L. Mueller, R.F. Haseloff, J. Piontek, I.E. Blasig, Structure and function of claudins, Biochim Biophys Acta 1778(3) (2008) 631-45.

[81] C. Van Itallie, C. Rahner, J.M. Anderson, Regulated expression of claudin-4 decreases paracellular conductance through a selective decrease in sodium permeability, J Clin Invest 107(10) (2001) 1319-27.

[82] C.M. Van Itallie, J.M. Anderson, Claudins and epithelial paracellular transport, Annu Rev Physiol 68 (2006) 403-29.

[83] G. Krause, L. Winkler, C. Piehl, I. Blasig, J. Piontek, S.L. Muller, Structure and function of extracellular claudin domains, Ann N Y Acad Sci 1165 (2009) 34-43.

[84] M. Furuse, K. Furuse, H. Sasaki, S. Tsukita, Conversion of zonulae occludentes from tight to leaky strand type by introducing claudin-2 into Madin-Darby canine kidney I cells, J Cell Biol 153(2) (2001) 263-72.

[85] S. Tsukita, M. Furuse, M. Itoh, Multifunctional strands in tight junctions, Nat Rev Mol Cell Biol 2(4) (2001) 285-93.

[86] C.M. Van Itallie, J. Holmes, A. Bridges, J.L. Gookin, M.R. Coccaro, W. Proctor, O.R. Colegio, J.M. Anderson, The density of small tight junction pores varies among cell types and is increased by expression of claudin-2, J Cell Sci 121(Pt 3) (2008) 298-305.

[87] K.R. Groschwitz, S.P. Hogan, Intestinal barrier function: molecular regulation and disease pathogenesis, J Allergy Clin Immunol 124(1) (2009) 3-20; quiz 21-2.

[88] B.R. Stevenson, J.D. Siliciano, M.S. Mooseker, D.A. Goodenough, Identification of ZO-1: a high molecular weight polypeptide associated with the tight junction (zonula occludens) in a variety of epithelia, J Cell Biol 103(3) (1986) 755-66.

[89] W. Hunziker, T.K. Kiener, J. Xu, Vertebrate animal models unravel physiological roles for zonula occludens tight junction adaptor proteins, Ann N Y Acad Sci 1165 (2009) 28-33.

[90] M. Furuse, M. Itoh, T. Hirase, A. Nagafuchi, S. Yonemura, S. Tsukita, S. Tsukita, Direct association of occludin with ZO-1 and its possible involvement in the localization of occludin at tight junctions, J Cell Biol 127(6 Pt 1) (1994) 1617-26.

[91] https://clinicalgate.com/intercellular-junctions/.

[92] P.D. Cani, S. Possemiers, T. Van de Wiele, Y. Guiot, A. Everard, O. Rottier, L. Geurts, D. Naslain, A. Neyrinck, D.M. Lambert, G.G. Muccioli, N.M. Delzenne, Changes in gut microbiota control inflammation in obese mice through a mechanism involving GLP-2-driven improvement of gut permeability, Gut 58(8) (2009) 1091-103.

[93] L. Shen, Tight junctions on the move: molecular mechanisms for epithelial barrier regulation, Ann N Y Acad Sci 1258 (2012) 9-18.

[94] A. Fasano, J.P. Nataro, Intestinal epithelial tight junctions as targets for enteric bacteria-derived toxins, Adv Drug Deliv Rev 56(6) (2004) 795-807.

[95] J.R. O'Hara, A.G. Buret, Mechanisms of intestinal tight junctional disruption during infection, Front Biosci 13 (2008) 7008-21.

[96] G. Samak, K.K. Chaudhry, R. Gangwar, D. Narayanan, J.H. Jaggar, R. Rao, Calcium/Ask1/MKK7/JNK2/c-Src signalling cascade mediates disruption of intestinal epithelial tight junctions by dextran sulfate sodium, Biochem J 465(3) (2015) 503-15.

[97] Q. Zhao, Y. Liu, L. Tan, L. Yan, X. Zuo, Adiponectin administration alleviates DSS-induced colonic inflammation in Caco-2 cells and mice, Inflamm Res 67(8) (2018) 663-670.

[98] M. Magnusson, K.E. Magnusson, T. Sundqvist, T. Denneberg, Increased intestinal permeability to differently sized polyethylene glycols in uremic rats: effects of low- and high-protein diets, Nephron 56(3) (1990) 306-11.

[99] M. Magnusson, K.E. Magnusson, T. Sundqvist, T. Denneberg, Impaired intestinal barrier function measured by differently sized polyethylene glycols in patients with chronic renal failure, Gut 32(7) (1991) 754-9.

[100] J.B. de Almeida Duarte, J.E. de Aguilar-Nascimento, M. Nascimento, R.J. Nochi, Jr., Bacterial translocation in experimental uremia, Urol Res 32(4) (2004) 266-70.

[101] N.D. Vaziri, B. Dure-Smith, R. Miller, M.K. Mirahmadi, Pathology of gastrointestinal tract in chronic hemodialysis patients: an autopsy study of 78 cases, Am J Gastroenterol 80(8) (1985) 608-11.

[102] N.D. Vaziri, J. Yuan, K. Norris, Role of urea in intestinal barrier dysfunction and disruption of epithelial tight junction in chronic kidney disease, Am J Nephrol 37(1) (2013) 1-6.

[103] E. Bourke, M.D. Milne, G.S. Stokes, Caecal pH and ammonia in experimental uraemia, Gut 7(5) (1966) 558-61.

[104] J.D. Swales, J.D. Tange, D.J. Evans, Intestinal ammonia in uraemia: the effect of a urease inhibitor, acetohydroxamic acid, Clin Sci 42(1) (1972) 105-12.

[105] J.Y. Kang, The gastrointestinal tract in uremia, Dig Dis Sci 38(2) (1993) 257-68.

[106] N.D. Vaziri, J. Yuan, S. Nazertehrani, Z. Ni, S. Liu, Chronic kidney disease causes disruption of gastric and small intestinal epithelial tight junction, Am J Nephrol 38(2) (2013) 99-103.

[107] N.D. Vaziri, J. Yuan, A. Rahimi, Z. Ni, H. Said, V.S. Subramanian, Disintegration of colonic epithelial tight junction in uremia: a likely cause of CKD-associated inflammation, Nephrol Dial Transplant 27(7) (2012) 2686-93.

[108] https://www.hmpdacc.org/.

[109] A. Ramezani, Z.A. Massy, B. Meijers, P. Evenepoel, R. Vanholder, D.S. Raj, Role of the Gut Microbiome in Uremia: A Potential Therapeutic Target, Am J Kidney Dis 67(3) (2016) 483-98.

[110] C. Cosola, M.T. Rocchetti, A. Sabatino, E. Fiaccadori, B.R. Di Iorio, L. Gesualdo, Microbiota issue in CKD: how promising are gut-targeted approaches?, J Nephrol 32(1) (2019) 27-37.

[111] D.N. Frank, A.L. St Amand, R.A. Feldman, E.C. Boedeker, N. Harpaz, N.R. Pace, Molecular-phylogenetic characterization of microbial community imbalances in human inflammatory bowel diseases, Proc Natl Acad Sci U S A 104(34) (2007) 13780-5.

[112] Z. Chen, L. Guo, Y. Zhang, R.L. Walzem, J.S. Pendergast, R.L. Printz, L.C. Morris, E. Matafonova, X. Stien, L. Kang, D. Coulon, O.P. McGuinness, K.D. Niswender, S.S. Davies, Incorporation of therapeutically modified bacteria into gut microbiota inhibits obesity, J Clin Invest 124(8) (2014) 3391-406.

[113] M. Malaguarnera, M. Vacante, T. Antic, M. Giordano, G. Chisari, R. Acquaviva, S. Mastrojeni, G. Malaguarnera, A. Mistretta, G. Li Volti, F. Galvano, Bifidobacterium longum with fructo-oligosaccharides in patients with non alcoholic steatohepatitis, Dig Dis Sci 57(2) (2012) 545-53.

[114] N.D. Vaziri, J. Wong, M. Pahl, Y.M. Piceno, J. Yuan, T.Z. DeSantis, Z. Ni, T.H. Nguyen, G.L. Andersen, Chronic kidney disease alters intestinal microbial flora, Kidney Int 83(2) (2013) 308-15.

[115] L. Vitetta, A.W. Linnane, G.C. Gobe, From the gastrointestinal tract (GIT) to the kidneys: live bacterial cultures (probiotics) mediating reductions of uremic toxin levels via free radical signaling, Toxins (Basel) 5(11) (2013) 2042-57.

[116] A.L. Servin, Pathogenesis of human diffusely adhering Escherichia coli expressing Afa/Dr adhesins (Afa/Dr DAEC): current insights and future challenges, Clin Microbiol Rev 27(4) (2014) 823-69.

[117] J.H. Cummings, Fermentation in the human large intestine: evidence and implications for health, Lancet 1(8335) (1983) 1206-9.

[118] G. Reshes, S. Vanounou, I. Fishov, M. Feingold, Cell shape dynamics in Escherichia coli, Biophys J 94(1) (2008) 251-64.

[119] Y.Y. Chen, D.Q. Chen, L. Chen, J.R. Liu, N.D. Vaziri, Y. Guo, Y.Y. Zhao, Microbiome-metabolome reveals the contribution of gut-kidney axis on kidney disease, J Transl Med 17(1) (2019) 5.

[120] Z. Sun, X. Wang, R. Andersson, Role of intestinal permeability in monitoring mucosal barrier function. History, methodology, and significance of pathophysiology, Dig Surg 15(5) (1998) 386-97.

[121] J.R. Turner, Molecular basis of epithelial barrier regulation: from basic mechanisms to clinical application, Am J Pathol 169(6) (2006) 1901-9.

[122] A.M. Marchiando, W.V. Graham, J.R. Turner, Epithelial barriers in homeostasis and disease, Annu Rev Pathol 5 (2010) 119-44.

[123] D.E. Fouts, M. Torralba, K.E. Nelson, D.A. Brenner, B. Schnabl, Bacterial translocation and changes in the intestinal microbiome in mouse models of liver disease, J Hepatol 56(6) (2012) 1283-92.

[124] L.V. McFarland, Use of probiotics to correct dysbiosis of normal microbiota following disease or disruptive events: a systematic review, BMJ Open 4(8) (2014) e005047.

[125] M. Lamprecht, S. Bogner, G. Schippinger, K. Steinbauer, F. Fankhauser, S. Hallstroem, B. Schuetz, J.F. Greilberger, Probiotic supplementation affects markers of intestinal barrier, oxidation, and inflammation in trained men; a randomized, double-blinded, placebo-controlled trial, J Int Soc Sports Nutr 9(1) (2012) 45.

[126] P. Gupta, H. Andrew, B.S. Kirschner, S. Guandalini, Is lactobacillus GG helpful in children with Crohn's disease? Results of a preliminary, open-label study, J Pediatr Gastroenterol Nutr 31(4) (2000) 453-7.

[127] A. Ramezani, D.S. Raj, The gut microbiome, kidney disease, and targeted interventions, J Am Soc Nephrol 25(4) (2014) 657-70.

[128] S.T. Abedon, S.J. Kuhl, B.G. Blasdel, E.M. Kutter, Phage treatment of human infections, Bacteriophage 1(2) (2011) 66-85.

[129] M. Kedinger, K. Haffen, P. Simon-Assmann, Intestinal tissue and cell cultures, Differentiation 36(1) (1987) 71-85.

[130] L. Smetanova, V. Stetinova, Z. Svoboda, J. Kvetina, Caco-2 cells, biopharmaceutics classification system (BCS) and biowaiver, Acta Medica (Hradec Kralove) 54(1) (2011) 3-8.

[131] F. Leonard, E.M. Collnot, C.M. Lehr, A three-dimensional coculture of enterocytes, monocytes and dendritic cells to model inflamed intestinal mucosa in vitro, Mol Pharm 7(6) (2010) 2103-19.

[132] I. Behrens, P. Stenberg, P. Artursson, T. Kissel, Transport of lipophilic drug molecules in a new mucus-secreting cell culture model based on HT29-MTX cells, Pharm Res 18(8) (2001) 1138-45.

[133] C. Hilgendorf, H. Spahn-Langguth, C.G. Regardh, E. Lipka, G.L. Amidon, P. Langguth, Caco-2 versus Caco-2/HT29-MTX co-cultured cell lines: permeabilities via diffusion, inside- and outside-directed carrier-mediated transport, J Pharm Sci 89(1) (2000) 63-75.

[134] K.M. Wood, G.M. Stone, N.A. Peppas, The effect of complexation hydrogels on insulin transport in intestinal epithelial cell models, Acta Biomater 6(1) (2010) 48-56.

[135] I. Lozoya-Agullo, F. Araujo, I. Gonzalez-Alvarez, M. Merino-Sanjuan, M. Gonzalez-Alvarez, M. Bermejo, B. Sarmento, Usefulness of Caco-2/HT29-MTX and Caco-2/HT29-MTX/Raji B Coculture Models To Predict Intestinal and Colonic Permeability Compared to Caco-2 Monoculture, Mol Pharm 14(4) (2017) 1264-1270.

[136] F. Pan, L. Han, Y. Zhang, Y. Yu, J. Liu, Optimization of Caco-2 and HT29 co-culture in vitro cell models for permeability studies, Int J Food Sci Nutr 66(6) (2015) 680-5.

[137] T. Lesuffleur, A. Barbat, E. Dussaulx, A. Zweibaum, Growth adaptation to methotrexate of HT-29 human colon carcinoma cells is associated with their ability to differentiate into columnar absorptive and mucus-secreting cells, Cancer Res 50(19) (1990) 6334-43.

[138] C. Pontier, J. Pachot, R. Botham, B. Lenfant, P. Arnaud, HT29-MTX and Caco-2/TC7 monolayers as predictive models for human intestinal absorption: role of the mucus layer, J Pharm Sci 90(10) (2001) 1608-19.

[139] N. Li, D. Wang, Z. Sui, X. Qi, L. Ji, X. Wang, L. Yang, Development of an improved three-dimensional in vitro intestinal mucosa model for drug absorption evaluation, Tissue Eng Part C Methods 19(9) (2013) 708-19.

[140] A. Wikman, J. Karlsson, I. Carlstedt, P. Artursson, A drug absorption model based on the mucus layer producing human intestinal goblet cell line HT29-H, Pharm Res 10(6) (1993) 843-52.

[141] J. Perez-Vilar, R.L. Hill, The structure and assembly of secreted mucins, J Biol Chem 274(45) (1999) 31751-4.

[142] J.M. Otte, D.K. Podolsky, Functional modulation of enterocytes by gram-positive and gram-negative microorganisms, Am J Physiol Gastrointest Liver Physiol 286(4) (2004) G613-26.

[143] V. Lievin-Le Moal, A.L. Servin, The front line of enteric host defense against unwelcome intrusion of harmful microorganisms: mucins, antimicrobial peptides, and microbiota, Clin Microbiol Rev 19(2) (2006) 315-37.

[144] A. des Rieux, V. Fievez, I. Theate, J. Mast, V. Preat, Y.J. Schneider, An improved in vitro model of human intestinal follicle-associated epithelium to study nanoparticle transport by M cells, Eur J Pharm Sci 30(5) (2007) 380-91.

[145] K. Verhoeckx, P. Cotter, I. López-Expósito, C. Kleiveland, T. Lea, A. Mackie, T. Requena, D. Swiatecka, H. Wichers, in: K. Verhoeckx, P. Cotter, I. Lopez-Exposito, C. Kleiveland, T. Lea, A. Mackie, T. Requena, D. Swiatecka, H. Wichers (Eds.), The Impact of Food Bioactives on Health: in vitro and ex vivo models, Springer, Cham (CH), 2015.

[146] B. Srinivasan, A.R. Kolli, M.B. Esch, H.E. Abaci, M.L. Shuler, J.J. Hickman, TEER measurement techniques for in vitro barrier model systems, J Lab Autom 20(2) (2015) 107-26.

[147] F. Zucco, A.F. Batto, G. Bises, J. Chambaz, A. Chiusolo, R. Consalvo, H. Cross, G. Dal Negro, I. de Angelis, G. Fabre, F. Guillou, S. Hoffman, L. Laplanche, E. Morel, M. Pincon-Raymond, P. Prieto, L. Turco, G. Ranaldi, M. Rousset, Y. Sambuy, M.L. Scarino, F. Torreilles, A. Stammati, An inter-laboratory study to evaluate the effects of medium composition on the differentiation and barrier function of Caco-2 cell lines, Altern Lab Anim 33(6) (2005) 603-18.

[148] P. Shah, V. Jogani, T. Bagchi, A. Misra, Role of Caco-2 cell monolayers in prediction of intestinal drug absorption, Biotechnol Prog 22(1) (2006) 186-98.

[149] E. Walter, S. Janich, B.J. Roessler, J.M. Hilfinger, G.L. Amidon, HT29-MTX/Caco-2 cocultures as an in vitro model for the intestinal epithelium: in vitro-in vivo correlation with permeability data from rats and humans, J Pharm Sci 85(10) (1996) 1070-6.

[150] R.A. Rocha, D. Velez, V. Devesa, In vitro evaluation of intestinal fluoride absorption using different cell models, Toxicol Lett 210(3) (2012) 311-7.

[151] M. Calatayud, M. Vazquez, V. Devesa, D. Velez, In vitro study of intestinal transport of inorganic and methylated arsenic species by Caco-2/HT29-MTX cocultures, Chem Res Toxicol 25(12) (2012) 2654-62.

[152] A. Khadem, A.-S. M, M. Sevastiyanova, C. Gougoulias, Lumance enhances the intestinal barrier function and ameliorates barrier disruption caused by LPS in IPEC-J2 cells line, Innovad 1-3.

[153] A. Woting, M. Blaut, Small Intestinal Permeability and Gut-Transit Time Determined with Low and High Molecular Weight Fluorescein Isothiocyanate-Dextrans in C3H Mice, Nutrients 10(6) (2018).

[154] M. Wolman, I. Klatzo, E. Chui, F. Wilmes, K. Nishimoto, K. Fujiwara, M. Spatz, Evaluation of the dye-protein tracers in pathophysiology of the blood-brain barrier, Acta Neuropathol 54(1) (1981) 55-61.

[155] https://www.sigmaaldrich.com/technical-documents/protocols/biology/fluorescein-isothiocyanate-dextran.html.

[156] Fluorescein isothiocyanate dextran, TdB Consultancy (2010) 1-5.

[157] J. Anderl, J. Ma, L. Armstrong, Improved Assays for Quantification of In Vitro Vascular Permeability, Millipore 10-14.

[158] R.W. Burry, Controls for immunocytochemistry: an update, J Histochem Cytochem 59(1) (2011) 6-12.

[159] Immunocytochemistry (ICC) Handbook, Novus Biologicals 1-24.

[160] V.A.N.S. AA, C.H. Lee, Pour plates or streak plates?, Appl Microbiol 18(6) (1969) 1092-3.

[161] https://www.thermofisher.com/order/catalog/product/T10282?SID=srch-srp-T10282#/T10282?SID=srch-srp-T10282.

[162] F. Antunes, F. Andrade, F. Araujo, D. Ferreira, B. Sarmento, Establishment of a triple co-culture in vitro cell models to study intestinal absorption of peptide drugs, Eur J Pharm Biopharm 83(3) (2013) 427-35.

[163] C. Pereira, F. Araujo, C.C. Barrias, P.L. Granja, B. Sarmento, Dissecting stromal-epithelial interactions in a 3D in vitro cellularized intestinal model for permeability studies, Biomaterials 56 (2015) 36-45.

[164] IN Cell Analyzer 2000, GE Healthcare (2011).

[165] S. Berg, D. Kutra, T. Kroeger, C.N. Straehle, B.X. Kausler, C. Haubold, M. Schiegg, J. Ales, T. Beier, M. Rudy, K. Eren, J.I. Cervantes, B. Xu, F. Beuttenmueller, A. Wolny, C. Zhang, U. Koethe, F.A. Hamprecht, A. Kreshuk, ilastik: interactive machine learning for (bio)image analysis, Nat Methods (2019).

[166] A.E. Carpenter, T.R. Jones, M.R. Lamprecht, C. Clarke, I.H. Kang, O. Friman, D.A. Guertin, J.H. Chang, R.A. Lindquist, J. Moffat, P. Golland, D.M. Sabatini, CellProfiler: image analysis software for identifying and quantifying cell phenotypes, Genome Biol 7(10) (2006) R100.

[167] J. Schindelin, I. Arganda-Carreras, E. Frise, V. Kaynig, M. Longair, T. Pietzsch, S. Preibisch, C. Rueden, S. Saalfeld, B. Schmid, J.Y. Tinevez, D.J. White, V. Hartenstein, K. Eliceiri, P. Tomancak, A. Cardona, Fiji: an open-source platform for biological-image analysis, Nat Methods 9(7) (2012) 676-82.

[168] N. Singhal, M. Kumar, P.K. Kanaujia, J.S. Virdi, MALDI-TOF mass spectrometry: an emerging technology for microbial identification and diagnosis, Front Microbiol 6 (2015) 791.

[169] D.R. Hill, J.R. Spence, Gastrointestinal Organoids: Understanding the Molecular Basis of the Host-Microbe Interface, Cell Mol Gastroenterol Hepatol 3(2) (2017) 138-149.

[170] S.E. Blutt, S.E. Crawford, S. Ramani, W.Y. Zou, M.K. Estes, Engineered Human Gastrointestinal Cultures to Study the Microbiome and Infectious Diseases, Cell Mol Gastroenterol Hepatol 5(3) (2018) 241-251.

# SUPPLEMENTARY FIGURES

# 8 SUPPLEMENTARY FIGURES

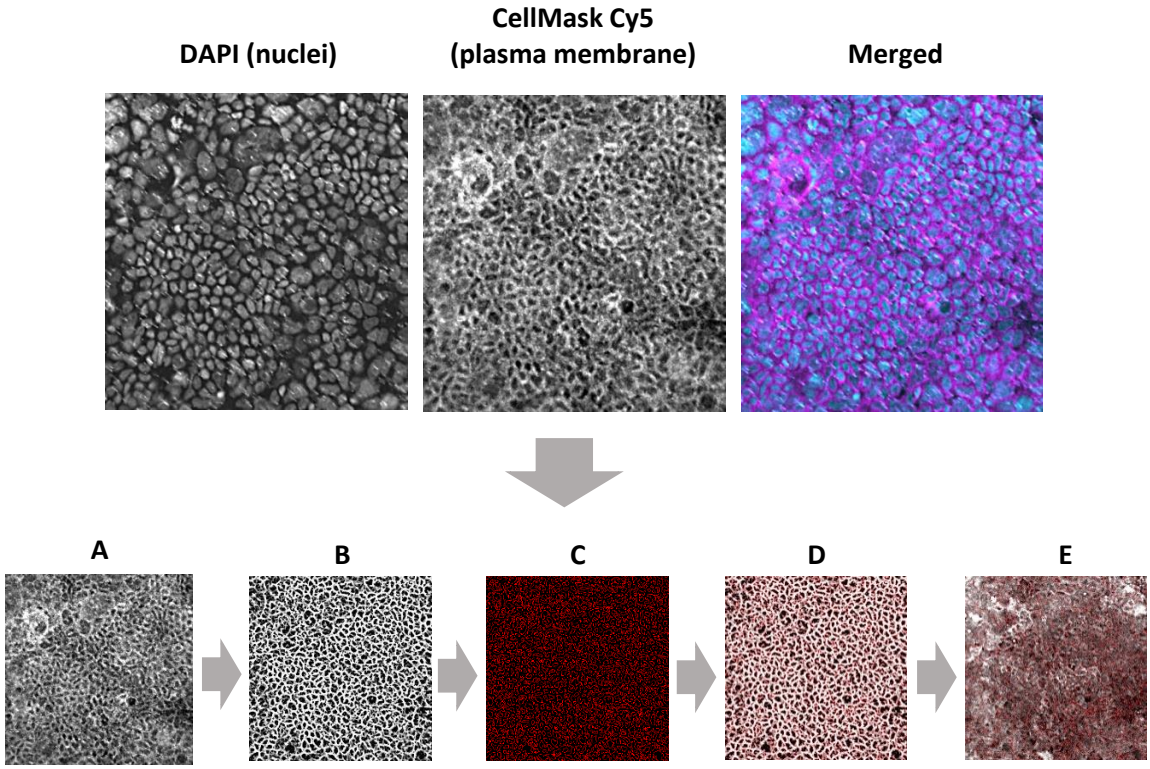


**Supplementary figure 1. Steps followed until quantification of TJs. (A)** CellMask Cy5 (plasma membrane). Result of IN Cell Analyzer 2000 (GE Healthcare). **(B)** Identification of plasma membranes. Result of Ilastik [165]. **(C)** Segmentation of plasma membranes. Result of CellProfiler [166]. **(D)** Overlay (B) + (C). Result of CellProfiler [166]. **(E)** Overlay (B) + (C) + antibodies of TJs to quantify fluorescence intensity on the TJs. Result of CellProfiler [166].

# ACKNOWLEDGMENTS

# 9 ACKNOWLEDGMENTS

This work was financed by FEDER - Fundo Europeu de Desenvolvimento Regional funds through the COMPETE 2020 - Operational Programme for Competitiveness and Internationalisation (POCI), PORTUGAL 2020 and by portuguese funds through FCT - Fundação para a Ciência e a Tecnologia/Ministério da Ciência, Tecnologia e Ensino Superior in the framework of the project “MicroMOB: The microbiome mobility pathway in chronic kidney disease and its role in infection and systemic inflammation” (PTDC/MEC-MCI/29777/2017) and the project "Institute for Research and Innovation in Health Sciences" (POCI-01-0145-FEDER-007274) as well as by the project NORTE-01-0145-FEDER-000012 , supported by Norte Portugal Regional Operational Programme (NORTE 2020), under the PORTUGAL 2020 Partnership Agreement, through the FEDER. Also, we would like to acknowledge the support of the i3S Scientific Platform BioSciences Screening, member of the national infrastructure PPBI - Portuguese Platform of Bioimaging (PPBI-POCI-01-0145-FEDER-022122).